Safety of a Multi-Vehicle System in Mixed Communication Environments

by

Animesh Chakravarthy

Submitted to the Department of Aeronautics and Astronautics
in partial fulfillment of the requirements for the degree of

Doctor of Philosophy

at the

MASSACHUSETTS INSTITUTE OF TECHNOLOGY

February 2007

Author .....
Department of Aeronautics and Astronautics
November 2006

Certified by .....
Eric Feron
Visiting Professor of Aeronautics and Astronautics, MIT
Dutton/Ducoffe Professor of Aerospace Software Engineering,
Georgia Institute of Technology
Thesis Supervisor

Certified by .....
Jaime Peraire
Professor of Aeronautics and Astronautics
Thesis Advisor

Certified by .....
James D. Paduano
Senior Research Engineer, Aurora Flight Sciences Corporation
Thesis Advisor

Certified by .....
Kyungyeol Song
Principal Engineer, Mide Technology Corporation
Thesis Advisor

Accepted by .....
Jaime Peraire
Chairman, Department Committee on Graduate Students

Safety of a Multi-Vehicle System in Mixed Communication Environments

by

Animesh Chakravarthy

Submitted to the Department of Aeronautics and Astronautics
on November 2006, in partial fulfillment of the
requirements for the degree of
Doctor of Philosophy

Abstract

Recent news events and statistics demonstrate the frequent occurrence of pile-up crashes on highways. A predominant reason for the occurrence of such crashes is that current vehicles (including those equipped with an Automatic Cruise Control system) do not provide the driver with advance information of events occurring far ahead of him/her. The use of inter-vehicular communication to provide advance warnings to enhance automotive safety is therefore being actively discussed in the research community. In this thesis, we investigate scenarios wherein only a subset of the vehicles in a multi-vehicle stream, are equipped with such advance warning capabilities. These vehicles (equipped with the capability to receive far-ahead information) are arbitrarily distributed among other unequipped vehicles that are capable of receiving only local, near-neighbor information. It is seen that there are conditions wherein even a partial equipment of the system can be beneficial (to both the equipped and the unequipped vehicles in a mixed vehicle stream). We demonstrate this through both simulations and a theoretical analysis. Towards this end, two distinct modeling approaches are adopted: microscopic and macroscopic.

The microscopic modeling approach uses ordinary differential equations to model each driver-vehicle unit and its interactions with its neighbors. A single-lane model is employed; and the problem is formulated as a collision avoidance problem. Sufficient conditions on the number of equipped vehicles, as well as their distributions in a mixed vehicle string are obtained; under these conditions, it is guaranteed that collisions do not occur. The macroscopic modeling approach, on the other hand, uses partial differential equations that govern the average behavior of groups of vehicles. In this approach, a multi-lane formulation is employed. This thesis examines the influence of partial equipment of the advance warning system on some of the wave effects that are known to exist in traffic flows, in particular, shocks and large negative velocity gradient waves that travel unattenuated or get amplified as they pass through the traffic. We examine the influence of the equipped vehicles in attenuating such waves. The resulting velocity gradients are parametrized as a function of the percentage of equipped vehicles. A prototype of an advance warning system was also developed and

road tests were conducted to test the concept. These road tests have demonstrated the system's performance to be satisfactory, subject to good communication links, for the class of scenarios tested.

Thesis Supervisor: Eric Feron
Title: Visiting Professor of Aeronautics and Astronautics, MIT
Dutton/Ducoffe Professor of Aerospace Software Engineering,
Georgia Institute of Technology

Acknowledgments

I would like to express my heartfelt thanks to Prof. Eric Feron, for giving me the opportunity to work with him, at MIT. He has pointed me in the direction in which this research has evolved; under his guidance, I believe I have attained enough confidence to assume leadership roles in my career.

No amount of thanks would be sufficient to express my deepest gratitude to Prof. Jaime Peraire. His constant encouragement instilled tremendous confidence in me. I constantly looked forward to my meeting with him; and his support to me has been tremendous - far far beyond what words can ever mention.

I truly have a lump in my throat, as I mention Dr. Kyungyeol Song. He simply is one of the nicest persons I have ever come across; and only he would understand when I say that I have a deep deep bond with him. Always cheerfully available for any discussions, he has provided tremendous inputs to this research. He is a truly extraordinary person; and I am, and shall always remain, immensely grateful to him.

I would also like to acknowledge my thanks to the other faculty with whom I have had the good fortune of being associated, either by way of taking their courses or otherwise. In particular, I would like to thank Prof. Nicolas Hadjiconstantinou, Dr. James Paduano, Prof. Richard Battin, Dr. Dionisios Margetis, Prof. Alex Megretski, Prof. John Deyst and Prof. Emilio Frazzoli.

I owe deep thanks to my lab-mates and office-mates, in particular, Emily Craparo, Zhi-Hong Mao, Jan De Mot, Masha Ishutkina, Ji-Hyun Yang, Tom Schouwenaars, Sommer Gentry, Jerome LeNy, Keith Santarelli, Danielle Tarraf, Mardavij Roozbehani. Some of them have been my study mates while preparing for those dreaded quals and I have benefitted tremendously from my interactions with them.

My other friends at MIT whom I shall always thank include Sudeep Lahiri, David Willis, Anand Srinivas, Umair Ahsun, Parthiv Shah and Debasish Sahoo. Whenever I felt low or down in the dumps, I knew I just had to spend a few minutes with them, before feeling cheerful again. I shall always remember the help I have always received from the administrative staff at LIDS, in particular, Doris Inslee, Lisa Gaummond, Angela Copyak.

Moving away from MIT and towards India, I am at a loss for words on how to thank Prof. Debasish Ghose of IISc, Bangalore and Dr. Srinathkumar who was formerly the head of the National Control Law Team (of which I have been a part). They have been my truest and most selfless mentors. I most humbly offer them my most sincere thanks.

I must acknowledge my other colleagues and friends in the Control Law Team and outside - Shyam Chetty, Girish Deodhare, Amitabh Saraf, Vijay Patel, Shrikkant Rao, Lakshmi, and of course, Viswanath Talasila and Krishna Prasad. Shyam and Girish in particular motivated me through the initial turbulent times in my Ph.D, and I always looked forward to the cheery emails of Vishy and KP. My association with Amitabh has helped me tremendously in inculcating a clear-headed mindset, when approaching any research problem.

I owe deep thanks to my family for bringing me this far - my parents and my grandmother - to them I owe deep gratitude.

And finally, Moonmoon. Moonmoon, thank you for being with me throughout. Without you, I simply would not have made it. And here's to Sabrina, our little bundle of joy, born in the same week as my thesis defense(!)

Contents

List of Figures

Chapter 1

Introduction

1.1 Background and Motivation

Rear end collisions are a major cause of multiple car crashes, especially during bad weather conditions [1, 2, 3, 4]. According to statistics released by the NHTSA (National Highway Transportation Safety Administration) (Figure 1-1) there were over ten thousand fatalities in each of the years 1999 and 2000 occurring due to vehicular collisions. Further NTSB (National Transportation Safety Board) statistics reveal that, in the US there were 1.848 million crashes for the year 1999 alone. In response to these events, the US Department of Transportation has plans to equip at least 10-25% of all vehicles with an advanced warning system by the year 2010 [81].

The major cause for such crashes is that often each driver gets warned of an impending slowdown ahead only when the brake-lights of the car/group of cars immediately in front of him/her turn on. This is particularly true during bad weather conditions, or while driving behind a large vehicle (which obstructs a driver's field of vision) which is when a driver is unable to look as far ahead, as he/she otherwise normally would have. This is also true in the context of current highly inhomogenous vehicle fleets that comprise cars, trucks, SUVs, etc. So, if we consider a platoon of cars travelling along, and the lead car executes an abrupt deceleration, this information is propagated from car to car in a staggered fashion (Figure 1-2(a)), as the brake-lights of each car come on, one after the other. There is an associated delay τ for each car

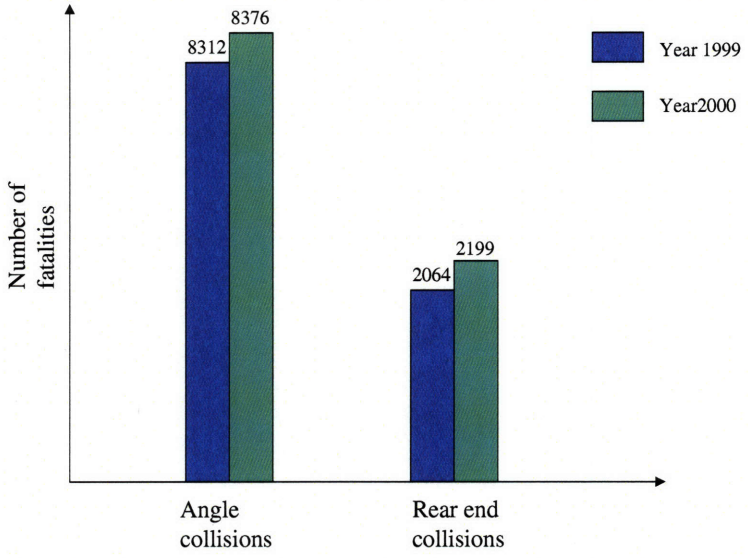

Figure 1-1: NHTSA Statistics indicating the occurrence of fatalities due to crashes

as the information propagates through the line of cars, (this delay typically comprises of the time it takes for each driver to realize that the front car's brake-lights are on, and to react with a corresponding deceleration that turns his/her own brake-lights on. It is a random variable with a typical value of around 0.5-1 seconds). Thus if car 1 (i.e. the lead car) poses a hazard by a sudden deceleration that turns on its brake-lights at time $t = 0$, then the kth car ($k > 2$) gets warned of the slowdown ahead at $t = (k-2)\tau$, and turns on his/her own brake-lights $(k-1)\tau$ seconds after the first generation of the hazard. In this way, the driver's reaction time gets continuously accumulated as the information propagates through the line of cars. This illustrates how this mode of transmission of information of a slowdown (from car to car as in Figure 1-2(a)) can often be too slow, and does not allow the drivers that are far behind in the platoon, sufficient time to react. Car pile-up crashes are the result.

There exists an important analogy between the occurrence of car pile-up crashes and the shock waves occurring in compressible flow dynamics. Shock waves in traffic flow dynamics have been discussed in the literature. The earliest known work

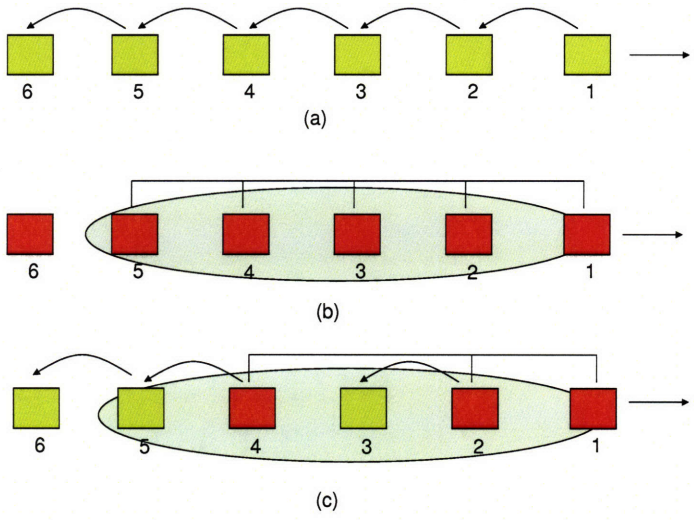

Figure 1-2: Schematic showing information propagation in different modes. (a) All vehicles are unequipped. (b) All vehicles are equipped. (c) Some vehicles are equipped. Equipped vehicles are shown in red.

appeared in [5].

The use of inter-vehicle communication for enhancement of vehicle safety is being discussed in the literature, *e.g.*, in [6, 12, 13, 7, 9, 10]. Researchers discuss concepts such as vehicular ad-hoc networks (VANETS) through which information can propagate in a wireless mode. For instance, if we consider a scenario wherein information of a hazard ahead can be transmitted wirelessly through a multi-vehicle stream; and if we assume that *all* the vehicles in the stream are equipped to receive such information, then this information propagation occurs as in Figure 1-2(b).

In a real-life scenario, however, it would be unrealistic to assume that all the cars in a platoon will indeed be equipped with inter-vehicular communication capabilities. In the context of vehicular safety, for example, it is reasonable to envisage scenarios wherein some vehicles are equipped to receive advance warning information, while others are not. Indeed, the long lifetime of passenger cars and other road vehicles guarantees that, at least for a while, not all cars will be equipped with advanced computation and communication capabilities. In addition, the appearance of such

capabilities is likely to be slower on low-end models than high-end models. It is pertinent therefore to examine the influence of an advance warning system, when only a (randomly selected) fraction of the total number of cars in the platoon are equipped with the system. In this case, information is propagated as in Figure 1-2(c). Thus if car 1 transmits a warning signal at time $t = 0$, then since cars 2 and 4 are equipped with the warning system, both of them receive the warning signal at $t = 0$ (if we assume infinite communication speeds). Furthermore, the unequipped cars 5 and 6 now receive (indirect) information of the slowdown at τ and 2τ, respectively, which contributes significantly to safety improvement, as compared to the case in Figure 1-2(a) when cars 5 and 6 receive the warning information only at $t = 3\tau$ and 4τ, respectively. Even if we assume finite propagation speeds (of the slowdown information through the equipped cars), the unequipped vehicles still benefit, because they receive indirect information of the slowdown ahead, earlier than they otherwise would have. The effects of this kind of partial deployment are studied in this thesis. We show that, in many cases, even if only a fraction of the cars are equipped, their influence on the traffic flow can be sufficient to alleviate the possibility of crashes even in the unequipped cars.

The goal of this research is to describe how an advance warning system enables pileup crashes to be averted, even in a mixed sensing environment wherein only a small number of vehicles are equipped with the warning system. This area of work can also be related to other more general problems of how a minority of informed individuals influence group behavior. For instance, biologists have long theorized that when a flock of birds are migrating from one place to another, it is actually only a small minority of the birds in the flock who have a clear idea of their final destination [28]. The other 'uninformed' birds merely follow the 'informed' birds in a follow-the-leader policy. In this way only a minority of informed birds are able to influence the overall behavior of the group. Likewise, in a vehicular traffic context, we examine how only a few equipped vehicles are able to modify the behavior of the overall multi-vehicle stream.

1.2 Overview of Related Research

The fast growing number of vehicles on networks of roads constantly motivates intense research activity in the field of traffic flow modeling [54]. Traditionally, there have been three approaches to describe the dynamics of traffic flow. The first and the most basic one is the microscopic modeling approach or the car-following modeling approach, which concerns the dynamic description of individual vehicles [16, 17, 18, 19]. In the microscopic modeling approach, the response of an individual vehicle to its predecessor is modeled using ordinary differential equations. A typical example is the follow-the-leader model [16], where the acceleration of each vehicle is assumed to be proportional to the difference in speeds between itself and its immediate predecessor. More sophisticated nonlinear models have also been synthesized [19].

The second approach for modeling traffic flow is the macroscopic modeling approach, which refers to the derivation of evolution equations for various macroscopic observable quantities of the vehicle flow, based on conservation equations. In macroscopic models, one does not look at the dynamics of the individual vehicles comprising the traffic flow. Instead, traffic is described (using partial differential equations - PDEs) as a compressible fluid formed by a multi-vehicle continuum. Analogs of the continuity and momentum equations used in fluid dynamics are then used to model the traffic.

The use of macroscopic models for studying traffic flows has a fairly long history. The Lighthill-Whitham-Richards (LWR) model [5, 29] represents the earliest use of macroscopic models to represent traffic flow. The LWR model is basically a first-order model that is based on a gas-dynamics-like continuity equation (representing the conservation of cars). Subsequently, second-order models have been developed by Payne-Whitham [30, 31] and also Phillips [72]. There has been some controversy in the past about the viability of second order models in general [32], and attempts have been made to address some of them in [34, 40].

The kinetic modeling approach, which is based on Boltzmann-type kinetic equations, represents an intermediate step between the microscopic and macroscopic mod-

els. Here, the traffic is treated as a gas of interacting particles. These interactions are described by an integro-differential dynamic equation in phase space that is the analogue of the Boltzmann equation in the kinetic theory of gases. Kinetic models in traffic flows were originally introduced by Prigogine and Herman [50], who proposed the use of a kinetic term to account for the vehicular interactions. These models have been further refined by Paveri-Fontana [51]. Based on Paveri-Fontana's equations, Helbing then derived a (gas dynamic based) third-order macroscopic traffic model [40] (this model included an equation for the velocity variance), and also a second order traffic model [41], that is anisotropic in nature. Helbing also derived a two species traffic model where the two species were cars and trucks [41], as also did Hoogendoorn and Bovy [43]. There have also been second-order models developed by Aw and Rascle [34, 35, 36] - these models however, are not based on gas-dynamics foundations.

The above models have been used extensively for the analysis of multi-vehicle systems. Using microscopic models, a multi-vehicle system has been treated as a countably infinite interconnection of nonlinear systems. Concepts of string stability [8, 20, 61, 62] have been extensively studied and even applied to design controllers for automatic vehicle-following systems. Similarly, macroscopic models generated using PDEs have also been studied for kinematic waves [31], shock waves [5] and traffic propagation stability [63, 64].

The use of inter-vehicle communication for enhancement of vehicle safety is being actively discussed in the literature. Publications in this regard include [6, 7, 9, 10, 80, 13]. The use of vehicle-to-vehicle networks in a "Cooperative Adaptive Cruise Control" scheme, which uses communicated information to improve on ordinary cruise control systems, is discussed in [6, 7]. In [80], the notion of safety of a string when the lead vehicle undergoes an emergency deceleration is formulated; and necessary and sufficient conditions for the safety of the string are determined, when the following vehicles are notified of this deceleration. In [13], safety of automated and manual highway systems with respect to resulting rear-end collision frequency and severity, is compared.

There has also been work done on mixed systems in the recent past [14, 15]. These papers study mixed systems comprising of semi-automated and manual vehicles, wherein the semi-automated vehicles are equipped with an ICC (Intelligent Cruise Control). These mixed systems are analyzed in the contexts of string stability (for the purposes of pollution emission) and shock waves. The mixed systems studied in these papers, however, do not assume inter-vehicle communication.

A considerable amount of work remains to be done, on the use of inter-vehicle communication for enhancement of vehicle safety, in a *mixed* sensing environment. Such an environment is comprised of a mixture of vehicles, some of which possess the capability of inter-vehicle communication, while others do not. Some of the key questions that need to be addressed involve determining the minimum percentage (or market penetration) of the equipped vehicles that are required to prevent pileup crashes and alleviate shock waves. We therefore believe that there is value in the analysis of mixed systems with partial inter-vehicle communication, involving information propagation as in Fig. 1-2(c). This thesis is a step in that direction, and addresses the specific issues of car pile-up crashes, shock waves and their alleviation.

1.3 Thesis Outline

In this thesis, we discuss a means to alleviate the possibility of car pile-up crashes. For this, we discuss a slowdown warning concept, whereby cars are equipped with a slowdown warning system. A car equipped with such a system has the ability to (i) Automatically transmit a slowdown warning signal whenever it decelerates abruptly, or its velocity becomes dangerously low for highway driving conditions, and (ii) Receive a slowdown warning signal, and alert the driver accordingly, if it deems the signal to be relevant. With such a system, information of a slowdown can be propagated at a much higher speed to all the cars (compared to when they are all unequipped) (as in Figure 1-2(b)). This allows sufficient time for the car drivers to react appropriately to avoid the crash. A schematic representation of our proposed slowdown warning system concept is shown in Figure 1-3.

The system comprises of a GPS receiver, a wireless transceiver, as well as a laptop computer. Using the GPS receiver, a car equipped with the warning system can determine its position and speed. The computer analyzes this information, and in the event of any abrupt deceleration or abnormally low speed, it transmits a warning signal to the other cars through a wireless transceiver. Each recipient car then determines whether the signal is indeed relevant to it and if so, it issues a warning signal to the driver, alerting him/her of the impending slowdown. On the other hand, if the computer deems the warning signal to be irrelevant to the car it resides in, then no warning is issued to the driver.

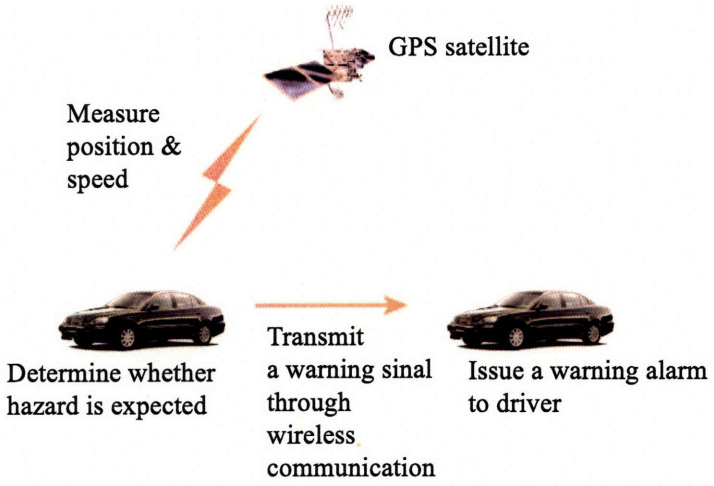

Figure 1-3: Schematic view

The role of the slowdown warning system in enhancing vehicular safety (in a scenario wherein only a partial subset of vehicles are equipped with the system) is studied along two distinct, parallel paths: (a) Using Microscopic models (b) Using Macroscopic models. In the first part, we use microscopic models to model each driver-vehicle system. The individual vehicles (and their interconnections) are modeled by ordinary differential equations (ODEs) and the problem is formulated as a single-lane problem. The notion of safety is defined as one of collision avoidance. In other words, we examine the role of the slowdown warning system in alleviating the collisions that can occur when a car executes an abrupt deceleration. The question that we seek

to address is the determination of the required number of equipped vehicles (in a mixed vehicle stream) that can guarantee zero collisions. We define multiple modes of behavior of the driver (Figure 1-4). In particular, we define two modes of driver behaviour: one before the alerting signal is broadcast, and one after the driver receives the alerting signal. We define each of these states as a discrete state in the hybrid control system - associated with each of these states is a different human driver model. In the recent past, collision detection and resolution schemes for aircraft in Free Flight have been studied in this framework [22, 23].

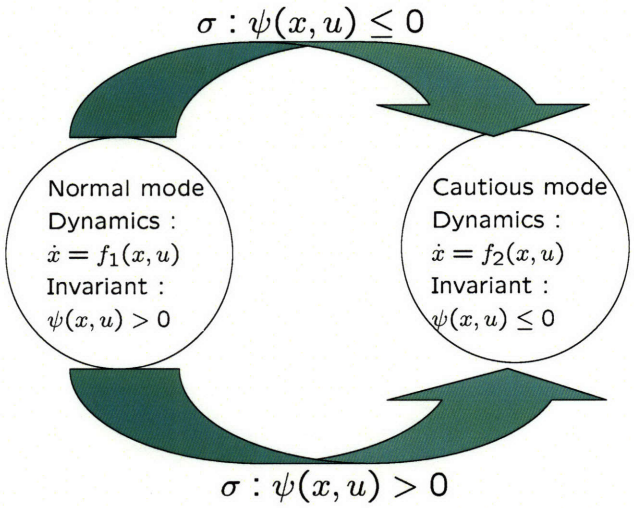

Figure 1-4: Vehicle driving modes

In the macroscopic modeling approach, on the other hand, we examine the average behavior of groups of vehicles. In this approach, the multi-vehicle system is modeled by partial differential equations (PDEs) and the problem is formulated as a multi-lane problem with the objective of alleviating large negative velocity gradients occurring on the highway. When a car executes an abrupt decleration, it initiates a compression wave that passes through the line of cars behind it. This compression wave then can (under some conditions) become stronger and stronger and eventually develop into a shock wave. As this shock wave passes through the line of cars, successive cars have to slam on their brakes and this increases the possibility of collisions. The presence of a few equipped vehicles, however, can help in smoothening the traffic flow, and

reducing the intensity of the shocks/large negative velocity gradients in the traffic. In this part of the work, we examine the role of the slowdown warning system in alleviating shocks/large negative velocity gradient waves in the traffic. Some of the questions that we seek to address include the determination of the required number of equipped vehicles (in a mixed vehicle stream) that will sufficiently weaken the negative velocity gradients.

This thesis is organized as follows. Chapter II discusses the microscopic modeling approach, wherein the safety problem is formulated as a collision avoidance problem, and the role of the slowdown warning system is to alleviate collisions. The problem formulation in the microscopic modeling approach assumes a single lane. We see how the phenomenon of string instability (viz., amplification of intervehicle spacing errors along a line of cars subsequent to an abrupt deceleration by the lead car) can lead to pileup crashes. We then see how equipping all the vehicles with a slowdown warning system can lead to a situation of string stability. We then demonstrate how equipping a few cars with a slowdown warning system leads to a situation of mixed string stability, which can still have a beneficial effect on the overall safety of the interconnected system of vehicles. We demonstrate this through both simulations and a theoretical analysis.

Chapter III then discusses the macroscopic modeling approach, wherein the safety problem is formulated as a shock alleviation problem, and the role of the slowdown warning system is to minimize/eliminate the strength of shocks/large negative velocity gradient waves on the highway. The problem is formulated as a multi-lane problem in this approach.

A prototype of the slowdown warning system was built, and we conducted actual road tests to test the efficacy of the system. These are discussed in Chapter IV, which discusses the system architecture and some of the communication and algorithmic issues involved. We also discuss details of related road tests that were performed after equipping a few cars with such a system. Finally, Chapter V presents the conclusions.

A brief summary of the main contributions of this thesis are as follows :

- In the microscopic modeling approach (discussed in Chapter II), this thesis studies the phenomenon of mixed string stability in the context of collision avoidance; and identifies certain sufficient conditions on the number and distribution of equipped vehicles, that will guarantee zero collisions in a mixed vehicle string.

- In the macroscopic modeling approach (discussed in Chapter III), this thesis arrives at a model for advance information propagation through a mixed vehicle scenario; studies the phenomenon of shocks in such a scenario; and parametrizes the shocks/negative velocity gradient waves for prototype initial conditions, as a function of the extent of equipment and signal transmission range in a mixed vehicle string.

- In the experimental section (discussed in Chapter IV), this thesis presents a safe method to test the slowdown warning concept for a specific class of pileup crash scenarios; and the results obtained using this method. These demonstrate driver behavior in cars unequipped and equipped with a slowdown warning system.

Chapter 2

Microscopic Modeling Approach

In this chapter, each individual driver-vehicle unit and its interactions with its neighbors is modeled using ordinary differential equations. A single-lane model is assumed. It is demonstrated how a scenario of all vehicles unequipped could lead to a situation of string instability; while equipping all vehicles with the slowdown warning system could lead to a situation of string stability. It is then demonstrated how a scenario of having some vehicles equipped could lead to a situation of mixed string stability. Sufficient conditions on the number and distribution of equipped vehicles (within a mixed vehicle string) are obtained, under which it is guaranteed that zero collisions occur. A lower bound on the probability of obtaining zero collisions is presented.

2.1 Introduction

In this chapter, we use microscopic models to demonstrate the benefits that accrue from a slowdown warning system. We formulate the problem as a collision avoidance problem; in other words, we see how the presence of a slowdown warning system can help alleviate collisions, that otherwise would have occurred. We first give a brief description of a finite state model of a human driver with/without a slowdown warning system, and then present simulation results that demonstrate the beneficial aspects of a slowdown warning system even in situations of partial equipment. These simulations demonstrate the possible occurrence of string instability under some initial conditions,

that can lead to pile-up crashes. It is then seen how equipping all the vehicles with a slowdown warning system can lead to a situation of string stability. We then see how a situation wherein there is a partial equipment of vehicles with the slowdown warning system, can lead to a scenario of mixed string stability (which means that some parts of the vehicular string are string stable, while other parts are not string stable) whereby as long as the equipped vehicles are present in a sufficient number, and their distributions lie in a defined set of possible distributions, then collisions will not occur even in the unequipped vehicles. We then perform a theoretical analysis that demonstrates certain sufficient conditions under which it is guaranteed that collisions cannot occur.

2.2 Finite state model of a driver

To account for the change in driver behavior in response to brake lights and/or advance slowdown warnings, we assumed the driver to be a finite-state system (ref Figure 1), whereby he could be in one of three different modes. Modeling the driver as a finite state system has been done before, for eg., [18]. Before we go into a discussion of the modes, we briefly introduce some nomenclature.

There are N vehicles in a platoon, numbered $1, 2, ..., N$, with car 1 being the lead car, and i denoting the ith vehicle. Some of the cars are equipped with the slowdown warning system, while the others are not. Define :

- E : The set of vehicles that are equipped with the slowdown warning system.

- U : The set of vehicles that are not equipped with the slowdown warning system.

- $sl\_rec(i)$ = A flag indicating whether a vehicle $i \epsilon E$ (i.e. an equipped car) is currently receiving a slowdown warning. A value of 1 indicates that a warning

is being received, while 0 indicates otherwise.

- $b\_l(i)$ = A flag indicating whether a vehicle i (which may be equipped or unequipped) currently has its brake lights on. A value of 1 indicates that its brake lights are on, while 0 indicates otherwise.
  The velocities of the cars are denoted by $V_1, V_2, ..., V_N$ while the inter car separations are denoted by $s_{1,2}, s_{2,3}, ..., s_{N-1,N}$.

At time $t = 0$, it is assumed that all the n cars are travelling at equal velocities, and the inter car separations are all equal. The lead car then suddenly decelerates, and emits a slow-down warning signal that is received by all the equipped cars behind it. The instant the equipped cars receive this signal, the drivers of these cars go into an alert mode and smoothly increase the distance between themselves and the car immediately in front of them. The unequipped cars, on the other hand, receive no such signal - only when the brake-lights of the car immediately in front of them come on, do these drivers go into an alert mode. However, they do not have the time to increase the distance between themselves and the car in front. We assume that the distance a car maintains to his/her immediate predecessor is equal to the product of the velocity of the following car and a quantity referred to as the time headway.

Thus, at any given time, the driver of the ith (following) car can be in one of three modes, viz. q_1, q_2 or q_3, and he/she transitions from one mode to another, depending on the flags $sl\_rec(i)$ and $b\_l(i-1)$. The descriptions of the modes are as follows :

1. Mode q_1: This is the initial mode in which all the drivers reside, when both the flags $sl\_rec(i)$ and $b\_l(i-1)$ are zero. This mode is characterized by 'normal' driver dynamics, manifested by 'normal' time delays. We denote the driver dynamics in this mode by $\dot{x} = f_1(x, u)$. A driver can reside in mode q_1 for long periods of time. In this mode, he/she tries to maintain a 'normal' distance between his car and the one immediately ahead of him/her (this distance is characterized by shorter time headways).

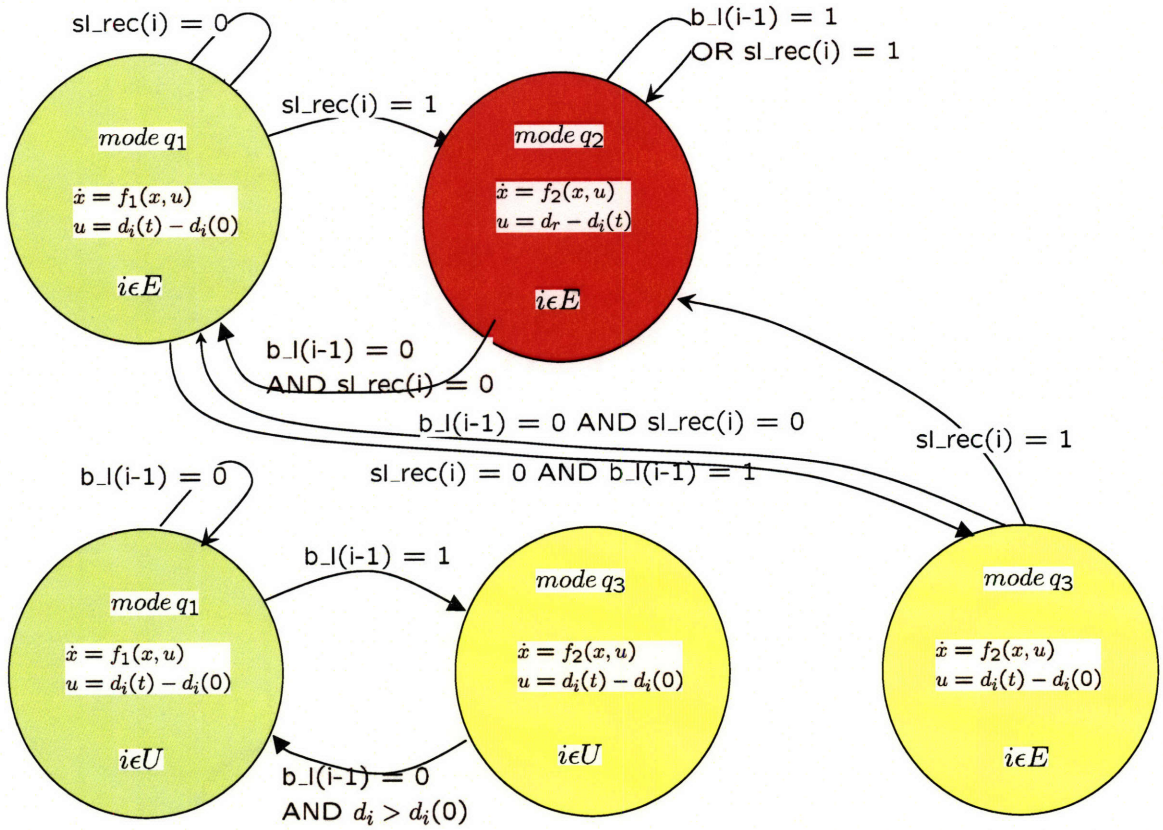

Figure 2-1: Finite state model of a car driver

2. Mode q_2: Only the drivers of the equipped cars can be in this mode. These drivers transition from mode q_1 to q_2 if and only if they receive a slowdown warning signal. This mode is characterized by (a) Faster driver dynamics, manifested by shorter time delays compared to q_1 (it is denoted by the equation $\dot{x} = f_2(x,u)$) and (b) A higher value of reference distance/time headway $d_{ref}(i)$, compared to q_1. Mode q_2 is a high alert mode, in which a driver resides for only a short duration, before reverting back to q_1.

3. Mode q_3: The drivers of both the equipped as well as the unequipped cars can reside in this mode. The drivers of the unequipped cars transition from q_1 to q_3

if and only if the brake-lights of the car ahead of them come on, while the drivers of the equipped cars transition from q_1 to q_3 if and only if the brake-lights of the car ahead of them come on, and additionally, they are not in receipt of a slowdown warning. This mode is characterized by the faster driver dynamics, represented by $\dot{x} = f_2(x, u)$ and the 'normal' reference distance (with a shorter time headway). A driver resides in mode q_3 only for a short duration of time.

Each of these modes, and the transitions thereof, are schematically represented in Figure 1, for equipped and unequipped cars. Note that this figure holds for all following cars.

2.3 Numerical Simulations

Before we theoretically analyze the effect of slowdown warning systems on the safety of traffic flow, we demonstrate the results of numerical simulations as an introduction of our proposed concept. Consider a string of cars driving on a single-lane highway. We assume that at $t = 0$, they are all driving with equal speeds and equal inter-car distances. The string of cars is modeled as an inter-connected system, with each car-driver system forming one element of the inter-connected system. The acceleration response of the driver of the ith car is modeled by the following equation, presented in [17], [18]:

$$\begin{aligned} \frac{dv_i(t)}{dt} &= K_1 \cdot (s_{i-1,i}(t-\tau) - Tv_i(t-\tau)) + \\ &\quad K_2 \cdot (v_{i-1}(t-\tau) - v_i(t-\tau)), \\ \frac{ds_{i-1,i}(t)}{dt} &= v_{i-1}(t) - v_i(t) \end{aligned} \tag{2.1}$$

where v_i indicates the velocity of the ith car and $s_{i-1,i}$ represents the inter-car distance between the ith and the $(i-1)$th cars, with car 1 being the lead car. τ indicates the response delay of each car-driver system. K_2 represents the sensitivity of each driver to the velocity difference between his/her car and the one immediately ahead

while K_1 is the sensitivity to the difference between the desired inter-car distance and the true inter-car distance. The desired inter-car distance of each driver (to the car ahead) is proportional to his/her own velocity, with the proportionality constant being T (the time headway). We work with a simplified model in which we assume all the drivers to possess identical dynamics.

Consider the following scenario, in which all the cars are initially travelling at typical highway speeds of about 30 meters/sec, (i.e. 67.5 mph), with the inter-car distance being 36 meters (i.e. $T = 1.2sec$). We assume τ to be a ball-park value of 0.6 seconds, and then determine K_1 and K_2 such that it ensures stable, non-oscillatory behavior for each two-car system. (These were obtained using guidelines available, for example, in [21]). At $t = 5sec$, the lead car begins to execute an abrupt deceleration, and decelerates continuously for 5 seconds. We now present simulations showing the effect of the lead car's deceleration (on the cars behind), when information of this deceleration is transmitted in each of the modes demonstrated in Figure 1-2 of Chapter 1.

Refer to Figure 2-2, which shows the velocity and inter-car distance profiles of 10 cars, when the information of the lead car's deceleration is transmitted from car to car, as in Figure 1(a). It can be seen that the values of the minimum car velocity and minimum inter-car distance keep decreasing with increasing car index, until car 6 is rear-ended by car 7, and crashes occur for all the cars behind. It can be seen from the figure that if there were more cars behind car 10, they too would all collide, thus leading to a pile-up. This is the phenomenon of string instability [20], [14].

String instability refers to the amplification of velocity errors as these errors travel along a string of vehicles. If we define $\epsilon_1(t) = V_1(t) - V_2(t)$, $\epsilon_2(t) = V_2(t) - V_3(t), ..., \epsilon_{N-1}(t) = V_{N-1}(t) - V_N(t)$, then a string of vehicles is said to be l_p stable if :

$||\epsilon_1(t)||_p \leq ||\epsilon_2(t)||_p \leq ..... \leq ||\epsilon_N(t)||_p$,

where p indicates the pth norm. In the context of pile-up crashes, we are interested in the amplification (or otherwise) of the ∞ norm of the velocity errors, i.e. we are interested in l_∞ string stability.

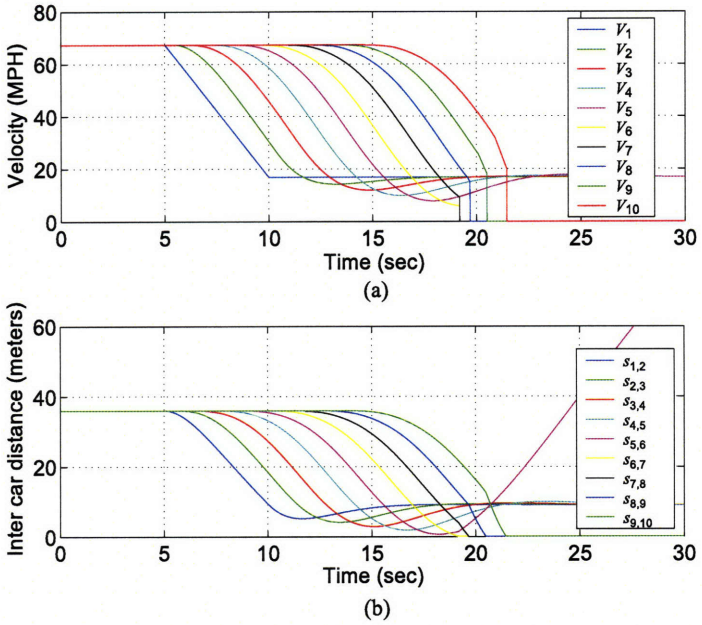

Figure 2-2: All cars unequipped

The occurrence of such a pile-up can be attributed to the following reason : with all cars maintaining initially shorter time headways, information of the deceleration of the lead car is transmitted from car to car in a staggered fashion, viz., by the brake-lights of the successive cars coming on one after the other, and this rate of information travel is too slow to give the driver sufficient time to react to avoid the imminent collision. It can also be inferred that the higher the value of τ, the smaller is the car index from which pile-up crashes begin to originate. In general, the shorter the time headway maintained by a vehicle (to the one ahead of it), the more likely the onset of string instability; at higher time headways, string instability does not manifest.

Now, consider a scenario when all the 10 cars are equipped with the slowdown warning system, and the lead car executes an identical deceleration profile. In this case, all the cars get informed of the slowdown ahead, near simultaneously, from the instant the lead car begins to decelerate (i.e. information of the lead car's deceleration is propagated as in Figure 1-2(b) of Chapter 1). They are therefore able to react much earlier (car 10, for example, is able to react τ seconds after the lead car begins to

decelerate, as opposed to 9τ seconds that it would otherwise have taken, if all cars were unequipped). We make the reasonable assumption that on receipt of the slowdown warning signal, the driver of each equipped car transitions to a slightly lower value of τ than when he was unequipped (in these simulations, we assume $\tau = 0.4$ sec for an equipped car - this signifies the increased alertness of the driver on receipt of the warning signal). Furthermore, the driver of each equipped car attempts to increase his/her time headway to the car in front of him/her, in anticipation of the imminent slowdown. The result is shown in Figure 2-3, where, on receipt of the warning signal, each driver tries to increase the time headway to the car immediately ahead (from the original $T = 1.2sec$ to $T = 1.65sec$). The trend of decreasing values of the minimum car velocity and minimum inter-car distance (with increasing car index) is no longer seen. This would be true even for any arbitrary number of cars behind car 10, if they too were equipped.

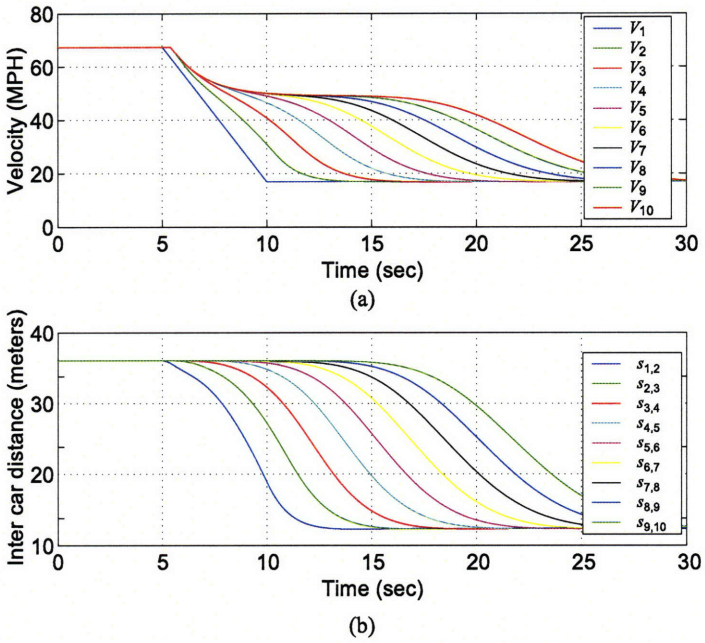

Figure 2-3: All cars equipped

As mentioned earlier, it is unreasonable to assume that in a real-life scenario, all the cars would indeed be equipped with a slowdown warning system. It is pertinent, therefore, to examine the influence of the system when only a fraction of the cars are

equipped. In other words, only some cars possess long distance sensing capabilities, while other cars possess only local (i.e. near neighbor) sensing capabilities. It turns out however, that in many cases, even if a fraction of the cars are equipped, this can still be sufficient to break the trend of decreasing intervehicle spacings as it propagates down the line of cars, and this can prevent pile-up crashes. This is illustrated in Figure 2-4, where only cars 7 and 9 are equipped. It is seen that after the lead car decelerates, there is an onset of decreasing intervehicle spacings in cars 2 to 6. However, the fact that car 7 is equipped breaks this trend, and in fact, the minimum value of V_7 (as also x_6) is higher than V_6 (respectively, x_5). Furthermore, since car 8 is unequipped, it re-initiates the trend of decreasing intervehicle spacings and therefore the minimum value of V_8 (as also x_7) is indeed lower than that of V_7 (respectively, x_6); yet it is higher than that in the case when car 7 was unequipped (see Figure 2-2). Similarly, since car 9 is equipped, not only is the minimum value of x_8 high enough, but also that of x_9 is higher than what it was when car 9 was unequipped. Consequently, no crashes occur. This shows that it is possible that even if a fraction of the cars are equipped, they are able to ensure the safety of not only themselves, but the unequipped cars as well.

2.4 Pileup crash: Mathematical definition and conditions for Safety

We use the following notation : F and f represent the same signal (or system) in the frequency and time domain, respectively, i.e., $F(s) = L(f) = \int_0^\infty f(t)e^{-st}dt$. The symbol s represents the Laplace variable. $\|f\|_\infty$ denotes $\sup_{t>0}|f|$, while $\|F\|_\infty$ denotes $\sup_{\omega>0}|F(j\omega)|$. Both$\|f\|_1$ and $\|F\|_1$ denote $\int_0^\infty |f(t)|\,dt$.

Consider a string of N vehicles driving on a single-lane with the dynamics of each vehicle defined by

$$V_i(s) = G_i(s)V_{i-1}(s) \ , \tag{2.2}$$

for all $i \in N$, where V_i represents the longitudinal velocity of the ith vehicle. $G_i(s)$ is

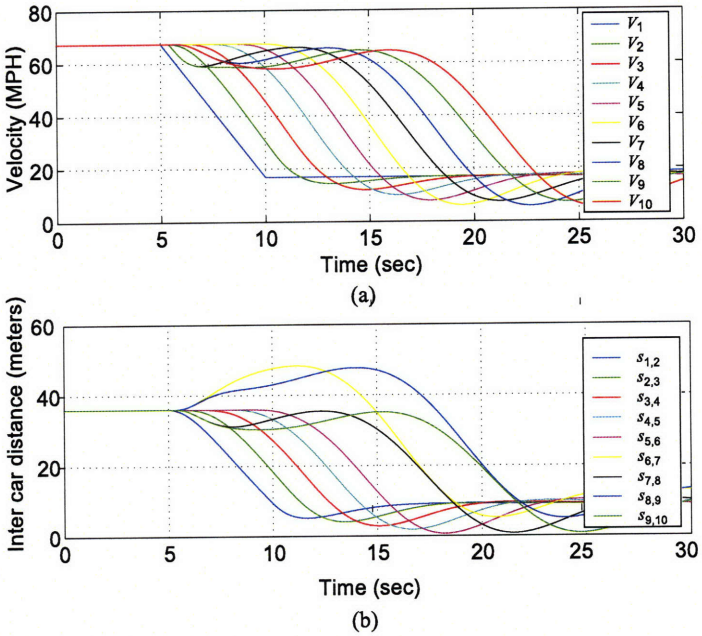

Figure 2-4: Only cars 7 and 9 equipped

Figure 2-5: Interconnected system of vehicles

the transfer function connecting the velocity response of the ith vehicle to that of the $(i-1)$th vehicle (See Figure 2-5). While the simulation results of Section II (that use Equation 2.1) assume a $G_i(s)$ of the form $G_i(s) = \dfrac{K_1 + sK_2}{s^2e^{s\tau} + s(K_1T + K_2) + K_1}$, the statements made in this section are true for arbitrary $G_i(s)$. We assume that all the vehicles in this interconnected system are driving with equal initial speeds and equal initial intervehicle spacings. The lead vehicle then executes an abrupt deceleration (possibly in response to some hazard ahead of it) and this induces a chain reaction that leads to a pileup crash in the system. Our objective in this section is to determine the conditions under which the pileup crash occurs/can be avoided.

Definition 1 A *pile-up crash* is said to occur in the interconnected system of vehicles, if there exists a time t and an index n such that

$$x_i(t) - x_{i+1}(t) < 0 \text{ for } n \leq i \leq N \ , \tag{2.3}$$

where x_i is the position of the ith vehicle (x_1 is the position of the lead vehicle) and x_i are measured in a direction such that $x_i(0) > x_{i+1}(0) \forall i$. The condition in Equation 2.3 is equivalent to

$$\|\Delta\left(x_i - x_{i+1}\right)\|_\infty > x_i(0) - x_{i+1}(0) \text{ for } n \leq i \leq N \ , \tag{2.4}$$

where $\Delta\left(x_i(t) - x_{i+1}(t)\right) = \left(x_i(t) - x_{i+1}(t)\right) - \left(x_i(0) - x_{i+1}(0)\right)$ represents the fluctuation in the intervehicle spacing between the ith and $(i+1)$th vehicles and $x_i(0) - x_{i+1}(0)$ represents the corresponding initial intervehicle spacing. The above condition implies that a crash between two adjacent vehicles occurs when the maximum fluctuation of the spacing between them exceeds its initial value. On the other hand, there will be no pileup crash in the interconnected system of vehicles, if

$$\|\Delta\left(x_i - x_{i+1}\right)\|_\infty \leq x_i(0) - x_{i+1}(0) \text{ for all } i. \tag{2.5}$$

Lemma 1 For an interconnected system of vehicles in Equation 2.2, the fluctuation

of the intervehicle spacing $\Delta(x_i - x_{i+1})$ can be written as

$$\frac{\Delta(X_i - X_{i+1})}{\Delta(X_{i-1} - X_i)} = \left[\frac{1 - G_{i+1}}{1 - G_i} G_i\right] = \widehat{G}_i \ . \tag{2.6}$$

Also, $\Delta(x_i - x_{i+1})$ can be written in terms of the velocity of the lead vehicle V_1 as

$$\Delta(x_i - x_{i+1}) = L^{-1}\left\{\left[\prod_{k=2}^{i} G_k\right] \frac{(1 - G_{i+1})}{s} V_1\right\} \tag{2.7}$$

Proof : Equations 2.6 and 2.7 can be easily derived using

$$\begin{aligned} \Delta x_1 &= x_1(t) - x_1(0) = L^{-1}\left\{\frac{1}{s} V_1\right\}, \text{ and} \\ \Delta X_i &= G_i \Delta X_{i-1} = G_i G_{i-1} \Delta X_{i-2} = \\ &= \cdots = \left[\prod_{k=2}^{i} G_k\right] \Delta X_1 \ . \end{aligned} \tag{2.8}$$

The condition for a pileup crash can be described in terms of $\widehat{G}_i$, as shown in the following theorem.

Theorem 1 Consider an interconnected system of N vehicles governed by Equation 2.2, with all vehicles driving with equal initial speeds and equal initial intervehicle spacing s_0. Then, if the lead vehicle executes an abrupt deceleration, it is guaranteed that there will be no pileup crash if

1. $\|\widehat{g}_i(t)\|_1 \leq 1$ for all i, and
2. $\|\Delta(x_1 - x_2)\|_\infty \leq s_0$

Here, $\widehat{g}_i$ represents the impulse response of the transfer function $\widehat{G}_i$.

Proof : Since $\Delta(X_i - X_{i+1}) = \widehat{G}_i \Delta(X_{i-1} - X_i)$ from Equation 2.6, we have

$$\|\Delta(x_i - x_{i+1})\|_\infty \leq \|\widehat{g}_i\|_1 \|\Delta(x_{i-1} - x_i)\|_\infty \ . \tag{2.9}$$

Therefore, if $\|\widehat{g}_i\|_1 \leq 1$ for all i, we see that $\|\Delta(x_i - x_{i+1})\|_\infty \leq \|\Delta(x_{i-1} - x_i)\|_\infty$ for all i, which implies that the maximum fluctuation of intervehicle spacing decreases

with increasing car index. Under this condition, it is evident that if $\|\Delta(x_1 - x_2)\|_\infty \leq s_0$, then $\|\Delta(x_i - x_{i+1})\|_\infty \leq s_0$ for all i. This satisfies the condition for no pileup crash occurrence by Equation 2.5. Therefore, if $\|g_i(t)\|_1 \leq 1$ for all i, and $\|\Delta(x_1 - x_2)\|_\infty \leq s_0$, it is guaranteed that there will be no pileup crash in the system.

The condition in Theorem 1 is equivalent to the condition for l_∞ string stability of the interconnected system [20], [14].

We should note that the condition $\|\widehat{g}_i\|_1 > 1$ for some i does not necessarily imply that there will be a pileup crash in the interconnected system, because $\|\Delta(x_i - x_{i+1})\|_\infty$ can be smaller than $\|\Delta(x_{i-1} - x_i)\|_\infty$, even when $\|\widehat{g}_i\|_1 > 1$. At the same time however, if $\|\widehat{g}_i\|_1 > 1$, then in the absence of further knowledge of the deceleration profile of the lead vehicle, one cannot *guarantee* the absence of a pile-up crash. (This statement is particularly true for large deceleration magnitudes of the lead vehicle). Note however that the system satisfying the condition in Theorem 1 will never have a pileup crash in any event.

2.5 Influence of a slowdown warning system

In this section, we investigate the role of the slowdown warning system in mitigating the generation of a pileup crash in a mixed sensing environment. In order to describe the effect of the slowdown warning system, we propose to model the dynamic behavior of a vehicle using a finite number of operating modes. We assume that all drivers are initially driving in a 'normal mode', and on receipt of a slowdown warning signal, the drivers of all the equipped cars transform to a 'cautious mode'. In this context, we therefore assume that, on receipt of a slowdown warning signal, $G_i(s)$ can be either $U(s)$ or $E(s)$, i.e.,

$$V_i = \begin{cases} U(s)V_{i-1}, \text{ if } i\text{th vehicle is unequipped} \\ E(s)V_{i-1}, \text{ if } i\text{th vehicle is equipped} \end{cases}, \tag{2.10}$$

In general, $U(s)$ is characterized by high values of τ accompanied by small values of T; while $E(s)$ is characterized by low values of τ accompanied by high values of T.

In other words, a driver in an equipped vehicle, on receipt of the slowdown warning signal, becomes more alert and increases his/her time headway to the car in front of him/her. The differences between $U(s)$ and $E(s)$ (for the driver dynamics presented in Equation 2.1) are clearly seen in Figure 2-6. In this figure, the frequency response of the vehicle dynamics is plotted for different values of T and τ. It can be seen that for a given value of T, as τ increases, it has the effect of increasing the magnitude of the frequency response. At the same time, for a given τ, as T increases, this has the effect of decreasing the frequency response magnitude.

Using the above guidelines, we assume that $U(s)$ and $E(s)$ have the following characteristics.

$$\begin{aligned} &1.\ \|U(s)\|_\infty > 1 \text{ and } |U(0)| = 1 \\ &2.\ \|E(s)\|_\infty = |E(0)| = 1, \text{ and } e(t) > 0\ \forall t > 0\ , \end{aligned} \tag{2.11}$$

where $e(t)$ is the impulse response of $E(s)$.

We believe that the models for $U(s)$ and $E(s)$ correctly reflect the behaviors of drivers of unequipped vs. equipped cars. In particular, the presence of resonant peaks generated by long reaction delays (when they are accompanied by short time headways) is such that, for long car streams, avoidance of pile-up crashes cannot be guaranteed. This can be seen as follows. If all the vehicles are unequipped, i.e. $G_i(s) = U(s)\ \forall i$, then $\widehat{G}_i(s) = U(s)\ \forall i$ by Equation 2.6, and therefore, $\|\widehat{g}_i\|_1 = \|u(t)\|_1 > 1\ \forall i$. By the analysis in Section III, we have seen that this condition on $\|\widehat{g}_i\|_1$ is indicative of the possibility of occurrence of a pileup crash.

On the other hand, the assumption on $E(s)$ in Equation 2.11 is imposed to guarantee that there is no pileup crash in the interconnected system when all vehicles are equipped with the slowdown warning system. That is, when all the vehicles are equipped, we have $\|\widehat{g}_i\|_1 = \|e(t)\|_1 = 1\ \forall i$ ($\because \widehat{G}_i(s) = E(s)\ \forall i$), and therefore, $\|\Delta(x_i - x_{i+1})\|_\infty \leq s_0$ for all i, which satisfies the condition for no pileup crash occurrence.

Figure 2-7(a) shows an example of a velocity profile, wherein a car decelerates

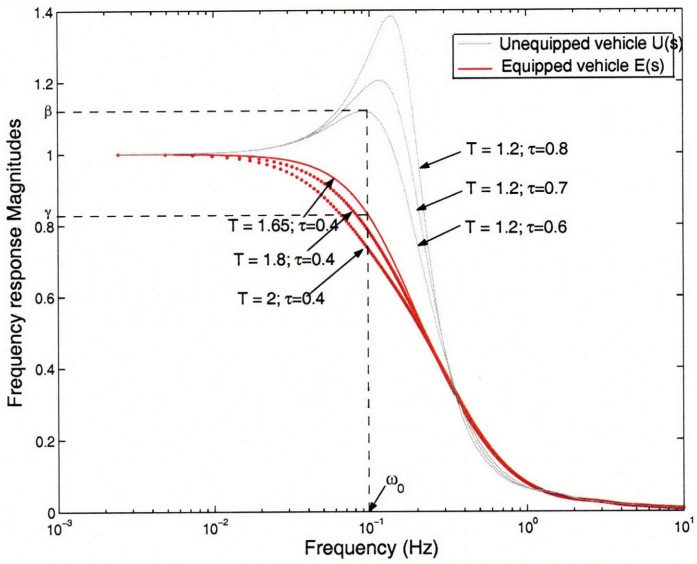

Figure 2-6: Frequency responses of $U(s)$ and $E(s)$

sharply from an initial velocity of 30 meteres/sec and comes to a complete stop over a time span of a little more than one second. The corresponding Fourier Transform of this signal is shown in Figure 2-7(b), from which it can be seen that there is substantial magnitude content of the signal at the frequency ω_0 shown in Figure 2-6.

Figure 2-8 shows the impulse responses of $U(s)$ and $E(s)$ for different values of T and τ. Smaller values of T, accompanied by larger values of τ (that characterise $U(s)$) lead to oscillatory impulse responses (with the amplitude of oscillation decreasing with decreasing τ). On the other hand, larger values of T, accompanied by smaller values of τ (that characterise $E(s)$) lead to non-oscillatory responses.

Figures 2-6 and 2-8 indicate that in the case of an equipped vehicle, the larger the increase in the time headway T that a driver attains (subsequent to the receipt of a slowdown warning signal), the greater the attenuation that that equipped vehicle exerts on the errors propagating through the mixed string of vehicles. This fact is also brought out in the following ten car simulation, in which cars $7, 8, 9$ and 10 are equipped. In this simulation, three different scenarios of headway increase are considered, viz. $T = 1.65, 1.8, 2$ seconds. It can be clearly seen that the larger the headway increase, the higher the higher are the minimum values of velocity and

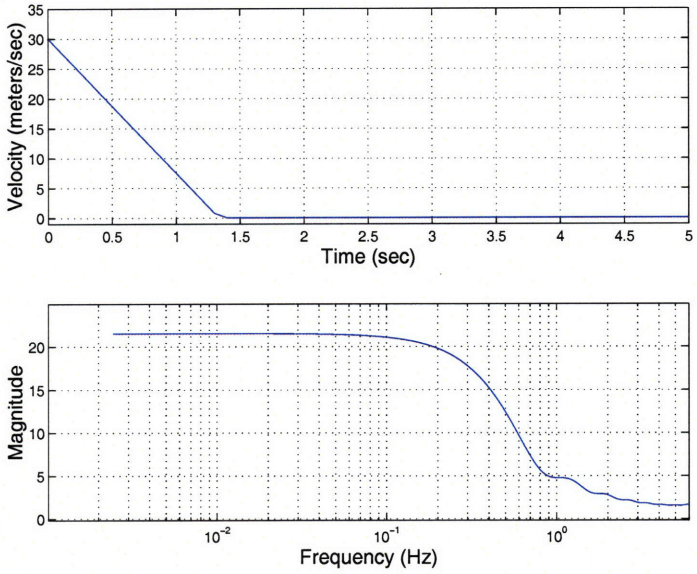

Figure 2-7: An example velocity profile and its corresponding frequency content

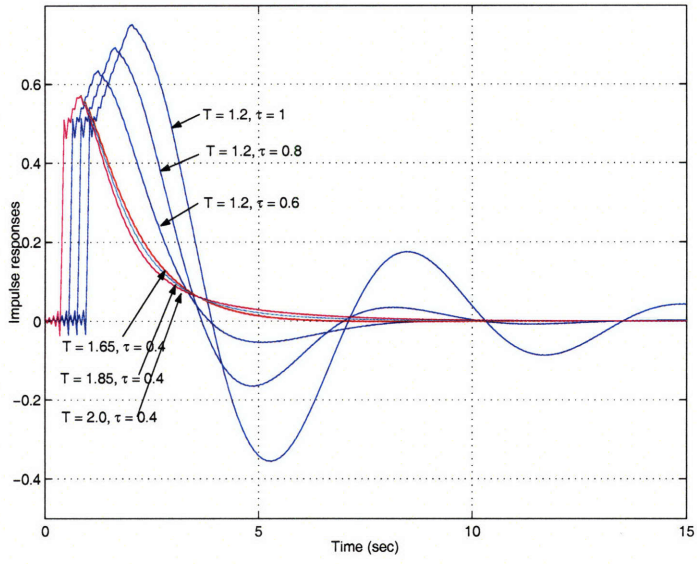

Figure 2-8: Impulse responses of $U(s)$ and $E(s)$

inter-car distance (to the car ahead) of the equipped cars.

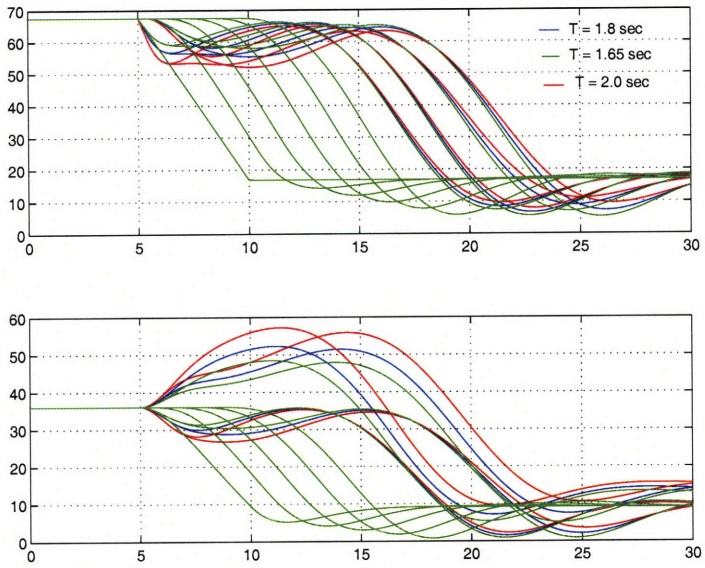

Figure 2-9: Effect of varying headway increases of an equipped vehicle on receipt of the slowdown warning signal

We now consider a mixed sensing environment in which only a small number of vehicles are equipped with the slowdown warning system. The following theorem provides a sufficient condition that guarantees that a pileup crash does not occur in the system of vehicles.

Theorem 2 Consider an interconnected system of N vehicles governed by Equation 2.2, with all vehicles driving at equal initial speeds with equal intervehicle spacing s_0, and L out of N vehicles are equipped with the slowdown warning system. Assume that the lead vehicle executes an abrupt deceleration, such that when all vehicles are unequipped, a pileup crash is initiated at the nth vehicle (i.e., $\|\Delta(x_i - x_{i+1})\|_\infty > s_0$ for $n \leq i \leq N-1$). Then, under the same deceleration profile of the lead vehicle, there will be no pileup crash if

$$L \geq M \,, \tag{2.12}$$

where $M = N - n + 1$ is the number of vehicles that would have crashed if all vehicles were unequipped.

Proof : First, we consider the nth and $(n-1)$th vehicle (note that under the

assumptions made in this Theorem, there is no collision between these two vehicles). When all vehicles are unequipped, Equation 2.7 gives

$$\Delta\left(x_{n-1}-x_n\right)=L^{-1}\left\{U^{n-2}\frac{(1-U)}{s}V_1\right\}\ , \tag{2.13}$$

and therefore,

$$\left\|\Delta\left(x_{n-1}-x_n\right)\right\|_\infty \leq \alpha\left\|u(t)\right\|_1^{n-2}\ , \tag{2.14}$$

where

$$\alpha=\left\|\int_0^t\left(v_1(t)-u(t)*v_1(t)\right)dt\right\|_\infty\ . \tag{2.15}$$

Here, '$*$' is a convolution integration in the time domain, i.e. $(u*v_1)(t)=\int_0^t u(t-\tau)v_1(\tau)d\tau$. Now, if we have

$$\alpha\left\|u(t)\right\|_1^{n-2}\leq s_0 \tag{2.16}$$

then from Equations 2.14 and 2.16, we see that

$$\left\|\Delta\left(x_{n-1}-x_n\right)\right\|_\infty \leq \alpha\left\|u(t)\right\|_1^{n-2}\leq s_0 \tag{2.17}$$

is true. This will ensure that

$$\left\|\Delta\left(x_{n-1}-x_n\right)\right\|_\infty \leq s_0 \tag{2.18}$$

is true. Equation 2.16 thus guarantees that there will be no collision between the $n-1$th and nth vehicles for *any* deceleration profile of the lead vehicle (Note that this is only a sufficient condition for there to be no collision between the $n-1$th and nth vehicles. Due to this assumption, the results presented in this Theorem are conservative).

Next, we show by induction that

$$\left\|\Delta\left(x_{n+k-1}-x_{n+k}\right)\right\|_\infty \leq \alpha\left\|u(t)\right\|_1^{n-2}, \tag{2.19}$$

is true for $k=1,2,...,N-n+1$, if there are at least k equipped vehicles among

them, which will prove that there will be no pileup crash among the vehicles for $1 \leq i \leq (n+k-1)$. It is obvious that if $L \geq M$, there are at least k equipped vehicles for $1 \leq i \leq (n+k-1)$.

1. For $k = 1$ (i.e., there is one equipped vehicle among $1 \leq i \leq n$).
   In this case, we only need to show that $\|\Delta(x_n - x_{n+1})\|_\infty \leq s_0$ because we have assumed that the deceleration of the leading vehicle does not cause any crash among the vehicles for $1 \leq i \leq n-1$. Since

$$\begin{aligned} \Delta(x_n - x_{n+1}) &= L^{-1}\left\{\left[\prod_{i=2}^{n} G_i\right]\frac{(1-G_{n+1})}{s}V_1\right\} \\ &= L^{-1}\left\{U^{n-2}E\frac{(1-U)}{s}V_1\right\}, \end{aligned} \tag{2.20}$$

   we have,

$$\begin{aligned} \|\Delta(x_n - x_{n+1})\|_\infty &\leq \alpha \|u(t)\|_1^{n-2} \|e(t)\|_1 \\ &= \alpha \|u(t)\|_1^{n-2} \\ &\quad (\because \|e(t)\|_1 = 1) \\ &\leq s_0 \ \text{(from Equation 2.16)}. \end{aligned} \tag{2.21}$$

   Therefore, there would be no pileup crash among the vehicles for $1 \leq i \leq n$, if there is one equipped vehicle among them.

2. For $k = m$ (i.e., there are m equipped vehicles among $1 \leq i \leq n+m-1$).
   Now, we assume that the theorem is true for $k = m$, i.e., that there will be no pileup crash among the vehicles for $1 \leq i \leq (n+m-1)$, if there are m equipped vehicles among them. In other words, we assume

$$\|\Delta(x_i - x_{i+1})\|_\infty \leq s_0 \text{ for all } 1 \leq i \leq n+m-1\ . \tag{2.22}$$

   Under this condition, we will show that the theorem is true for $k = m+1$, i.e., there will be no pileup crash among the vehicles for $1 \leq i \leq (n+m)$, if there

are $m+1$ equipped vehicles among them. Here, we only need to show that $\|\Delta(x_{n+m} - x_{n+m+1})\|_\infty \leq s_0$ because the condition in Equation 2.22 has been assumed to be true. Since

$$\begin{aligned} &\Delta(x_{n+m} - x_{n+m+1}) \\ &= L^{-1}\left\{\left[\prod_{i=2}^{n+m} G_i\right]\frac{(1-G_{n+m+1})}{s}V_1\right\} \\ &= L^{-1}\left\{U^{n-2}E^{m+1}\frac{(1-U)}{s}V_1\right\}, \end{aligned} \tag{2.23}$$

we have

$$\begin{aligned} \|\Delta(x_{n+m} - x_{n+m+1})\|_\infty &\leq \alpha \|u(t)\|_1^{n-2} \|e(t)\|_1^{m+1} \\ &= \alpha \|u(t)\|_1^{n-2} \\ &\leq s_0 \text{ (from Equation 2.16).} \end{aligned} \tag{2.24}$$

Therefore, there would be no pileup crash among the vehicles for $1 \leq i \leq n+m$, if there are $m+1$ equipped vehicles among them, which proves the theorem for $k = m+1$. If we select $k = M \triangleq N - n + 1$, it is obvious that there would be no pileup crash among the vehicles for $1 \leq i \leq N$, if there are M equipped vehicles among them. ■

In the above theorem, it should be noted that there is no constraint on the distribution of the equipped vehicles within the N vehicle system. In other words, as long as $L \geq N - n + 1$, there will be no pileup crash in the entire interconnected system, for any distribution of the equipped vehicles.

For example, assume that $N = 100$ and $M = 20$. That is, consider an interconnected system comprising of 100 vehicles driving with equal initial speeds and equal initial intervehicle spacings. Assume that, when all vehicles are unequipped, the lead vehicle decelerates so as to induce a chain reaction that causes a pileup crash from the $81st$ vehicle onwards (the last 20 vehicles crash). In this case, a pileup crash could be completely avoided if we arbitrarily equip 20 of the 100 vehicles with the slowdown

warning system.

The theorem in Equation 2.12 is a sufficient condition to avoid a pileup crash. In other words, there could be situations where the number of equipped vehicles is smaller than M, but this is still adequate to avoid the pileup crash completely. The condition for no pileup crash in Theorem 2 is conservative, because we have assumed that Equation 2.16 needs to be satisfied to guarantee that there is no collision between the $(i-1)$th and the ith vehicles. However, even if Equation 2.16 is violated, it does not necessarily mean that the $(i-1)$th vehicle collides with the ith vehicle. For the same reason, the condition $\|\Delta(x_{n+m} - x_{n+m+1})\|_\infty \leq s_0$ in Equation 2.24 could be achieved, even when $\alpha \|u(t)\|_1^{n-2} > s_0$. However, Theorem 2 cannot provide information about what happens when $L < M$.

In order to investigate the occurrence of a pileup crash for $L < M$ and derive a condition for no pileup crash that is less conservative condition than Equation 2.12, we make another assumption on the dynamics of the interconnected vehicle system and the deceleration profile of the lead vehicle. That is, we assume that $G_k(s)$ and V_1 satisfy the following inequality,

$$\|\Delta(x_i - x_{i+1})\|_\infty \leq \alpha \left\| \prod_{k=2}^{i} G_k \right\|_\infty \tag{2.25}$$

Clearly, the condition in Equation 2.25 is not guaranteed in general. However, Equation 2.25 turns out to be true for the $G_k(s)$ represented by Equation 2.1 and a V_1 representing a typical deceleration. Using the assumption in Equation 2.25 allows us to derive a much less conservative condition (for pileup crash avoidance) than the one in Equation 2.12.

While a formal proof that demonstrates that Equation 2.25 holds true (in the scenarios of interest in this paper) is yet to be shown, we believe the following simulations will convince the reader of its correctness. We first performed the simulations with three unequipped cars. In these simulations, the lead car was assumed to have a velocity profile of the form shown in Figure 2-10, and simulations were performed with variable ΔV and ΔT, with ΔV and ΔT representing the quantities

shown in the figure. For each different $(\Delta V, \Delta T)$ combination, we determine the value of $\|\Delta(x_2 - x_3)\|_\infty$. It turns out that the condition $\frac{\|\Delta(x_2-x_3)\|_\infty}{\alpha} \leq \|G_2\|_\infty$ is always satisfied for the different $(\Delta V, \Delta T)$ combinations considered (see Fig. 9). Thus, we numerically verified that Equation 2.25 is satisfied for the case $i = 2$. We then further verified (again, numerically) that Equation 2.25 is satisfied for general i. A typical result supporting this is given in Fig. 10, wherein, for a specific $(\Delta V, \Delta T)$ combination, plots of $\|\Delta(x_i - x_{i+1})\|_\infty$ and $\alpha \left\| \prod_{k=2}^{i} G_k \right\|_\infty$ are shown. This plot is typically representative of the trend shown by the left and right hand side quantities of Equation 2.25 (for a lead vehicle decleration profile of the form in Fig. 2-10), and thus show that Equation 2.25 is satisfied, at least in our context (though it is not true in general).

The less conservative condition (obtained as a consequence of using 2.25) is given in the following theorem.

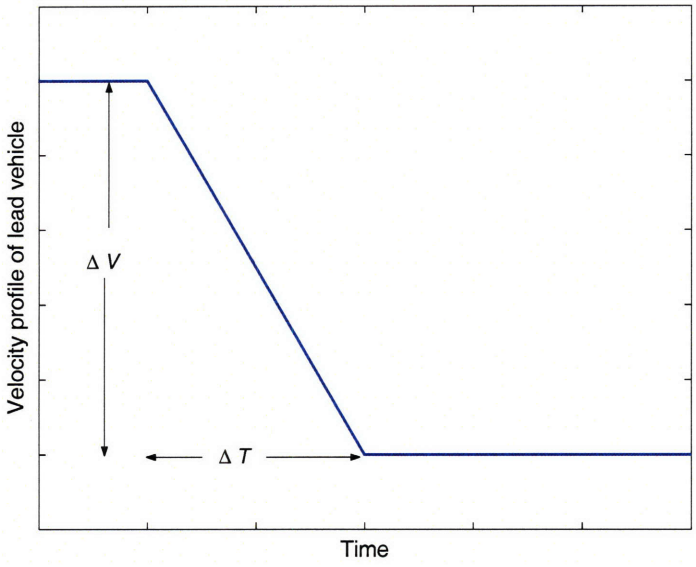

Figure 2-10: Typical velocity profile of lead vehicle

While Figure 2-11 shows the relation between the amplification factor, $\|U\|_1$ and $\|U\|_\infty$ for a single value of $\tau = 0.6$ seconds, Figure 2-13 then shows the corresponding relation for varying values of τ. The relation for $\tau = 0.2, 0.4, 0.8, 1$ second are shown in the figure. It can be seen that with increasing values of τ, the amplification factor

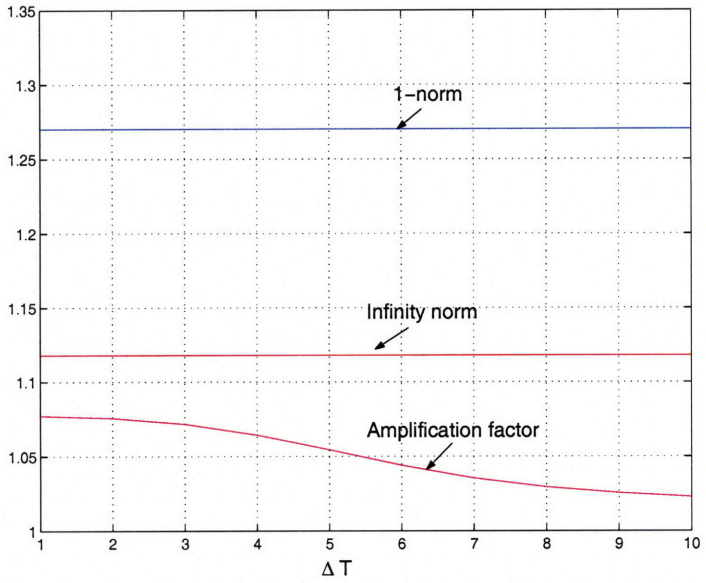

Figure 2-11: Relation among $\|U\|_1$, $\|U\|_\infty$, and actual amplification factor.

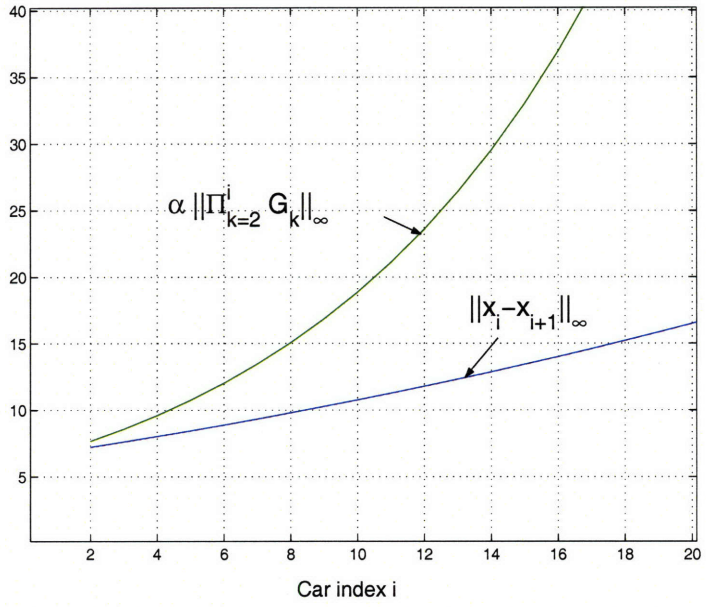

Figure 2-12: Results of numerical simulations that verify Equation 25

increases (as was also evidenced from Figures 2-6 and 2-8); yet, at the same time, the amplification factor remains consistently lower than $\|U\|_\infty$.

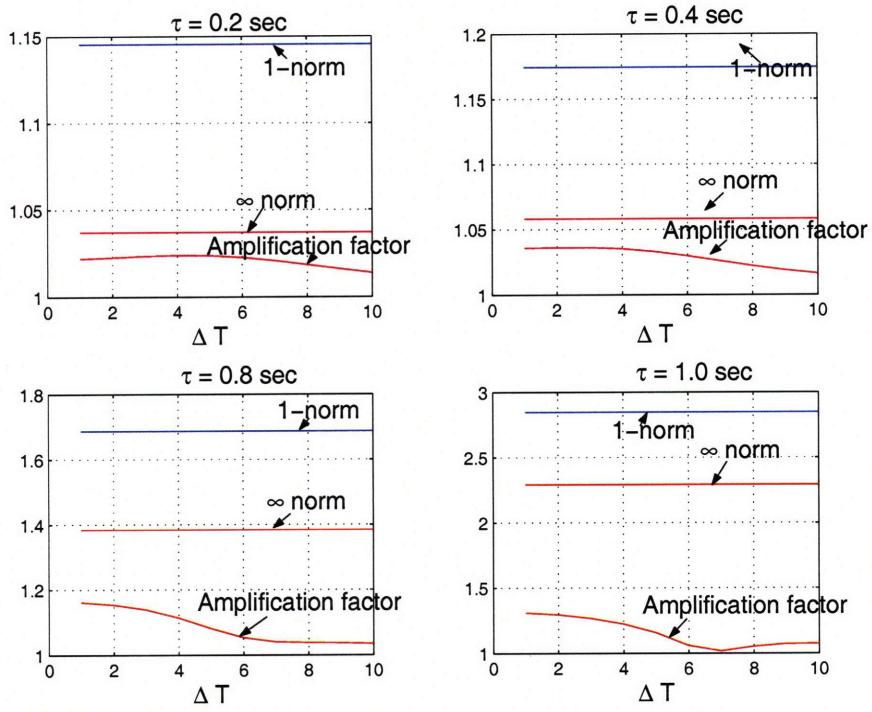

Figure 2-13: Effect of varying τ on the relation among $\|U\|_1$, $\|U\|_\infty$, and actual amplification factor.

Theorem 3 Consider the same situation as in Theorem 2, i.e., there are N vehicles driving with equal initial speeds and equal intervehicle spacing s_0, L out of N vehicles are equipped with the slowdown warning system, and the lead vehicle decelerates abruptly such that (when all cars are unequipped) a pileup crash is initiated at the nth vehicle, i.e., $\|\Delta(x_i - x_{i+1})\|_\infty > s_0$ for $n \leq i \leq N-1$. Let L_k be the number of equipped vehicles between the first and the $(n+k-1)$th vehicle (by definition, $L_{N-n+1} = L$). Under the same deceleration profile of the lead vehicle and the assumption in Equation 2.25, there will be no pileup crash in the interconnected system, if

$$L_k \geq \lfloor k\lambda \rfloor \text{ for } 1 \leq k \leq N-n+1, \tag{2.26}$$

where

$$\lambda = \frac{\log \beta}{\log \beta - \log \gamma} \ . \tag{2.27}$$

Here, $\beta = \|U(s)\|_\infty = |U(j\omega_0)| > 1$, ω_0 is the frequency at which $|U(j\omega)|$ is maximum, $\gamma = |E(j\omega_0)| < 1$, and $\lfloor x \rfloor$ denotes the smallest integer greater than x. (Figure 2-6 demonstrates β and γ for a representative choice of $U(s)$ and $E(s)$). Therefore, the total number of equipped vehicles L should be greater than $\lfloor M\lambda \rfloor$ to guarantee that there will be no pileup crash, where $M = N - n + 1$ is the number of vehicles that would have crashed if all vehicles were unequipped.

Proof : Basically, we follow the same procedure used for the proof in Theorem 2. When all vehicles are unequipped, Equation 2.7 gives

$$\Delta(x_{n-1} - x_n) = L^{-1}\left\{U^{n-2}\frac{(1-U)}{s}V_1\right\} \ , \tag{2.28}$$

and therefore we have from Equation 2.25,

$$\|\Delta(x_{n-1} - x_n)\|_\infty \leq \alpha\beta^{n-2} \ . \tag{2.29}$$

As in the previous proof, we assume

$$\alpha\beta^{n-2} \leq s_0 \ , \tag{2.30}$$

so that the condition $\|\Delta(x_{n-1} - x_n)\|_\infty \leq s_0$ is always achieved for any deceleration of the lead vehicle. Now, we will show that

$$\|\Delta(x_{n+k-1} - x_{n+k})\|_\infty \leq \alpha\beta^{n-2}, \tag{2.31}$$

is true for $k = 1, 2, ..., N - n + 1$, if Equation 2.26 is satisfied (i.e., there are at least $\lfloor k\lambda \rfloor$ equipped vehicles among them). This will prove that there will be no pileup crash among the vehicles for $1 \leq i \leq (n + k - 1)$. We will prove this by induction.

1. For $k = 1$

   In this case, there should exist at least one equipped vehicle $1 \leq i \leq n$ because

λ is always less than one. Under this condition, we have

$$\begin{aligned}\Delta\left(x_n - x_{n+1}\right) &= L^{-1}\left\{\left[\prod_{i=2}^{n} G_i\right]\frac{(1-G_{n+1})}{s}V_1\right\} \\ &= L^{-1}\left\{U^{n-2}E\frac{(1-U)}{s}V_1\right\}\ ,\end{aligned} \tag{2.32}$$

which will yield

$$\begin{aligned}\left\|\Delta\left(x_n - x_{n+1}\right)\right\|_\infty &\leq \alpha\left\|U^{n-2}E\right\|_\infty \text{(from Equation 2.25)} \\ &\leq \alpha\beta^{n-2}\gamma \\ &\leq \alpha\beta^{n-2}\ \ (\because \gamma < 1) \\ &\leq s_0 \text{ (from Equation 2.30).}\end{aligned} \tag{2.33}$$

Therefore, there would be no pileup crash among the vehicles for $1 \leq i \leq n$, if there is one equipped vehicle among them.

2. For $k = m$ (i.e., there are $\lfloor m\lambda \rfloor$ equipped vehicles among $1 \leq i \leq n+m-1$). Now, we assume that the theorem is true for $k = m$, i.e., that there will be no pileup crash among the vehicles for $1 \leq i \leq (n+m-1)$, if there are $\lfloor m\lambda \rfloor$ equipped vehicles among them. In other words, we assume

$$\left\|\Delta\left(x_i - x_{i+1}\right)\right\|_\infty \leq s_0 \text{ for all } 1 \leq i \leq n+m-1\ . \tag{2.34}$$

Under this condition, we will show that the theorem is true for $k = m+1$, i.e., there will be no pileup crash among the vehicles for $1 \leq i \leq (n+m)$, if there are $\lfloor (m+1)\,\lambda \rfloor \triangleq p$ equipped vehicles among them. Here, we only need to show that $\left\|\Delta\left(x_{n+m} - x_{n+m+1}\right)\right\|_\infty \leq s_0$ because the condition in Equation 2.34 has

been assumed to be true. Since

$$\begin{aligned}
&\Delta\left(x_{n+m}-x_{n+m+1}\right) \\
&=L^{-1}\left\{\left[\prod_{i=2}^{n+m} G_i\right]\frac{(1-G_{n+m+1})}{s}V_1\right\} \\
&=L^{-1}\left\{U^{n+m-1-p}E^p\frac{(1-U)}{s}V_1\right\} ,
\end{aligned} \tag{2.35}$$

we have

$$\begin{aligned}
\left\|\Delta\left(x_{n+m}-x_{n+m+1}\right)\right\|_\infty &\leq \alpha\left\|U^{n+m-1-p}E^p\right\|_\infty \\
&\leq \alpha\beta^{n+m-1}\left(\frac{\gamma}{\beta}\right)^p .
\end{aligned} \tag{2.36}$$

Since $\frac{\gamma}{\beta}<1$ and $(m+1)\lambda \leq p$, we have

$$\left(\frac{\gamma}{\beta}\right)^p \leq \left(\frac{\gamma}{\beta}\right)^{(m+1)\lambda} = \beta^{-m-1} \tag{2.37}$$

Using Equation 2.36 and 2.37, we have

$$\begin{aligned}
\left\|\Delta\left(x_{n+m}-x_{n+m+1}\right)\right\|_\infty &\leq \alpha\beta^{n+m-1}\beta^{-m-1} \leq \alpha\beta^{n-2} \\
&\leq s_0 \text{ (from Equation 2.16)}
\end{aligned} \tag{2.38}$$

Therefore, we see that there would be no pileup crash among the vehicles $1\leq i \leq n+m$, if there are p equipped vehicles among them, which proves the theorem for $k=m+1$. If we select $k=M \triangleq N-n+1$, it is obvious that there would be no pileup crash among the vehicles for $1\leq i \leq N$, if there are $\lfloor M\lambda \rfloor$ equipped vehicles among them. ■

It should be noted that the new condition $L \geq \lfloor M\lambda \rfloor$ to avoid a pileup crash is much less conservative than the condition $L \geq M$, because $\lambda < 1$. For example, the vehicle dynamics used in the simulation in Section 2.3 give $\beta = 1.12$ and $\gamma = 0.85$,

which yields $\lambda = 0.41$. Therefore, the number of equipped vehicles that will enable a pileup crash to be averted when $N = 100$ and $M = 20$ is $\lfloor 20 \times 0.41 \rfloor = 9$. That is, a pileup crash can be averted if we 'reasonably' distribute 9 equipped vehicles in the 100 vehicle stream with the slowdown warning system. Here, we use the term 'reasonably', in the context that the distribution of the equipped vehicles should satisfy the condition in Equation 2.26 of Theorem 3. Theorem 3 implies that when $L < M$, then in order to guarantee avoidance of a pileup crash, along with the condition $L \geq \lfloor M\lambda \rfloor$, at least $\lfloor k\lambda \rfloor$ equipped vehicles need to be present between the first and the $(n+k-1)$th vehicle for $1 \leq k \leq N-n+1$, .

However, it was found that the probability of satisfying the condition in Equation 2.26 (and thus avoiding a pileup crash completely) is quite acceptable in most cases. The probability of averting the pileup crash as N varies from 10 to 50 and $\lambda = 0.5$ is given in Figure 2-14, in which we assume for each N that 20% of vehicles crash when none are equipped (i.e.,M=$\lfloor 0.2N \rfloor$), and we equip $L = \lfloor M\lambda \rfloor$ of the N vehicles. For example, when $N = 20$, M and L become $M = \lfloor 0.2N \rfloor = 4$, and $L = \lfloor M\lambda \rfloor = 2$, respectively, and the probability of satisfying the condition in Equation 2.26 can be computed as

$$= \frac{\begin{array}{c}\text{Number of combinations of at least one vehicle equipped} \\ \text{between 1-17 and the other one equipped between 1-19}\end{array}}{\text{Number of combinations of 2 out of 20 vehicles equipped}} = \frac{(17 \times 18)/2}{\binom{20}{2}} = 0.8053, \tag{2.39}$$

where $\binom{n}{k}$ represents the number of combinations of n objects taken k at a time. Proceeding in the manner outlined in Equation 2.39, we can compute the probability of averting a pileup crash for general N, M and L. It can be seen from Figure 2-14 that there is a high probability (above 65%) of completely avoiding the pileup crash if we equip about 10% of the total number of vehicles. Of course, the pileup crash is guaranteed to be averted if we equip 20% of the vehicles.

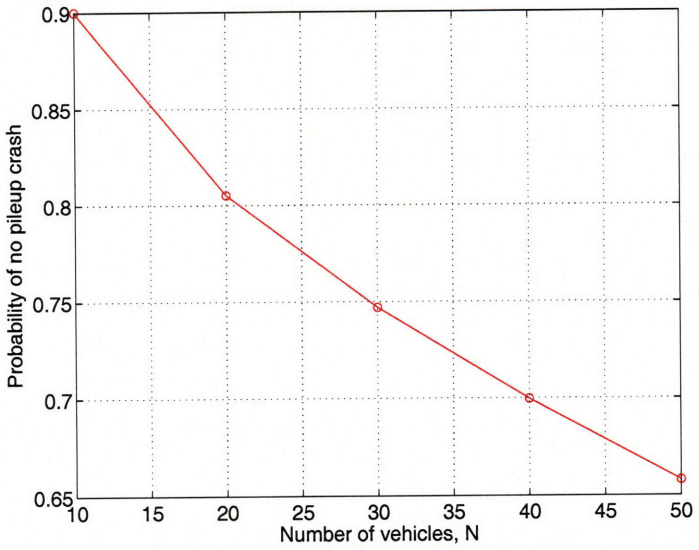

Figure 2-14: Probability to avoid a pileup crash completely for $L = \lfloor 0.1N \rfloor$.

2.6 A summary of what we have learnt

How are pileup crashes caused ?

While there could be several ways in which pileup crashes could be caused, it seems intuitive to think that large time delays accompanied by short following distances could act as a trigger to initiate pileup crashes. We see that large time delays and small time headways can indeed lead to the phenomenon of string instability - which implies amplification of velocity and inter-vehicle spacing errors, as these errors propagate through a line of vehicles. Thus, if a string is large enough, then these errors continue to amplify till they exceed a certain threshold, and this leads to pileup crashes. Conversely, short time delays accompanied by large time headways result in string stability. This phenomenon is brought out in Figures 2-2, 2-3 and 2-6.

What role can partial equipment of an advance warning system play in averting pileup crashes ?

When a driver receives an advance warning, it is reasonable to assume that he exhibits shorter time delays when responding to the vehicle ahead. We also make the reasonable assumption that he attempts to increase his following distance (i.e. time headway) to the car ahead. These two effects combine to make that portion of the

vehicular string that include him and his predecessor, string stable. If all the vehicles in a string are equipped, then the entire string is string stable. If only some vehicles are equipped, then there occurs the phenomenon of mixed string stability. It can be intuitively seen that even in situations when there are only some equipped vehicles in a string, then as long as the equipped vehicles are present in a sufficient number, and are well distributed in the vehicular string, then they can serve to keep the level of amplification of the velocity/inter-car distance errors below the threshold that would lead to pileup crashes. This phenomenon is demonstrated in Figure 2-4.

How many equipped vehicles need to be present in a given string, in order to alleviate a pileup crash completely, i.e. have zero collisions ?

In this thesis, this number is presented as a function of the number of vehicles that would have crashed, if all vehicles were unequipped. The statement of this result is given in Theorems 2 and 3. Note however, that this number is a conservative estimate. Furthermore, while Theorem 2 guarantees zero collisions under any arbitrary distribution of equipped vehicles, Theorem 3 guarantees zero collisions if the distribution of equipped vehicles belongs to a set of defined distributions given in the Theorem.

Given a string where the equipped vehicles are present in the requisite number stated by Theorem 3, but are otherwise arbitrarily distributed, what is the probability that they will lie in the set of requisite distributions (specified by Theorem 3), that will result in zero collisions ?

This is presented in Figure 2-14. Figure 2-14 thus gives the proability of zero collisions, as a function of the total number of vehicles. Note however that since this figure is based on the statement of Theorem 3, and Theorem 3 itself is conservative, therefore this probability curve represents a lower bound on the probability of zero collisions.

Chapter 3

Macroscopic Modeling Approach

In this chapter, the average behavior of groups of vehicles is studied using partial differential equations. A multi-lane model is assumed. It is demonstrated how scenarios when all vehicles are unequipped can lead to situations wherein large negative velocity gradients travel unattenuated or get amplified as they propagate along the highway. It is then demonstrated how the presence of a few equipped vehicles can attenuate these velocity gradients. The resulting velocity gradients are then parametrized as a function of the extent of equipment, in a mixed vehicle string. For a prototype Reimann Problem, it is demonstrated that about 15% equipment accompanied by a signal transmission range of 500 meters can lead to over 50% reduction in the velocity shock magnitude, as compared to when all vehicles are unequipped.

3.1 Introduction

In this chapter, we use macroscopic models to demonstrate the benefits that accrue from a slowdown warning system. Partial Differential Equation (PDE) based models are used, and a multi-lane scenario is assumed. We examine the influence of partial equipment of the slowdown warning system on some of the wave effects that are known to exist in traffic flows, in particular, shocks/large negative velocity gradient waves that travel unattenuated/get amplified as they pass through the traffic. We formulate the problem as a shock alleviation problem; in other words, we see how

the presence of a slowdown warning system can help alleviate/minimize the presence of large negative velocity gradients on the highway, that otherwise would have occurred. Furthermore, in this chapter, we assume a finite speed of propagation of the slowdown warning communication wave, as it travels through a line of vehicles. The PDE models used are based on gas dynamics foundations. We first explain the underlying Boltzmann equation that is used in a single species situation, i.e., when all vehicles are unequipped, and then illustrate the derivation of the macroscopic equations by taking moments of the Boltzmann equation. We then use DSMC (Direct Simulation Monte Carlo) methods to explain the link between the underlying Boltzmann equation (that essentially represents microscopic models of vehicles) and the macroscopic model. We then explain how the Boltzmann equation gets modified in a two species situation, when the two species assumed are cars and trucks. We then illustrate how this two species equation gets further modified when we assume that one of the species (i.e. the equipped vehicles) receives advance information of the slowdown ahead/degraded velocity conditions ahead, via a communication wave propagating with a finite speed through the equipped vehicles. With this model, we then present results that parametrize the strength of the velocity gradient waves, as a function of the percentage of equipment for different initial conditions - a Reimann Problem and initial conditions with negative velocity gradients that grow steeper and steeper as time evolves (when all vehicles are unequipped).

3.2 Derivation of macroscopic equations for a single species - all vehicles unequipped

3.2.1 The underlying Boltzmann Equation

Consider a system of vehicles, indexed by α, with $\alpha = 1, 2, ...N$, as represented schematically in Figure 3-1. Let the state of vehicle α at time t be defined by $X_\alpha(t) = [x_\alpha(t), v_\alpha(t), v^o{}_\alpha(t)]$, where $x_\alpha(t)$, $v_\alpha(t)$ and $v^o{}_\alpha(t)$ represent the position, velocity and desired velocity, respectively of particle α. The dynamics of particle α are governed

by the following state space equations :

$$\frac{dx_\alpha}{dt} = v_\alpha \tag{1}$$

$$\frac{dv_\alpha}{dt} = \frac{v_\alpha^o - v_\alpha}{\tau_\alpha} + \Sigma_{\beta \neq \alpha} f_{\alpha\beta} + \xi_\alpha(t) \tag{2}$$

$$\frac{dv_\alpha^o}{dt} = 0 \tag{3}$$

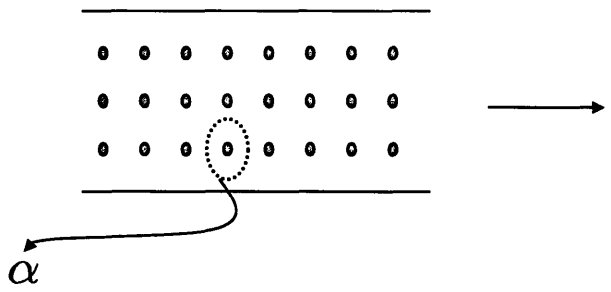

Figure 3-1: Schematic multi-vehicle scenario

While the meaning of equation (1) is obvious, equation (2) indicates that the acceleration/deceleration behavior of each driver-vehicle unit α is comprised of three factors :

(a) The desire of the driver to attain his desired velocity v_α^o. It is assumed that he/she tries to attain this desired velocity at an exponential rate, with time constant τ_α.

(b) The interaction effects due to the presence of other vehicles. $f_{\alpha\beta}$ indicates the interaction effect (i.e. the slowing down effect) of vehicle β on α. It comes into play when a vehicle β is driving ahead of vehicle α, with a velocity $v_\beta < v_\alpha$, and α is unable to overtake β (by passing). It is explained in more detail further below.

(c) The acceleration noise, represented by $\xi_\alpha(t)$ for vehicle α. This noise is assumed to be Gaussian white noise, i.e. it has zero mean with specified co-variance as follows:

$$< \xi_\alpha(t) >= 0 \quad \forall \quad \alpha \tag{4}$$

$$< \xi_\alpha(t)\xi_\beta(\tau) >= 2D\delta_{\alpha\beta}\delta(t-\tau) \tag{5}$$

where $< h >$ indicates the expected value of h. Finally, equation (3) indicates that the desired velocity of each driver is a constant for all time. Note that this does not necessarily mean that all the drivers have the same desired velocity.

We define $\tilde{\rho}(x, v, v^o, t)$ as the phase space density - in other words it is a multivariable probability density function (in three dimensions) such that $\tilde{\rho}(x, v, v^o, t)\Delta x \Delta v \Delta v^o$ represents the average no. of particles present in the interval $[x - \Delta x/2, x + \Delta x/2]$, with velocity in the interval $[v - \Delta v/2, v + \Delta v/2]$, and desired velocity in the interval $[v^o - \Delta v^o/2, v^o + \Delta v^o/2]$, at a time $t' \in [t - \Delta t/2, t + \Delta t/2]$.

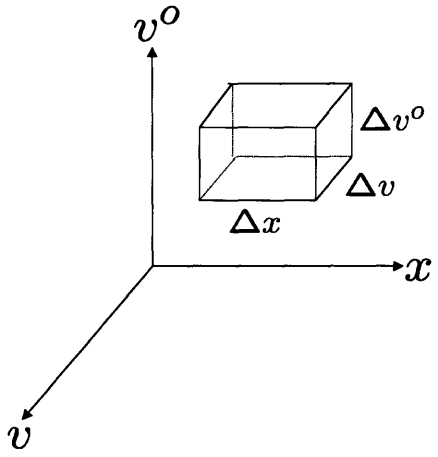

Figure 3-2: Illustration of the phase space

Thus, if $\Delta n(x, v, v^o, t')$ represents the number of vehicles in the box schematically shown in Figure 3-2 at some time t', then

$$\tilde{\rho}(x, v, v^o, t) = \frac{1}{\Delta x \Delta v \Delta v^o \Delta t} \int_{t'-\Delta t/2}^{t'+\Delta t/2} \Delta n(x, v, v^o, t') dt \tag{6}$$

In order for $\tilde{\rho}(x, v, v^o, t)$ to indicate a meaningful average, the averaging lengths Δx, Δv and Δv^o are important. For $\tilde{\rho}(x, v, v^o, t)$ to indicate a meaningful average of a specific single traffic situation, it is necessary that the lengths Δx, Δv and Δv^o be microscopically large, but macroscopically small. On the other hand, for $\tilde{\rho}(x, v, v^o, t)$ to be meaningful in the limit of $\Delta x \to 0$, $\Delta v \to 0$, $\Delta v^o \to 0$, it has to be constructed as an ensemble average of macroscopically identical (but microscopically distinct) traffic scenarios.

If we define $\frac{d\hat{v}}{dt} \equiv \frac{v^o - v}{\tau}$, then one can write the evolution of $\tilde{\rho}(x, v, v^o, t)$ as governed by the continuity equation in phase space density as follows (this has analogies to the Boltzmann equation in gas dynamics) :

$$\frac{\partial\tilde{\rho}}{\partial t}+\frac{\partial}{\partial x}(\tilde{\rho}\frac{dx}{dt})+\frac{\partial}{\partial v}(\tilde{\rho}\frac{d\hat{v}}{dt})+\frac{\partial}{\partial v^o}(\tilde{\rho}\frac{dv^o}{dt})=(\frac{\partial\tilde{\rho}}{\partial t})_{int}+\frac{\partial(\tilde{\rho}D)}{\partial v^2} \tag{7}$$

It can be seen that the terms on the left hand side of the above equation arise due to the time variation of $\tilde{\rho}$ as well as the convection of $\tilde{\rho}$ in phase-space. On the right hand side, $(\frac{\partial\tilde{\rho}}{\partial t})_{int}$ represents the instantaneous changes in the phase space density that occur due to the slowing down interactions between the vehicles. This is given by the Boltzmann interaction term. The interaction term can be thought of as comprising two parts :

$$(\frac{\partial\tilde{\rho}}{\partial t})_{int}=\frac{\partial\tilde{\rho}^+}{\partial t}+\frac{\partial\tilde{\rho}^-}{\partial t} \tag{8}$$

where $\frac{\partial\tilde{\rho}^+}{\partial t}$ represents the effect of an instantaneous increase in $\tilde{\rho}(\cdot)$, and $\frac{\partial\tilde{\rho}^-}{\partial t}$ represents the effect of an instantaneous decrease in $\tilde{\rho}(.)$.

We first consider events that lead to an instantaneous increase in $\tilde{\rho}(x,v,v^o,t)$. Consider two distinct velocity classes v and w, where it is to be understood that a vehicle belonging to velocity class v has its velocity in the range $[v-\Delta v/2, v+\Delta v/2]$; and a vehicle belonging to velocity class w has its velocity in the range $[w-\Delta w/2, w+\Delta w/2]$. Assume $w > v$. Then when a faster vehicle belonging to velocity class w encounters a slower vehicle belonging to velocity class v and travelling ahead of it, then either of two events could occur :

a) The faster vehicle overtakes the slower vehicle (by passing). Such an event is assumed to occur with a probability p; and if it occurs, it occurs instantaneously, and with no change in the velocities of either of the two vehicles.

b) The faster vehicle does not pass the slower vehicle, but instead adapts its velocity instantaneously to that of the slower vehicle. Such an event occurs with probability $(1-p)$. Occurrence of this event leads to an instantaneous increase in the number of vehicles of class v, accompanied by an instantaneous decrease in the number of vehicles of class w. In other words, if we assume for instance that both vehicles belong to the same desired velocity class v^o, then this event leads to an instantaneous increase in $\tilde{\rho}(x,v,v^o,t)$, accompanied by an instantaneous decrease in $\tilde{\rho}(x,w,v^o,t)$. The rate at which this event occurs is obtained from the following reasoning :

Consider a single stochastic vehicle A, belonging to velocity class v, and desired ve-

locity class v^o. Then, we can see that : Number of interactions that vehicle A encounters with all vehicles belonging to the (slower) velocity class w and desired velocity class w^o in time dt = Number of vehicles belonging to velocity class w and desired velocity class w^o that the vehicle A encounters, in time $dt = \tilde{\rho}(x, w, w^o, t)dwdw^o|v-w|dt$.

Therefore, number of interactions that vehicle A encounters with vehicles belonging to *all* other slower velocity classes, in time $dt = \int dw^o \int_{w<v} dw\tilde{\rho}(x, w, w^o, t)|v - w|dt$.

Number of interactions of all vehicles of velocity class v and desired velocity class v^o with vehicles belonging to all other slower classes, in time dt = Number of vehicles of velocity class v and desired velocity class v^o at x X Number of interactions that a single vehicle in velocity class v and desired velocity class v^o encounters

$= \tilde{\rho}(x, v, v^o, t)dxdv \int dw^o \int_{w<v} dw\tilde{\rho}(x, w, w^o, t)|v - w|dt$

$= \tilde{\rho}(x, v, v^o, t)dxdvdt \int dw^o \int_{w<v} dw\tilde{\rho}(x, w, w^o, t)|v - w|$

Multiplying the above by $(1-p)$ which indicates the probability of not overtaking, we finally get that $\frac{\partial \tilde{\rho}^+}{\partial t}$, which is actually the number of interactions of vehicles of velocity class v and desired velocity class v^o with vehicles belonging to all other slower classes computed per unit time, per unit length and per unit velocity is given by :

$$\frac{\partial \tilde{\rho}^+}{\partial t} = (1-p)\tilde{\rho}(x, v, v^o, t) \int dw^o \int_{w<v} \tilde{\rho}(x, w, w^o, t)|v - w| \tag{9}$$

In a similar fashion, one can see that if the slower vehicle of velocity class w is travelling in front of the faster vehicle of velocity class v, (i.e. $w < v$) (and both vehicles belong to the desired velocity class v^o); then if the faster vehicle adapts its velocity instantaneously to that of the slower vehicle, it leads to an instantaneous decrease in $\tilde{\rho}(x, v, v^o, t)$. By an analogous reasoning, one can obtain that :

$$\frac{\partial \tilde{\rho}^-}{\partial t} = -(1-p)\tilde{\rho}(x, v, v^o, t) \int dw^o \int_{w>v} dw\tilde{\rho}(x, w, w^o, t)|v - w| \tag{10}$$

After substituting eqns. (1),(2),(3) (9) and (10) into equation (7), we get the following :

$$\frac{\partial \tilde{\rho}}{\partial t} + \frac{\partial}{\partial x}(\tilde{\rho}v) + \frac{\partial}{\partial v}(\tilde{\rho}\frac{v^o - v}{\tau}) = (1-p)\int_v^\infty dw \int_0^\infty dw^o|v-w|\tilde{\rho}(x, w, w^o, t)\tilde{\rho}(x, v, v^o, t) -$$

$$(1-p)\int_0^v dw \int_0^\infty dw^o|w - v|\tilde{\rho}(x, w, w^o, t)\tilde{\rho}(x, v, v^o, t) + \frac{\partial(\tilde{\rho}D)}{\partial v^2} \tag{11}$$

We then integrate both sides of the above equation with respect to dv^o. Doing so, and defining $\int dv^o\tilde{\rho}(x, v, v^o, t) = \hat{\rho}(x, v, t)$, eqn. (11) takes the form :

$$\frac{\partial\hat{\rho}}{\partial t} + \frac{\partial}{\partial x}(\hat{\rho}v) + \frac{\partial}{\partial v}(\hat{\rho}\frac{v^o - v}{\tau}) = (1-p)\int_v^\infty dw|v-w|\hat{\rho}(x,w,t)\hat{\rho}(x,v,t) - (1-p)\int_0^v dw|w-v|\hat{\rho}(x,w,t)\hat{\rho}(x,v,t) + \frac{\partial(\hat{\rho}D)}{\partial v^2} \quad (12)$$

We will revisit the above formula in Section 4 of this Chapter, when we perform molecular simulations using the DSMC Method.

3.2.2 Method of moments to obtain Macroscopic Equations

Multiplying both sides of Equation (11) by $v^k(v^o)^l$ and then integrating with respect to $dv^o dv$, one gets the following two equations for the zeroth and first velocity moments (and the zeroth desired velocity moment) respectively :

$$\frac{\partial m_{0,0}}{\partial t} + \frac{\partial m_{1,0}}{\partial x} = 0 \quad (13)$$

$$\frac{\partial m_{1,0}}{\partial t} + \frac{\partial m_{2,0}}{\partial x} + \frac{1}{\tau}(m_{1,0} - m_{0,1}) = m_{1,0}m_{1,0} - m_{2,0}m_{0,0} \quad (14)$$

where $m_{k,l}$ is defined as

$$m_{k,l} = \int\int dv^o dv v^k (v^o)^l \tilde{\rho}(x,v,v^o,t) \quad (15)$$

with $m_{-1,l} = 0$ by defintion.

It can be inferred from (15) that $m_{0,0}$ represents the average spatial density $\rho(x,t)$ as follows :

$$m_{0,0} = \int dv^o \int dv\tilde{\rho}(x,v,v^o,t) = \int dv\hat{\rho}(x,v,t) = \rho(x,t) \quad (16)$$

Similarly, it can be inferred from (15) that $m_{1,0}$ is given by :

$$m_{1,0} = \int dv^o \int vdv\tilde{\rho}(x,v,v^o,t) \quad (17)$$

i.e., $m_{1,0} = \rho(x,t)V(x,t)$

where $V(x,t)$ represents the average velocity defined by:

$$V(x,t) =< v >= \frac{\int dv^o \int vdv\tilde{\rho}(x,v,v^o,t)}{\rho(x,t)} \quad (18)$$

It can also be inferred from (15) that $m_{2,0}$ is given by :

$$m_{2,0} = \int dv^o \int v^2 dv\tilde{\rho}(x,v,v^o,t) \quad (19)$$

$$\text{i.e. } m_{2,0} = \rho(x,t)(V(x,t)^2 + \theta(x,t)) \quad (20)$$

where $\theta(x,t)$ represents the velocity variance defined as :

$$\theta(x,t) =< (v - V(x,t))^2 >= \frac{\int dv^o \int [v - V(x,t)]^2 dv\tilde{\rho}(x,v,v^o,t)}{\rho(x,t)} \quad (21)$$

Substituting for $m_{0,0}$, $m_{1,0}$ and $m_{2,0}$ in equations (13) and (14), the following macroscopic equations are obtained :

$$\frac{\partial \rho}{\partial t} + \frac{\partial(\rho V)}{\partial x} = 0 \tag{20}$$

$$\frac{\partial V}{\partial t} + V\frac{\partial V}{\partial x} = \frac{-1}{\rho}\frac{\partial(\rho\theta)}{\partial x} + \frac{V_e - V}{\tau} \tag{21}$$

where $V_e(x,t)$ represents the average equilibrium velocity and is given by :

$$V_e(x,t) = V^o - (1-p)\rho\tau\theta \tag{22}$$

Equations (20), (21) and (22) represent the form of macroscopic equations that can be derived from the work done by [50], [51], [72]. These equations however do into take into account two aspects: (a) The assumption that vehicular interactions are inherently anisotropic, i.e. that a vehicle responds to the traffic situation ahead of it, and not to the situation behind it; (b) The fact that each vehicle has non-zero length and that vehicular braking interactions occur when there is still a finite space between two vehicles.

The above two aspects were treated in [41], and using an Enskog-like approach, the following Boltzmann equation was arrived at:

$$\frac{\partial \hat{\rho}}{\partial t} + \frac{\partial}{\partial x}(\hat{\rho}v) + \frac{\partial}{\partial v}(\hat{\rho}\frac{v^o - v}{\tau}) = \frac{(1-p)}{p}\int_v^\infty dw|v-w|\hat{\rho}_a(x,w,t)\hat{\rho}(x,v,t) - \frac{(1-p)}{p}\int_0^v dw|w-v|\hat{\rho}(x,w,t)\hat{\rho}_a(x,v,t) + \frac{\partial(\hat{\rho}D)}{\partial v^2}. \tag{23}$$

(The above equation may be compared with Equation 12). This Equation removes the isotropic nature inherent in Equation (12) by defining a quantity $\hat{\rho}_a(x,v,t)$, which is essentially the same as $\hat{\rho}(x_a,v,t)$, where $x_a = x + (l + VT)$. By defining $\hat{\rho}_a(x,v,t)$ in the RHS of the Boltzmann Equation, Equation (23) is modeling the fact that the average vehicle responds to the traffic situation occurring at a distance $l + VT$ ahead of it. l represents the average vehicle length, and is given by $l = \frac{1}{\rho_{max}}$, while T represents the average time headway maintained by a vehicle to the vehicle in front of it (in the high density limit). ρ_{max} represents the maximum possible vehicular density that occurs, when all vehicles are lined up bumper to bumper.

Equation (23) also incorporates the finite space requirements for vehicular interactions by the insertion of the term $\frac{1}{p}$ that premultiplies the RHS of the original Boltzmann Equation (12). Since p is inherently a probability-like number, it is always less than or equal to 1, and consequently Equation (23) leads to an increase in the number of vehicular interactions (as compared with the gas-dynamic like interaction

term given in Equation (12). By subsequently further defining p as a function of ρ (discussed below), Equation (23) also ensures that with increasing vehicular density, the number of vehicular interactions increase, as well as the probability of overtaking decreases; both of which make sense from a physical standpoint.

By taking the first and second moments of Equation (23), we again obtain Equations of the form (20) and (21), but this time, the expression for the equilibrium velocity V_e turns out to be of the form :

$$V_e(x,t) = V^o - P(\rho_a)B\rho\tau(\theta + \theta_a)/2. \tag{24}$$

In the above, ρ_a and θ_a represent the density and velocity variance computed at an interaction point x_a, in other words, $\rho_a = \rho(x_a)$, $\theta_a = \theta(x_a)$. Obtaining an expression for equilibrium velocity of the form given in Equation (24) required the assumption of a Gaussian velocity distribution, in other words, it assumes that the velocity distribution at any x, t is always Gaussian. More precisely, it makes the assumption that :

$$\hat{\rho}(x,v,t) = \rho(x,t)e^{(v-V(x,t))^2/(2\pi\theta(x,t))}. \tag{25}$$

The pre-factor $P = \dfrac{(1-p)}{p}$ (which takes into account both - the probability of not overtaking, as well as the finite space requirements of vehicles) is given by the expression :

$$P(\rho) = \frac{1-p(\rho)}{p(\rho)} = \frac{V^o\rho T^2}{\tau A_{max}(1-(\rho/\rho_{max})^2)}. \tag{26}$$

The above expression is obtained by assuming that at equilibrium, in the high density limit, vehicles try to maintain (on the average) a time headway of T to the vehicle ahead of them. The from of $P(\rho)$ is graphically depicted in Figure 3-3.

From the above, one can also represent $p(\rho)$, which represents the probability of overtaking, as in Figure 3-4. It can be seen that the model inherently assumes that the probability of overtaking decreases with increasing density of vehicles/km/lane.

The factor B (in Equation 24) that takes into account the anisotropic interaction effects, is given as

$$B(\delta_v) = \delta_v \frac{e^{-\delta_v^2/2}}{\sqrt{2\pi}} + (1+\delta_v^2)\int_{-\infty}^{\delta_v} dy \frac{e^{-y^2/2}}{\sqrt{2\pi}}. \tag{27}$$

where $\delta_v = (V - V_a)/\sqrt{\theta + \theta_a}$ with V_a and θ_a representing the average velocity and velocity variance computed at the interaction point x_a.

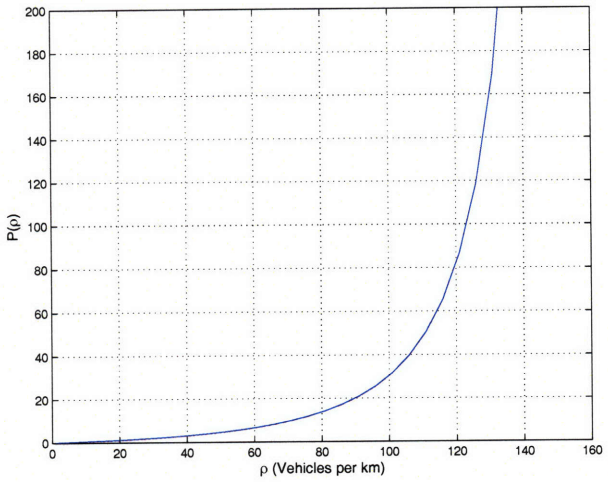

Figure 3-3: Profile of P as a function of ρ

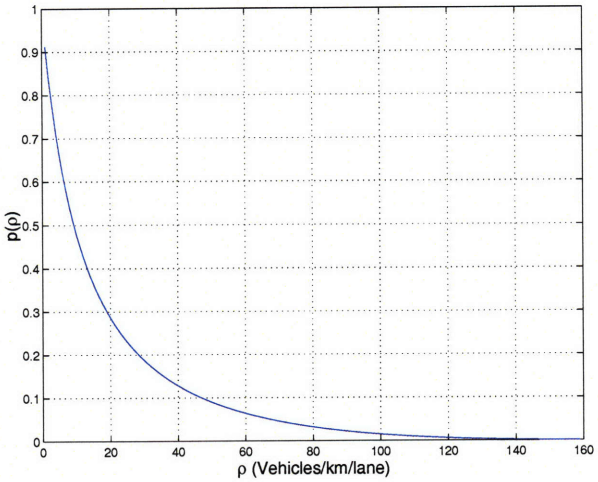

Figure 3-4: Profile of p as a function of ρ

One can see that Equations (13) and (14) (as also Equations (20) and (21)) represent a non-closed system of equations. Equations (13) and (20) governing the average density (which represents the zeroth velocity moment) depend on the average velocity (which is the first velocity moment). Equations (14) and (21) governing the average velocity in turn depend on the velocity variance (which is the second velocity moment). If we were to write down the PDE governing the evolution of the velocity variance, we would find that it depends on the skewness of the velocity distribution (which is the third velocity moment), and so on. In short, one gets a non-closed hierarchy of equations. An assumption of a Gaussian velocity distribution (as mentioned above and shown in Equation (25)) is used in conjunction with a closure expression for the velocity variance, (which is discussed below) to close the system of equations. Note that while eqn. (20) is already written in its conservative form, eqn. (21) can also be written in its conservative form as :

$$\frac{\partial(\rho V)}{\partial t} + \frac{\partial(\rho V^2 + \rho\theta)}{\partial x} = \rho\frac{V_e - V}{\tau}. \tag{28}$$

Equations (20) and (28) represent the form in which the continuity and momentum equations are used for their numerical solution.

3.3 Numerical data assumed

The following values have been assumed for the numerical data (when all vehicles are unequipped):

- Average desired velocity $Vo = 110$ km/hour. When all vehicles are unequipped, it is assumed that this velocity is set by the prevailing speed limit on the highway. In other words, it is assumed that all vehicles would like to drive at their maximum possible velocity, and the reason that they are unable to actually do so, is the presence of other vehicles on the highway.

- Average relaxation time $\tau = 15$ sec. This represents the average time constant of the exponential rate with which vehicles attain their desired velocity.

- The velocity variance $\theta(x,t)$ is assumed to be of the form $\theta = A(\rho)V(x,t)^2$, where $V(x,t)$ represents the average velocity. $A(\rho)$ is a density dependent pre-factor, that has been experimentally evaluated in [39], and found to be of the form :

  $A(\rho) = Ao + \Delta A(\tanh((\rho - \rho_c)/\Delta\rho) + 1)$

  where $Ao = 0.008; \Delta A = 2.5Ao; \rho_c = 0.27\rho_{max}; \Delta\rho = 0.05\rho_{max}; Amax = A(\rho_{max}) = 0.048$. This form of the velocity variance pre-factor is shown in Figure 3-5.

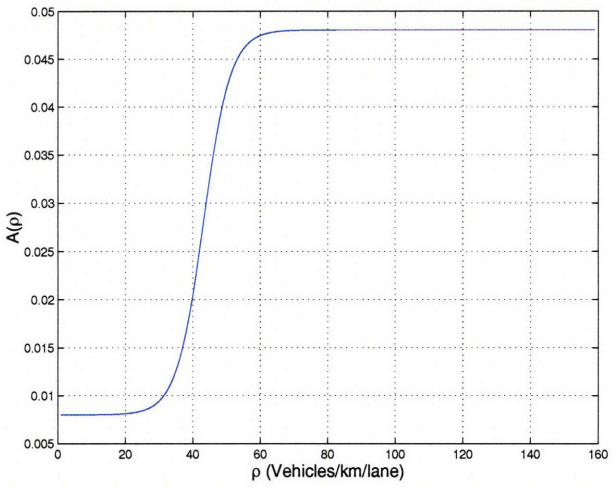

Figure 3-5: Variance Pre-factor Profile

- Maximum vehicle density $\rho_{max} = 160$ vehicles/km. This represents the maximum possible vehicle density when all the vehicles are at a standstill.

- Average time headway maintained $T = 1.5$ sec.

Using the above expressions, we get the profile of the average equilibrium velocity V_e as a function of ρ to be as given in Figure 3-6. Similarly, the velocity variance θ as a function of ρ is given in Figure 3-7.

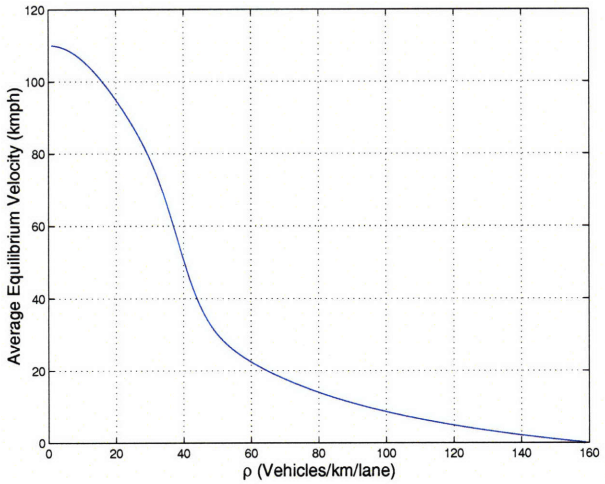

Figure 3-6: Equilibrium Average Velocity Profile

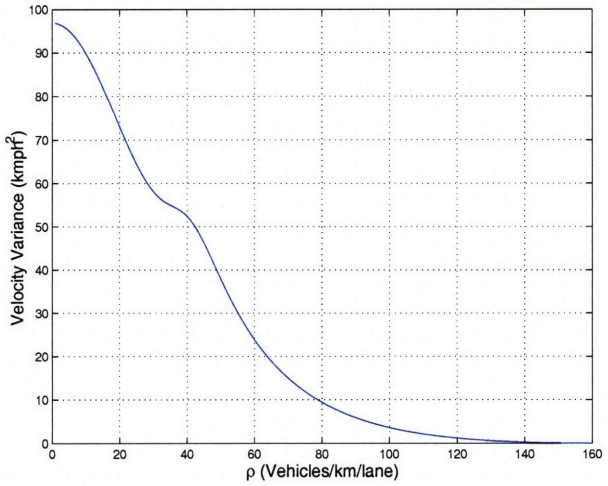

Figure 3-7: Velocity variance as a function of density

3.4 Demonstration of the link between the discrete and continuum models through DSMC

The aim of this section is to demonstrate the link between the discrete model adopted in Equations (1)-(3), along with the Boltzmann Equation, with the continuum model represented in Equations (20) and (28). In this section, we characterize the evolution of a set of particles from an arbitrary initial condition to an equilibrium condition. The equilibrium condition is defined by steady state, homogenous values of average velocity and velocity variance, for a given density.

Initial Conditions at the Discrete Level:

For the purposes of this section, we assume a circular highway of length 10 km with two lanes (with vehicles on both the lanes travelling in the same direction). The assumption of a circular highway allows us to ensure that vehicles exiting the highway at one point, re-enter the same highway. We do the demonstration for a vehicular density of $\rho = 20$ vehicles/km/lane. We therefor have a total of 400 vehicles on the 10 km length, two lane highway stretch. The initial positions of the vehicles are randomly determined as follows :

$x_{lh}(n_{lh}) = n_{lh}/20 - 0.01 + 0.02 * rand(1)$

$x_{rh}(n_{rh}) = n_{rh}/20 - 0.01 + 0.02 * rand(1),$

where $rand(1)$ indicates a random number uniformly distributed in $[0, 1]$. $n_{lh} \in [1, 200]$, $n_{rh} \in [1, 200]$ indicates a vehicle index number in the left and right lanes respectively; while $x_{lh}(n_{lh})$ and $x_{rh}(n_{rh})$ indicate the vehicle positions of the corresponding vehicle (in km). The initial velocities of the vehicles are randomly picked from a Gaussian distribution of specified mean and variance. In this section, we will consider two different initial conditions - these are as represented in Figure 3-8. Figure 3-9 shows one such sample of random initial distribution of velocities (these have been extracted from the second macroscopic intial condition shown in Figure 3-8), while Figure 3-10 represents one such sample of random initial inter-vehicle positions.

Through the run of the entire simulation, we also assume the presence of a vehicular acceleration noise. As indicated in Equations (4) and (5), this noise is assumed to

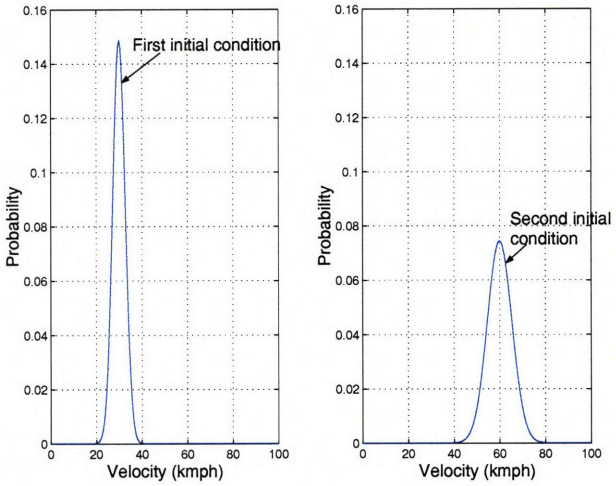

Figure 3-8: Representation of the two macroscopic initial conditions on velocity from which microscopic velocity samples are extracted

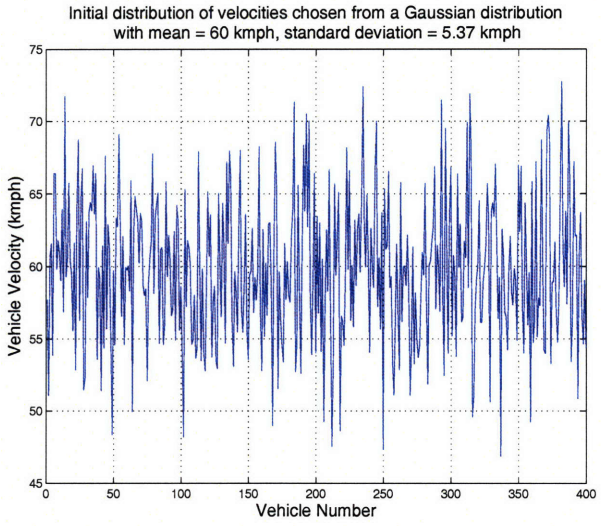

Figure 3-9: Initial Distribution of vehicular velocities

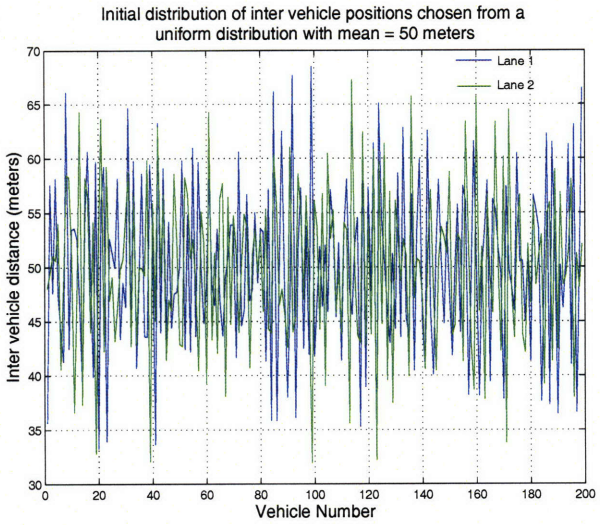

Figure 3-10: Initial Distribution of inter vehicular distances

be zero-mean, white noise with specified co-variance. The co-variance $2D$ of the noise is itself a function of the vehicular density (in accordance with the experimental data given in Figure 3-7. We have the relation $\theta_e = C - P\rho\tau\Gamma/2 + D\tau$ as a representation for the equilibrium velocity variance. In this relation, C represents the covariance of the velocity and the desired velocity of all the vehicles, and we can set this to be zero by setting the desired velocity of all the vehicles to be identical. With the further assumption of an equilibrium Gaussian velocity distribution, we can obtain the following figure of D vs. ρ, as given in Figure 3-11. In the simulations, we convert this acceleration noise to an equivalent velocity noise. The standard deviation σ of this velocity noise depends on the time step Δt. Figure 3-12 shows how the standard deviation of the velocity noise varies as a function of density and time step Δt. In our simulations, we use a time step $\Delta t = 0.05$ seconds, and for $\rho = 20$ vehicles/km/lane, this leads to $\sigma = 0.57$, as can be seen from Figure 3-12. Figure 3-13 then shows the velocity profile of a single driver driving on an empty stretch of a highway, with an assumed average velocity of 100 kmph , over a time span of 10000 seconds.

Discussion of the DSMC Method

We use DSMC (Discrete Simulation Monte Carlo) Methods to explain the link between the discrete vehicular model and the continuum model. The DSMC Method

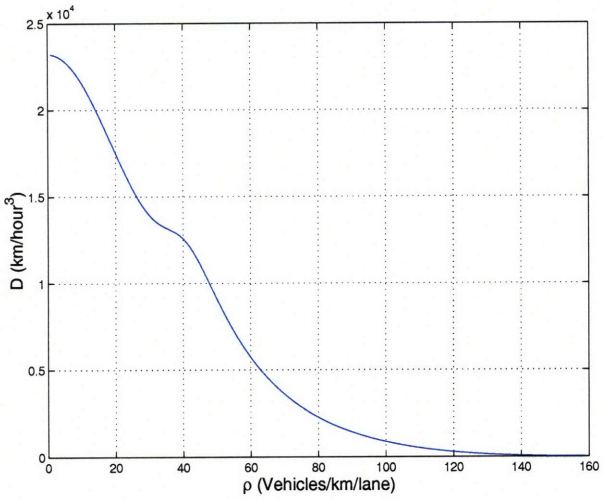

Figure 3-11: Variation of D as a function of ρ

was originally conceived by Bird to simulate molecular dynamics in gas flows. After the initialization process, the method postulates the following two operations to be performed, in sequence, in each time step Δt :

1) Update the position and velocity of each vehicle according to $\frac{dx}{dt} = v$; $\frac{dv}{dt} = \frac{V^o - v}{\tau} + \xi(t)$. This is the 'collisionless' process, wherein vehicular interactions are not considered.

2) Then, determine the number of vehicular interactions required to take place during that time step. Randomly, choose the vehicle pairs required to interact using an acceptance-rejection method (discussed below), so as to eventually process the total number of interactions required to be processed during that time step. Update the velocities of those vehicles that have interacted, by changing the velocity of the faster vehicle to equal that of the slower one, and leaving the velocity of the slower vehicle unchanged. Carry the left over fraction of unprocessed interactions to the next time step.

The reason that the process can be split into two steps is now discussed. The Boltzmann Equation can be written, using a shorthand notation, in the following form :

$$\frac{\partial \tilde{\rho}}{\partial t} = -H\tilde{\rho} + J\tilde{\rho} \tag{29}$$

where H is an operator that represents the effects of changes occurring in $\tilde{\rho}$ due to its convection in phase-space (i.e. the 'collisionless' process), and J is an operator that represents the effects of changes occurring in $\tilde{\rho}$ due to vehicular interactions (the 'collision' process). Then, we can write:

$$\tilde{\rho}(x, v, v^o, \Delta t) = \tilde{\rho}(x, v, v^o, 0) + \frac{\partial \tilde{\rho}(x, v, v^o, t)}{\partial t}|_{t=0} \Delta t$$

$$\Rightarrow \tilde{\rho}(x, v, v^o, \Delta t) = \tilde{\rho}(x, v, v^o, 0) - H\tilde{\rho}(x, v, v^o, 0)\Delta t + J\tilde{\rho}(x, v, v^o, 0)\Delta t$$

$$\Rightarrow \tilde{\rho}(x, v, v^o, \Delta t) = (1 - H\Delta t + J\Delta t)\tilde{\rho}(x, v, v^o, 0).$$

This in turn can be written as :

$$\tilde{\rho}(x, v, v^o, \Delta t) = (1 - H\Delta t)(1 + J\Delta t)\tilde{\rho}(x, v, v^o, 0) \tag{30}$$

by ignoring the second order terms in the above equation. The above equation thus states the principle of uncoupling the collisionless process from the collision process. In the first step, $\tilde{\rho}$ undergoes a change due to the operator H, and in the second stage, it undergoes a change due to the operator J.

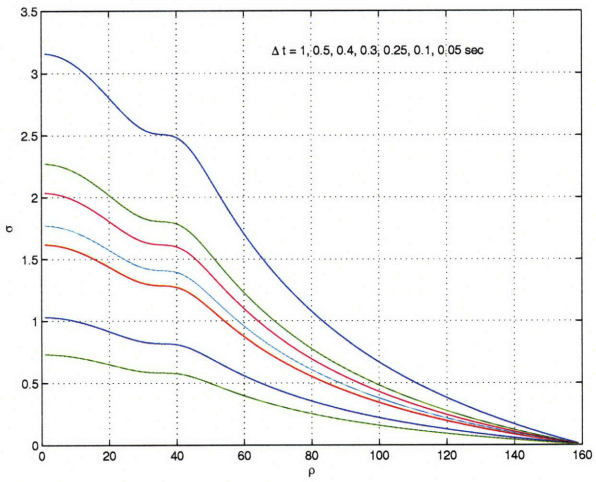

Figure 3-12: Standard deviation of vehicular noise as a function of density for varying Δt

In order to visualize the collision (i.e. vehicular interaction) process, we look at a pair of cells on the space-velocity plane, as shown in Figure 3-14. The number of collisions taking place between particles in a v cell and particles in a w cell (with both the velocity cells in the same x cell, and with $w < v$) during a time step Δt is obtained from the interaction terms of the Boltzmann equation (23) as :

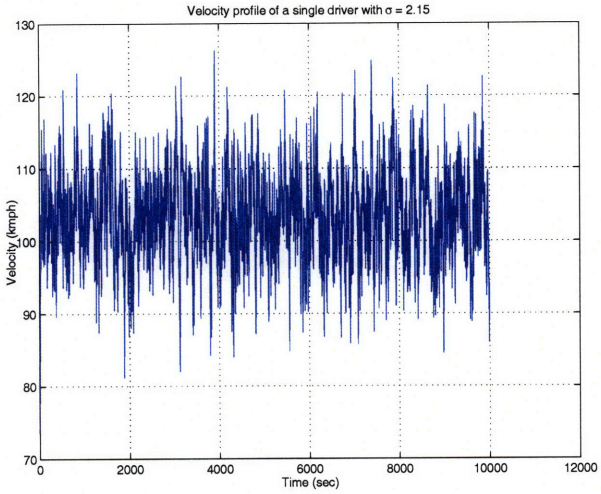

Figure 3-13: Individual Driver Noise

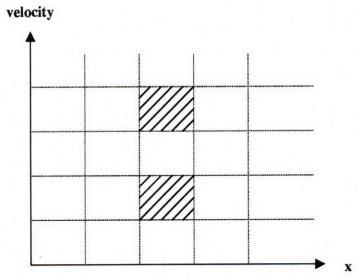

Figure 3-14: The space-velocity plane

$$\frac{(1-p(\rho))}{p(\rho)}\hat{\rho}(x,v,t)\hat{\rho}(x,w,t)|w-v|\Delta t\Delta x\Delta v \tag{31}$$

where Δx represents the width of an x cell and Δv represents the width of a velocity cell.

The total number of collisions taking place between particles in a v cell and particles in all the other velocity cells (lying in the same x cell, and with velocities less than v) during a time step Δt is then given as :

$$\frac{(1-p(\rho))}{p(\rho)}\hat{\rho}(x,v,t)(0.5\Sigma_{w<v}\hat{\rho}(x,w,t)|w-v|)\Delta t\Delta x\Delta v \tag{32}$$

where the summation sign is indicative of the trapezoidal integration being performed. Note that in the above collisions, the particles in the v cell represent the impeded particles, while the particles in all the other velocity cells with velocities less than v represent the impeding particles.

The total number of collisions taking place in a x cell during a time step Δt is then given by :

$$\frac{(1-p(\rho)}{p(\rho)}(0.5\Sigma_{v}\hat{\rho}(x,v,t)\Delta v(0.5\Sigma_{w<v}\hat{\rho}(x,w,t)|w-v|))\Delta t\Delta x\Delta v \tag{33}$$

Once we compute the total number of collisions to take place in a time step, it still remains to choose the particles that should actually collide (i.e. interact). Note that the probability of a collision between two particles is proportional to their relative velocity, i.e. a pair of particles with a higher velocity difference, is more probable to collide than a pair of particles with a lower velocity difference. In other words, given a pair of particles chosen at random, and given that their velocities are v and w, the probability of them having a collision is given by

$$P_{coll} = |w-v|/(0.5\Sigma_{v}\hat{\rho}(x,v,t)\Delta v(0.5\Sigma_{w<v}\Delta v\hat{\rho}(x,w,t)|w-v|)) \tag{34}$$

To suitably choose the particles that need to collide, we utilise an acceptance rejection procedure as follows: Pick two particles at random, and then compute P_{coll} for that pair of particles. Pick a random number uniformly distributed in $[0,1]$. If the number is less than P_{coll}, then accept the pair as a collision candidate; on the other hand, if the number is greater than P_{coll}, then reject the pair as a collision candidate. Continue this process until all the collisions in the cell have been processed.

Results of the Discrete Simulations

Figure 3-15 shows the velocity distribution of all the vehicles at time $t = 300$

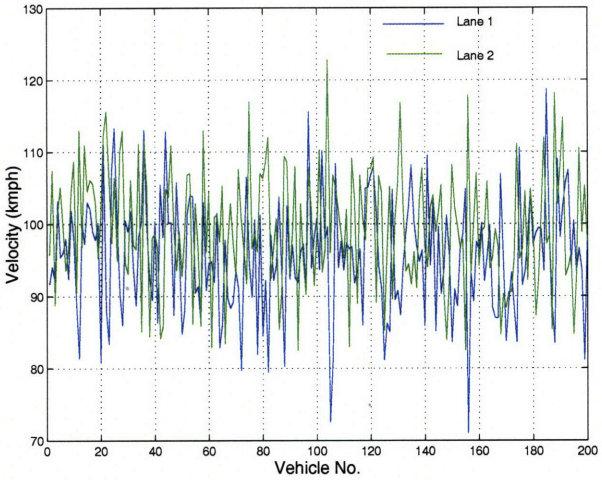

Figure 3-15: Velocity distribution of all the vehicles at $t = 300$ seconds

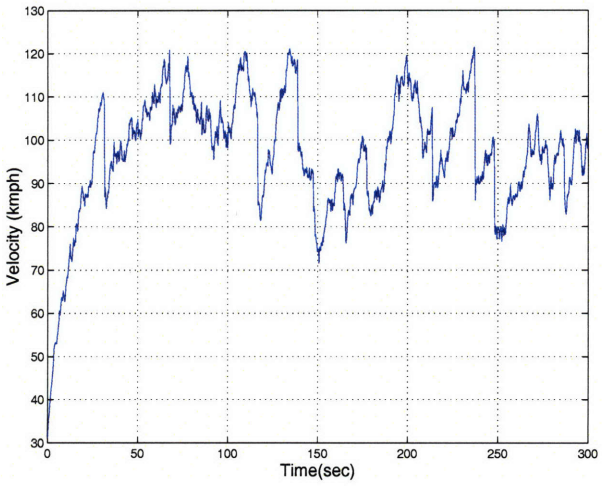

Figure 3-16: Velocity profile of a single vehicle picked at random

seconds, after they have evolved from the first initial condition given in Figure 3-8. Figure 3-16 shows the velocity profile of a randomly chosen vehicle, as a function of time. This figure clearly brings out all the different aspects of an individual vehicle's behavior - the desire to attain his chosen velocity v^o, the velocity reductions required to be performed everytime a slower vehicle is present in front that the trailing vehicle cannot overtake, as well as the velocity noise that is an intrinsic feature of every driver's behavior.

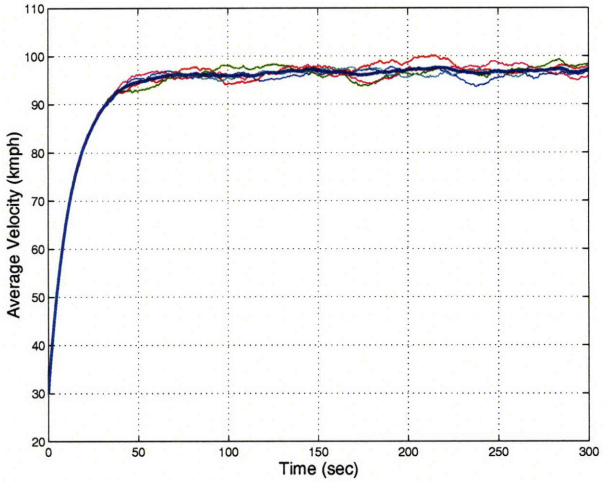

Figure 3-17: Relaxation of average velocity to its equilibrium value for 5 different simulations (i.e. 10 lanes) from different microscopic initial conditions that are derived from a single macroscopic initial condition

From data such as that given in Figure 3-15, and by evaluating this data at each time instant, we can compute the average velocity and velocity variance. Figure 3-17 shows the evolution of the average velocity of all the vehicles, as a function of time, from the first initial condition given in Figure 3-8. The five thin lines represent the average velocities obtained from five different simulations (with each simulation comprising of an average taken over two lanes). It can be seen that in each of the five simulations, the average velocity converges to an equilibrium value, and this convergence occurs at an exponential rate, and with a time constant of about 15 seconds. Furthermore, even though the five simulations are from the same macroscopic initial condition (given in Figure 3-8), they are from different microscopic intial conditions

(as explained earlier). The thick line then shows the average velocity after it has been further averaged over the five simulations. It can be clearly seen that the final average velocity very closely approximates the value given in the average equilibrium velocity vs. density diagram of Figure 3-6 (this figure shows an average velocity of about 95 kmph for the density of 20 vehicles/km/lane).

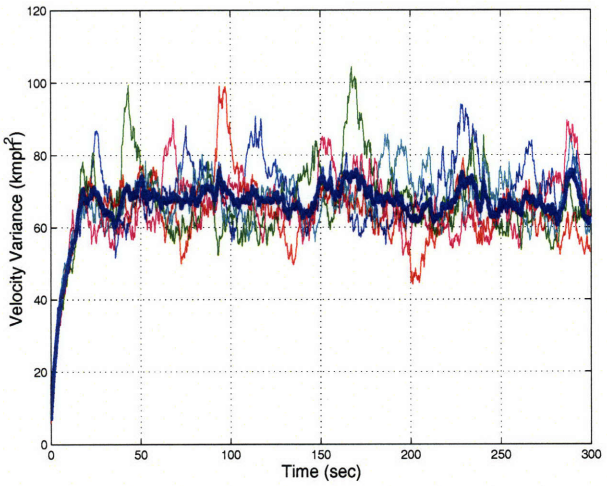

Figure 3-18: Relaxation of velocity variance to its equilibrium value for 5 different simulations (i.e. 10 lanes) from different microscopic initial conditions that are derived from a single macroscopic initial condition

From the same initial conditions used to obtain the results of Figure 3-17, we then look at plots of the evolution of velocity variance as a function of time. These are shown in Figure 3-18. In the case of velocity variance, the fact that there is convergence to an equilibrium value is not immediately apparent, when one looks at just a single simulation run. However, when we obtain the variance from the five simulation ensemble (as given by the thick line in the figure), one can begin to see convergence toward some sort of an equilibrium. Again, the relaxation to this equilibrium occurs exponentially. If we then take the time average of the velocity variance represented by the thick line, after it has relaxed to equilibrium, we find this value to very closely approximate the value given in the velocity variance vs. density diagram of Figure 3-7 (this figure shows a velocity variance of about 71 $kmph^2$ for the density of 20 vehicles/km/lane).

We then repeat the simulations for a second set of initial conditions, that are extracted from the second macroscopic initial condition shown in Figure 3-8. Figure 3-19 shows the relaxation of the average velocity to its equilibrium value, while Figure 3-20 shows the relaxation of the velocity variance to its equilibrium value. Again, while the relaxation of the average velocity to its equilibrium is visually apparent from a single simulation; the relaxation of velocity variance to an equilibrium becomes apparent only after extracting the variance from an ensemble of several simulations. These values are quite commensurate with the values obtained from the first initial condition. This is also brought out in Figures 3-21 and 3-22.

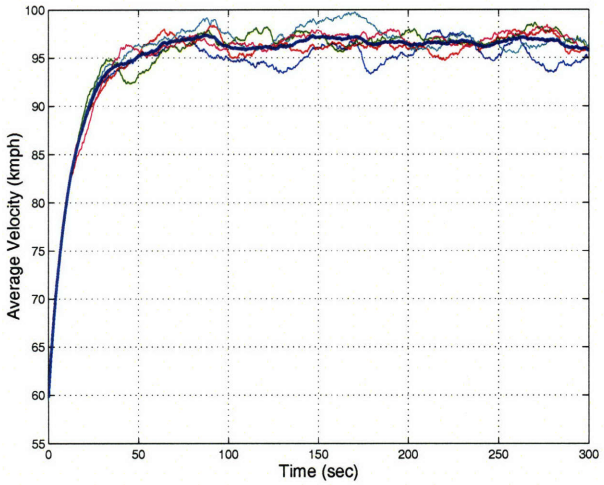

Figure 3-19: Relaxation of average velocity to its equilibrium value for 5 different simulations (i.e. 10 lanes) from different microscopic initial conditions that are derived from a single macroscopic initial condition

3.5 Derivation of macroscopic equations for two species - some vehicles equipped

3.5.1 The underlying Boltzmann Equation

Consider a system of equipped and unequipped vehicles, randomly mixed among each other, as shown in Figure 3-23. The unequipped vehicles are indexed by a subscript

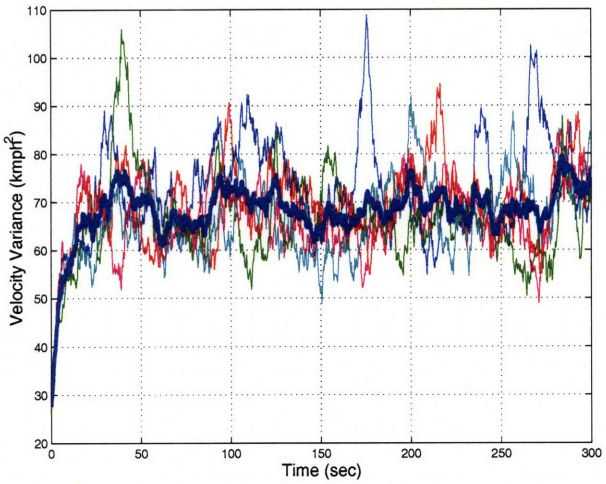

Figure 3-20: Relaxation of velocity variance to its equilibrium value for 5 different simulations (i.e. 10 lanes) from different microscopic initial conditions that are derived from a single macroscopic initial condition

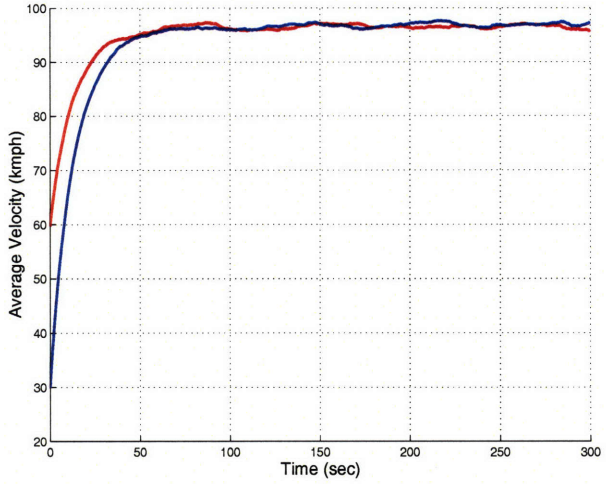

Figure 3-21: Relaxation of average velocity to its equilibrium value as obtained from an ensemble of 5 simulations (i.e. 10 lanes) from two different initial conditions

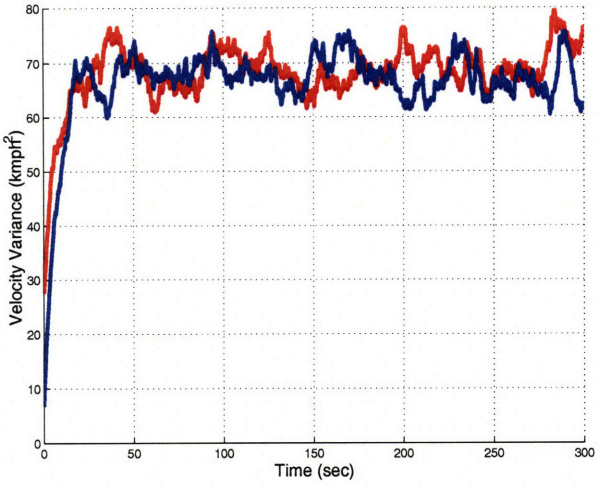

Figure 3-22: Relaxation of velocity variance as obtained from an ensemble of 5 simulations (i.e. 10 lanes) to its equilibrium value from two different initial conditions

u, while the equipped vehicles are indexed by a subscripte e. The state space vector of each unequipped vehicle is defined by $X_u(t) = [x_u(t), v_u(t), v^o{}_u(t)]$, where $x_u(t)$, $v_u(t)$ and $v^o{}_u(t)$ represent the position, velocity and desired velocity, respectively of the unequipped vehicle. Similarly, the state space vector of each equipped vehicle is defined by $X_e(t) = [x_e(t), v_e(t), v^o{}_e(t)]$, where $x_e(t)$, $v_e(t)$ and $v^o{}_e(t)$ represent the position, velocity and desired velocity, respectively of the equipped vehicle. The dynamics of u and e are then given by the following state space equations :

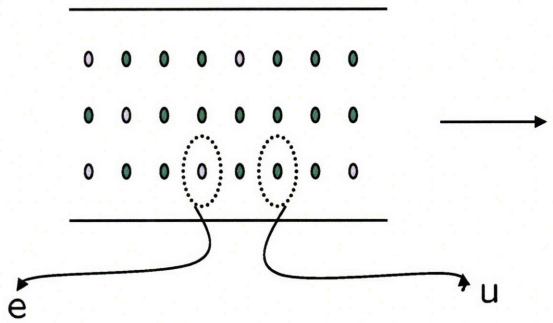

Figure 3-23: Schematic multi-vehicle scenario comprising of unequipped and equipped vehicles

$$\frac{dx_u}{dt} = v_u \tag{35}$$

$$\frac{dv_u}{dt} = \frac{v_u^o - v_u}{\tau_u} + \Sigma f_{uu} + \Sigma f_{eu} + \xi_u(t) \tag{36}$$

$$\frac{dv_u^o}{dt} = 0 \tag{37}$$

$$\frac{dx_e}{dt} = v_e \tag{38}$$

$$\frac{dv_e}{dt} = \frac{v_e^o - v_e}{\tau_e} + \Sigma f_{ue} + \Sigma f_{ee} + \xi_e(t) \tag{39}$$

$$v_e^o = v_{initial}^o, \quad t < t_o$$

$$v_e^o = v_{final}^o, \quad t \geq t_o \tag{40}$$

where t_o indicates the time instant at which the slowdown warning signal was received by that vehicle. Note that the time at which the warning is received, is different for different vehicles (owing to the finiteness of the signal transmission speed that we will implement in this formulation - we discuss this later).

In the above, Σf_{uu} represents the interaction effects caused to an unequipped vehicle due to the presence of other unequipped vehicles, while Σf_{ue} represents the interaction effects caused to an unequipped vehicle due to the presence of other equipped vehicles. Similarly, Σf_{ee} represents the interaction effects caused to an equipped vehicle due to the presence of other equipped vehicles, while Σf_{eu} represents the interaction effects caused to an equipped vehicle due to the presence of other unequipped vehicles. τ_u and τ_e represent the average relaxation times of the unequipped and equipped vehicles respectively; while ξ_u and ξ_e represent their respective acceleration noise. The acceleration noise of each vehicle is again assumed to be Gaussian white noise, with zero mean, and covariances given by D_u and D_e respectively.

We define $\tilde{\rho_u}(x, v, v^o, t)$ and $\tilde{\rho_e}(x, v, v^o, t)$ as the phase space density of the unequipped and equipped vehicles, respectively.

The Boltzmann equations for the unequipped and equipped vehicles are then given by an analogous reasoning as in the single species case :

$$\frac{\partial \tilde{\rho_u}}{\partial t} + \frac{\partial}{\partial x}(\tilde{\rho_u}\frac{dx}{dt}) + \frac{\partial}{\partial v}(\tilde{\rho_u}\frac{d\hat{v}}{dt}) + \frac{\partial}{\partial v^o}(\tilde{\rho_u}\frac{dv^o}{dt}) = (\frac{\partial \tilde{\rho_u}}{\partial t})_{int} + \frac{\partial(\tilde{\rho_u}D_u)}{\partial v^2} \tag{41}$$

$$\frac{\partial \tilde{\rho_e}}{\partial t} + \frac{\partial}{\partial x}(\tilde{\rho_e}\frac{dx}{dt}) + \frac{\partial}{\partial v}(\tilde{\rho_e}\frac{d\hat{v}}{dt}) + \frac{\partial}{\partial v^o}(\tilde{\rho_e}\frac{dv^o}{dt}) = (\frac{\partial \tilde{\rho_e}}{\partial t})_{int} + \frac{\partial(\tilde{\rho_e}D_e)}{\partial v^2}$$
$$+ \tilde{\rho_e}(x, v, t)\frac{P(v_{final}^o, x, t) - P(v_{initial}^o, x, t)}{T} \tag{42}$$

It can be seen that the above two equations are very similar in form to the Boltz-

mann equation for the single species (Equation (7)). The interaction terms however need to be modified to take care of cross-species interactions. It can be seen that we have

$$
\begin{aligned}
&(\frac{\partial\tilde{\rho_u}}{\partial t})_{int} = (1-p)\int_v^\infty dw \int_0^\infty dw^o |v-w| \tilde{\rho_u}(x,w,w^o,t)\tilde{\rho_u}(x,v,v^o,t) \\
&-(1-p)\int_0^v dw \int_0^\infty dw^o |w-v| \tilde{\rho_u}(x,w,w^o,t)\tilde{\rho_u}(x,v,v^o,t) \\
&+(1-p)\int_v^\infty dw \int_0^\infty dw^o |v-w| \tilde{\rho_e}(x,w,w^o,t)\tilde{\rho_u}(x,v,v^o,t) \\
&-(1-p)\int_0^v dw \int_0^\infty dw^o |w-v| \tilde{\rho_e}(x,w,w^o,t)\tilde{\rho_u}(x,v,v^o,t) \qquad (43)
\end{aligned}
$$

and analogously

$$
\begin{aligned}
&(\frac{\partial\tilde{\rho_e}}{\partial t})_{int} = (1-p)\int_v^\infty dw \int_0^\infty dw^o |v-w| \tilde{\rho_e}(x,w,w^o,t)\tilde{\rho_e}(x,v,v^o,t) \\
&-(1-p)\int_0^v dw \int_0^\infty dw^o |w-v| \tilde{\rho_e}(x,w,w^o,t)\tilde{\rho_e}(x,v,v^o,t) \\
&+(1-p)\int_v^\infty dw \int_0^\infty dw^o |v-w| \tilde{\rho_u}(x,w,w^o,t)\tilde{\rho_u}(x,v,v^o,t) \\
&-(1-p)\int_0^v dw \int_0^\infty dw^o |w-v| \tilde{\rho_u}(x,w,w^o,t)\tilde{\rho_u}(x,v,v^o,t) \qquad (44)
\end{aligned}
$$

and imposing the anisotropic and finite space requirements (as in the single species case), the above equations assume the form :

$$
\begin{aligned}
&(\frac{\partial\tilde{\rho_u}}{\partial t})_{int} = \tfrac{(1-p)}{p}\int_v^\infty dw \int_0^\infty dw^o |v-w| \tilde{\rho_{ua}}(x,w,w^o,t)\tilde{\rho_u}(x,v,v^o,t) \\
&-\tfrac{(1-p)}{p}\int_0^v dw \int_0^\infty dw^o |w-v| \tilde{\rho_u}(x,w,w^o,t)\tilde{\rho_{ua}}(x,v,v^o,t) \\
&+\tfrac{(1-p)}{p}\int_v^\infty dw \int_0^\infty dw^o |v-w| \tilde{\rho_{ea}}(x,w,w^o,t)\tilde{\rho_u}(x,v,v^o,t) \\
&-\tfrac{(1-p)}{p}\int_0^v dw \int_0^\infty dw^o |w-v| \tilde{\rho_e}(x,w,w^o,t)\tilde{\rho_{ua}}(x,v,v^o,t) \qquad (45)
\end{aligned}
$$

and analogously

$$
\begin{aligned}
&(\frac{\partial\tilde{\rho_e}}{\partial t})_{int} = \tfrac{(1-p)}{p}\int_v^\infty dw \int_0^\infty dw^o |v-w| \tilde{\rho_{ea}}(x,w,w^o,t)\tilde{\rho_e}(x,v,v^o,t) \\
&-\tfrac{(1-p)}{p}\int_0^v dw \int_0^\infty dw^o |w-v| \tilde{\rho_e}(x,w,w^o,t)\tilde{\rho_e a}(x,v,v^o,t) \\
&+\tfrac{(1-p)}{p}\int_v^\infty dw \int_0^\infty dw^o |v-w| \tilde{\rho_{ua}}(x,w,w^o,t)\tilde{\rho_u}(x,v,v^o,t) \\
&-\tfrac{(1-p)}{p}\int_0^v dw \int_0^\infty dw^o |w-v| \tilde{\rho_u}(x,w,w^o,t)\tilde{\rho_{ua}}(x,v,v^o,t) \qquad (46)
\end{aligned}
$$

where $\rho_{ua}(x,v,v^o,t) \equiv \rho_u(x_a,v,v^o,t)$ and $\rho_{ea}(x,v,v^o,t) \equiv \rho_e(x_a,v,v^o,t)$.

3.5.2 Macroscopic Equations and modeling the effects of a finite communication transmission speed

We define the following macroscopic quantities :

The average spatial densities of the unequipped and equipped vehicles (viz. $\rho_u(x,t)$

and $\rho_e(x,t)$ respectively) are defined as :

$$\rho_u(x,t) = \int dv^o \int dv \tilde{\rho_u}(x,v,v^o,t) \tag{47}$$

$$\rho_e(x,t) = \int dv^o \int dv \tilde{\rho_e}(x,v,v^o,t) \tag{48}$$

The average velocities of the unequipped and equipped vehicles (viz. $V_u(x,t)$ and $V_e(x,t)$ respectively) are defined as :

$$V_u(x,t) = \int dv^o \int v dv \frac{\tilde{\rho_u}(x,v,v^o,t)}{\rho_u(x,t)} \tag{49}$$

$$V_e(x,t) = \int dv^o \int v dv \frac{\tilde{\rho_e}(x,v,v^o,t)}{\rho_e(x,t)} \tag{50}$$

The velocity variances of the unequipped and equipped vehicles (viz. $\theta_u(x,t)$ and $\theta_e(x,t)$ respectively) are defined as :

$$\theta_u(x,t) = \int dv^o \int [v_u - V_u(x,t)]^2 dv \frac{\tilde{\rho_u}(x,v,v^o,t)}{\rho_u(x,t)} \tag{51}$$

$$\theta_e(x,t) = \int dv^o \int [v_e - V_e(x,t)]^2 dv \frac{\tilde{\rho_e}(x,v,v^o,t)}{\rho_e(x,t)} \tag{52}$$

Using the method of moments as in the single species case, the following macroscopic equations are obtained :

$$\frac{\partial \rho_u}{\partial t} + \frac{\partial(\rho_u V_u)}{\partial x} = 0 \tag{53}$$

$$\frac{\partial \rho_e}{\partial t} + \frac{\partial(\rho_e V_e)}{\partial x} = 0 \tag{54}$$

$$\frac{\partial V_u}{\partial t} + V_u \frac{\partial V_u}{\partial x} = \frac{-1}{\rho_u} \frac{\partial(\rho_u \theta_u)}{\partial x} + \frac{V_u^{eq} - V_u}{\tau} \tag{55}$$

$$\frac{\partial V_e}{\partial t} + V_e \frac{\partial V_e}{\partial x} = \frac{-1}{\rho_e} \frac{\partial(\rho_e \theta_e)}{\partial x} + \frac{V_e^{eq} - V_e}{\tau} \tag{56}$$

where $V_u^{eq}(x,t)$ represents the average equilibrium velocity of the unequipped vehicles and is given by :

$$V_u^{eq}(x,t) = V_u^o - PB_{uu}\rho_u \tau(\theta_u + \theta_{ua})/2 - PB_{ue}\rho_e \tau(\theta_u + \theta_{ea})/2 \tag{57}$$

where $V_e^{eq}(x,t)$ represents the average equilibrium velocity of the equipped vehicles and is given by :

$$V_e^{eq}(x,t) = V_e^o - PB_{eu}\rho_u \tau(\theta_e + \theta_{ua})/2 - PB_{ee}\rho_e \tau(\theta_e + \theta_{ee})/2 \tag{58}$$

In the above, $B_{ue}, B_{ee}, B_{eu}, B_{uu}$ have the same form as Bin Equation (27) except for the fact that we now have $B_{ue} = B(\delta v_{ue}); B_{uu} = B(\delta v_{uu}); B_{eu} = B(\delta v_{eu}); B_{ee} = B(\delta v_{ee});$, where $\delta v_{ue} = (V_u - V_{ea})/\sqrt{(\theta_u + \theta_{ea})}; \delta v_{eu} = (V_e - V_{ua})/\sqrt{(\theta_e + \theta_{ua})}; \delta v_{uu} = (V_u - V_{ua})/\sqrt{(\theta_u + \theta_{ua})}; \delta v_{ee} = (V_e - V_{ea})/\sqrt{(\theta_e + \theta_{ea})}$.

Note that while eqns. (53) and (54) are already written in conservative form, eqns.

(55) and (56) can also be written in its conservative form as :

$$\frac{\partial(\rho_u V_u)}{\partial t} + \frac{\partial(\rho_u V_u^2 + \rho_u \theta_u)}{\partial x} = \rho_u \frac{V_u^{eq} - V_u}{\tau} \tag{59}$$

$$\frac{\partial(\rho_e V_e)}{\partial t} + \frac{\partial(\rho_e V_e^2 + \rho_e \theta_e)}{\partial x} = \rho_e \frac{V_e^{eq} - V_e}{\tau} \tag{60}$$

In the above, we have $P = \frac{(\rho_u+\rho_e)T^2 V_{avg}^o}{\tau A_{\rho max}(1-((\rho_u+\rho_e)/\rho_{max})^2)}$ and $V_{avg}^o = (\rho_u V_u + \rho_e V_e)/(\rho_u + \rho_e)$. It is assumed that $\theta_u = A(\rho_u + \rho_e)V_u^2$ and $\theta_e = A(\rho_e + \rho_e)V_e^2$.

Equations (53), (54), (59) and (60) represent the form in which the continuity and momentum equations are used for their numerical solution.

The above equations are similar to the equations used in [41] when the two species of vehicles assumed were cars and trucks, and in that context, it was assumed that the desired velocities of the cars and trucks remained constant for all time. In the context of this work however, we assume that the equipped vehicles change their desired velocities instantaneously on receipt of the communication wave - we therefore define an additional variable $\gamma(x,t)$ and add in the following additional equations:

$$V_e^o = \gamma(x,t)V_{efinal}^o + (1 - \gamma(x,t))V_{einitial}^o \tag{61}$$

$$\frac{\partial \gamma}{\partial t} + a\frac{\partial \gamma}{\partial x} = 0, \tag{62}$$

where $\gamma(x,t)$ is a Heaviside step function defined such that $\gamma(x,t) = 0$ for that x (part of the highway that has not received the communication wave by time t), and $\gamma(x,t) = 1$ for all other x. Equation (61) thus implies that the moment an equipped vehicle at x receives the slowdown warning signal at a time t, its desired velocity changes instantaneously from its initial value $V_{einitial}^o$ (which is assumed to be the same as V_u^o - the desired velocity of the unequipped vehicles) to a final value of V_{efinal}^o (which is assumed to be approximately equal to the average velocity occurring at the degraded point far ahead, where a hazard has occurred). Equation (62) is a PDE that postulates the evolution of $\gamma(x,t)$ and in which $a < 0$ represents the communication speed. The boundary condition $\gamma(10,t) = 1$ is imposed.

We note that alternative formulations are also possible. For instance, if we assume that information of the location of the hazard is also broadcast to the equipped vehicles (along with the warning signal), then it is reasonable to assume that the driver of the equipped vehicle will adapt his desired velocity (as a function of distance to the hazard) so that he attains his final desired velocity by the time he reaches the

location of the hazard. In this case, we could rewrite Equation (61) as

$$V_e^o = \gamma(x,t)\left[(1-\alpha(x,t))V_{efinal}^o + \alpha(x,t)V_{einitial}^o\right] + (1-\gamma(x,t))V_{einitial}^o \quad (63)$$

where $\alpha(x,t)$ is a function that evolves according to the PDE

$$\frac{\partial \alpha}{\partial t} + V_e\frac{\partial \alpha}{\partial x} = -\frac{V_e}{d_0}, \quad (64)$$

with d_0 representing the average distance of an equipped car to the location of the hazard, when it first received the warning signal, and the initial condition on α is specified such that $\alpha(x,0) = 1$ for all x to the left of the hazard, and $\alpha(x,0) = 0$ for all x to the right of the hazard. The boundary condition on α would be $\alpha(0,t) = 1$.

3.6 Discussion of the initial conditions used

A good prototype of an initial condition used to test the influence of the slow-down warning system in a mixed equipment scenario, is the Reimann Problem. The Reimann Problem represents an initial condition comprising of a left state and a right state joined by a discontinuity, in each of the dependent variables, with the discontinuity occurring at the same spatial location for both variables. The left states are denoted by ρ_L and V_L, while the right states are denoted by ρ_R and V_R respectively. Schematically, such a condition is represented as shown in Figure 3-24.

In the Reimann Problems that we will consider, we will assume that $\rho_L < \rho_R$ and $V_L > V_R$. It can be seen that a large drop in average velocity, occurring over a short distance (in other words, a large negative spatial velocity gradient) is indicative of a potentially unsafe driving situation. We choose $\rho_L = 15$ vehicles/km/lane and $\rho_R = 140$ vehicles/km/lane. We assume that ρ changes from ρ_L to ρ_R over a length of 200 meters, which appears as a shock over a length scale of 10 km. Additionally, we will assume that the left and right states are both in their respective equilibrium (when all vehicles are unequipped). From Figure 3-6, it can be seen that this implies that $V_L = 105.67$ kmph and $V_R = 3.17$ kmph. Using the representation for velocity variance given above, we see that at the microscopic level, (with all vehicles unequipped), such a condition is indicative of a driver having to perform an instantaneous velocity change from an initial value that lies in the velocity probability density function $P(V_L)$

to a final value that lies in the velocity probability density function $P(V_R)$. $P(V_L)$ and $P(V_R)$ are represented in Figure 3-25. We use boundary conditions as follows : $\rho(0,t) = \rho(0,0); V(0,t) = V(0,0)$.

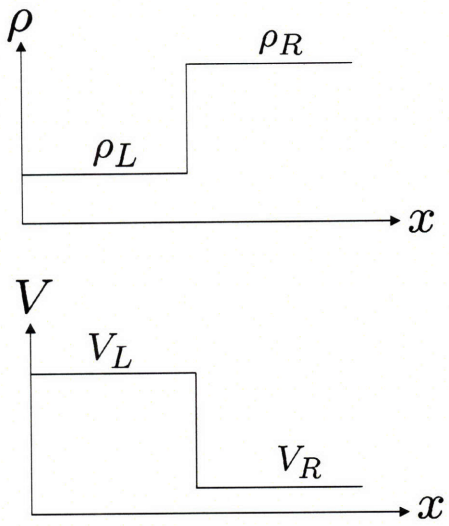

Figure 3-24: Reimann Problem

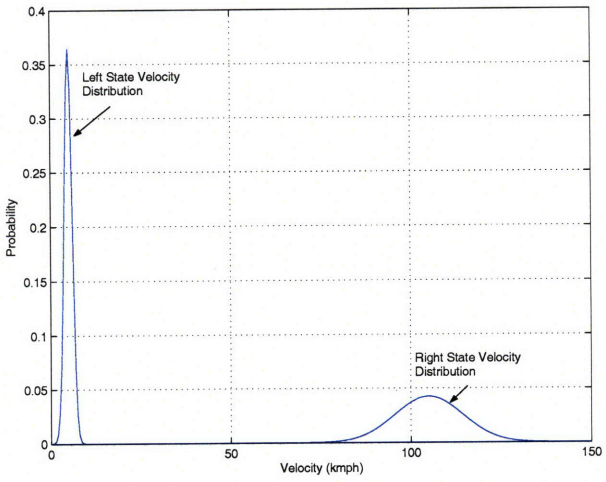

Figure 3-25: Initial conditions

A second initial condition of interest is one that is initially continous, but then propagates with time, in a manner such as to eventually form a shock. In other words, the initial (decreasing) average velocity profile steepens with time. It is of interest

to see how a partial equipment of the slowdown warning system can help arrest the wave steepening scenario that can exist (when all vehicles are unequipped), and to then parametrize this effect as a function of varying equipment.

For this purpose, we invoke an initial condition with identical left and right states as before, i.e. $\rho_L = 15$ vehicles/km/lane, $\rho_R = 140$ vehicles/km/lane and $V_L = 105.67$ kmph, $V_R = 3.17$ kmph; but instead of joining them by a discontinuity, we now join ρ_L to ρ_R by a gradual transition, so that the average density increases from ρ_L to ρ_R over a span of 2 km. The average velocity varies from V_L to V_R in a manner so that the average velocity is in equilibrium with the average density at each x.

3.7 PDE Solution Method used

The solution method used to solve the system of PDEs is the Lax Method (for the hyperbolic part) combined with an Implicit Euler Method (for the forcing function part). Given a system of PDE's of the form

$$\frac{\partial U}{\partial t} + \frac{\partial F(U)}{\partial x} = H$$

where $U(x,t), F(U)$ and $H(x,t)$ are vectors. The above representation assumes that the equations are written in conservative form, i.e. $F(U)$ represents the flux. Over each time step Δt, we first solve the system

$$\frac{\partial U}{\partial t} + \frac{\partial F}{\partial x} = 0 \tag{65}$$

using the Lax Method to obtain U^*, and then solve

$$\frac{\partial U}{\partial t} = H \tag{66}$$

using an Implicit Euler Method to obtain $U(x, t + \Delta t)$.

The Lax scheme is of the form

$$U_i^* = {U_i}^n - \tfrac{\Delta t}{\Delta x}({F_{i+\frac{1}{2}}}^n - {F_{i-\frac{1}{2}}}^n) \tag{67}$$

$$\text{where } {F_{i+\frac{1}{2}}}^n = 0.5({F_i}^n + {F_{i+1}}^n) - \frac{\lambda_i}{2}({U_{i+1}}^n - {U_i}^n) \tag{68}$$

$$\text{and } \lambda_i = \max_{[i,i+1]} \frac{\partial F}{\partial U} \tag{69}$$

λ_i denotes the magnitude of the largest eigenvalue of the Jacobian Matrix $\frac{\partial F}{\partial U}$, computed over the ith and $(i+1)$th cells.

After obtaining U_i^*, the same is then updated by an Implicit Euler Method as follows.

$$\frac{U_i^{n+1} - U_i^*}{\Delta t} = H(U_i^*) \tag{70}$$

3.8 Simulation results

Evolution of Initial Conditions when all vehicles are unequipped:

Figure 3-26 then shows the average density and average velocity profiles (for the Reimann Problem) as a function of space and time, when all the vehicles are unequipped. It can be seen that the initial large negative velocity gradient propagates, almost unattenuated, backwards along the highway. The wave speed at which it propagates is found as $\frac{\rho_L V_L - \rho_R V_R}{\rho_L - \rho_R} = -9.1 kmph$. Figure 3-27 shows the average driver trajectories on a space-time plane. On this figure too, the shock-like behavior is clearly seen.

The presence of a large negative gradient on an initial velocity condition can also be seen as a large negative perturbation on $\frac{\partial V}{\partial x}$. As can be seen from Figure 3-37, with all vehicles unequipped, $\frac{\partial V}{\partial x}$ attenuates in magnitude initially for a short while, only very slightly, and then propagates along unattenuated. If we define $||\frac{\partial V}{\partial x}||_\infty = \max_x \frac{\partial V}{\partial x}$ at a given time t, then the time history of $||\frac{\partial V}{\partial x}||_\infty$ is shown in Figure 3-38. In the next section, we will analyze how the same initial condition evolves in a situation of partial equipment with the slowdown warning system.

Figure 3-28 then shows the average density and average velocity profiles as they evolve with time, from the second initial condition. It is seen that the top portion of the velocity wave (and the bottom portion of the density wave) move forward relative to the highway, i.e. they have positive wave velocity; while the bottom portion of the velocity wave (as also the high density part of the density wave) move backwards, with a negative wave velocity. This kind of wave motion (wherein different parts of the wave have wave velocities of opposite signs), leads to further and further steepening of the wave, until eventually a shock is formed, that then moves backwards as a whole. The evolution of $||\frac{\partial V}{\partial x}||_\infty$ showing the gradual steepening of the wave is given in Figure 3-44, while Figure 3-43 gives the magnitude of ΔV, which represents the velocity change that occurs over the region where the value of $\frac{\partial V}{\partial x}$ is less than -100

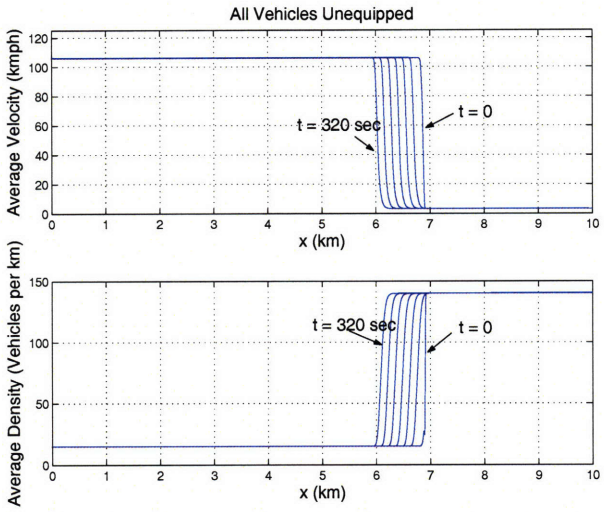

Figure 3-26: Average Velocity and Density profiles (All vehicles unequipped)

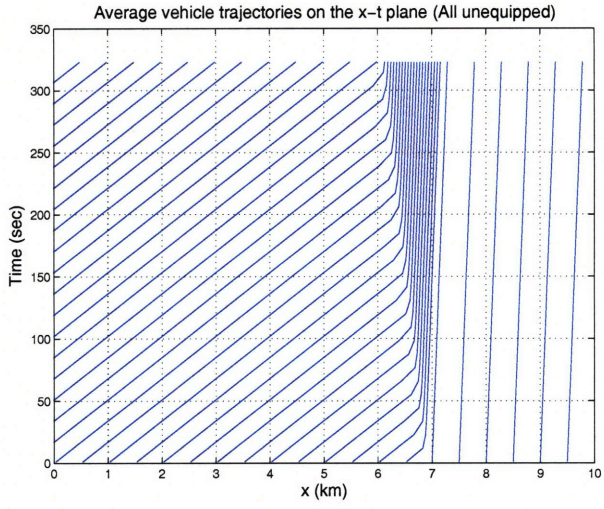

Figure 3-27: Average Vehicle trajectories on the x-t plane (All vehicles unequipped)

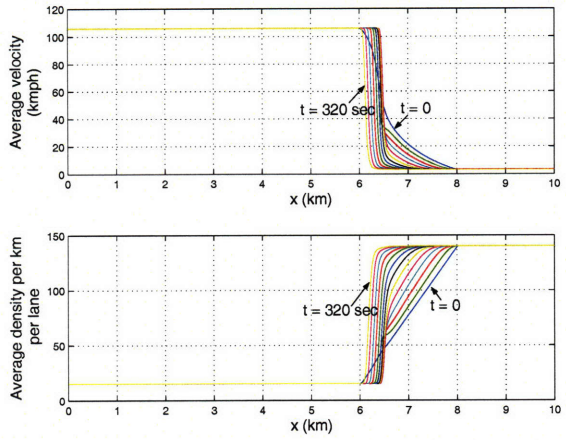

Figure 3-28: Average velocity and density profiles (all vehicles unequipped) for a continous initial condition

kmph/km. It is seen that over a span of approximately 5 minutes, ΔV increases to almost 100 kmph, which makes it almost identical to the initial condition of the first case we explored.

Evolution of First Initial Condition when some vehicles are equipped:

We now intend to test the above two initial conditions in a scenario of mixed equipment, schematically depicted in Figure 3-23. To this end, we assume that at $t = 0$, the average velocity of the equipped vehicles is identical to that of the unequipped vehicles. $\rho_u(x,t)$, $V_u(x,t)$ are used to represent the average density and average velocity of the unequipped vehicles, while $\rho_e(x,t)$ and $V_e(x,t)$ represent the average density and average velocity of the equipped vehicles. To test the effect of varying equipment, we vary ρ_u and ρ_e, so that $\frac{\rho_e(x)}{\rho_u(x)+\rho_e(x)}$ represents the percentage of equipment at each x, and we keep $\rho_u(x,0) + \rho_e(x,0) =$ a constant which is equal to the density of vehicles when they were all unequipped. In other words, $\rho_{uL}(x,0) + \rho_{eL}(x,0) = \rho_L(x,0)$; $\rho_{uR}(x,0) + \rho_{eR}(x,0) = \rho_R(x,0)$; $V_{uL}(x,0) = V_{eL}(x,0)$; $V_{uR}(x,0) = V_{eR}(x,0)$, where the values for ρ_L, ρ_R, V_L and V_R correspond to the values when all vehicles were unequipped (as discussed in the previous section).

For the first initial condition, we assume an average communication speed of 25 kmph, relative to the highway, and moving backwards. Such a communication speed can be achieved from an initial velocity of about 100 kmph, if the velocity threshold

is approximately 25 kmph, coupled with a transmission range of about 500 meters. In other words, everytime an equipped vehicle (that is travelling at an initial velocity of around 100 kmph) receives the warning signal and begins to slow down (in anticipation of the hazard ahead); and then throws the signal back by 500 meters once its velocity falls below a threshold of 25 kmph; then this will result in a communication wave travelling backwards at around 25 kmph (on an average), relative to the highway.

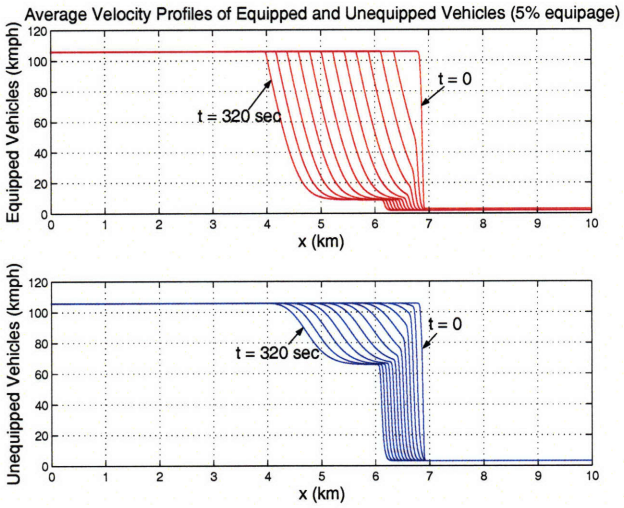

Figure 3-29: Average Velocity profiles of Equipped and Unequipped Vehicles (5% equipment)

Figure 3-29 shows the average velocity profiles of the equipped and unequipped vehicles respectively (for a 5% equipment scenario), while Figure 3-30 shows the average density profiles of the same. It can be seen that as the communication wave propagates through the equipped vehicles, causing them to slow down, the unequipped vehicles are also forced to slow down earlier than they otherwise would have (they thus receive indirect information of the hazard ahead). The wave velocity of the top portion of the average velocity of the unequipped vehicles has now become negative (it was formerly positive when they had no equipped vehicles among their midst); and this in turn has led to a lower magnitude of the average velocity shock experienced by the unequipped vehicles. Figure 3-31 shows the average vehicle trajectories of the equipped and unequipped vehicles, on a $x - t$ plane. The propagation of the

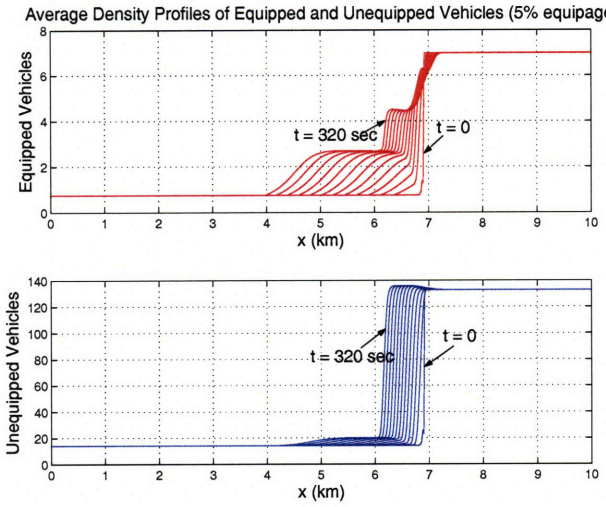

Figure 3-30: Average Density profiles of Equipped and Unequipped Vehicles (5% equipment)

communication wave is also seen.

Figure 3-34 then demonstrates the average velocity profiles of the unequipped vehicles, for varying degrees of equipment, while Figure 3-36 demonstrates the magnitude of the velocity shock as a function of time, for the different equipments. It is seen from Figure 3-36 that the largest reduction in ΔVthat can occur with a 5% increase in equipment, occurs in the $0-5\%$ range. With 10% equipment, the velocity shock magnitude in the unequipped vehicles is reduced almost by a factor of one-half, for equipments above 15%, the magnitude of benefit obtained (as measured from the reduction in shock strength of the unequipped vehicles per unit increase in the density of the equipped vehicles), is not significantly increased. This behavior is also manifested in Figure 3-37 as also Figure 3-38, which demonstrates $||\frac{\partial V_u}{\partial x}||_\infty$, as a function of time.

Evolution of Second Initial Condition when some vehicles are equipped:

After our discussion on the Reimann Problem, we now direct our attention towards the second initial condition studied earlier, i.e. a situation wherein an initially continuous condition, evolved with time, to get progressively steeper and eventually appear like a discontinuity. In this case, we test two different scenarios : in the first,

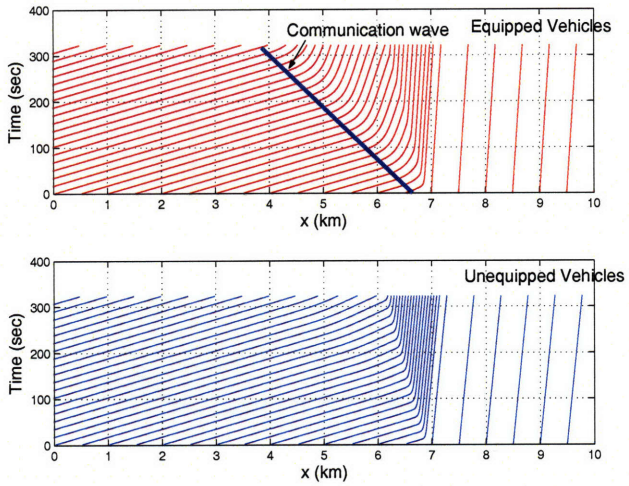

Figure 3-31: Average Vehicle trajectories of Equipped and Unequipped Vehicles on the x-t plane (5% equipment)

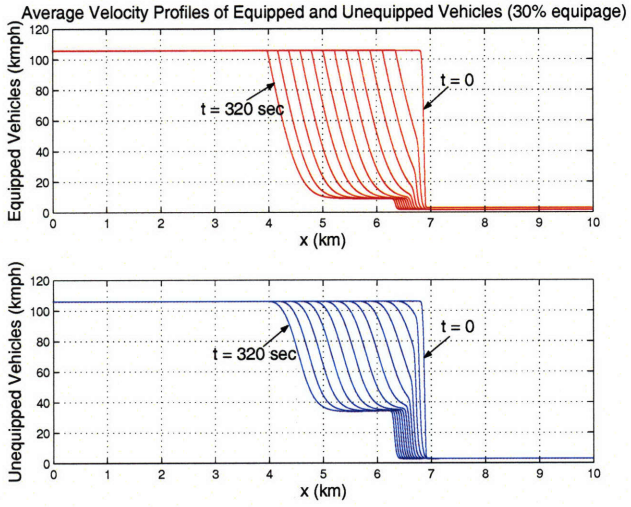

Figure 3-32: Average Velocity profiles of Equipped and Unequipped Vehicles (30% equipment)

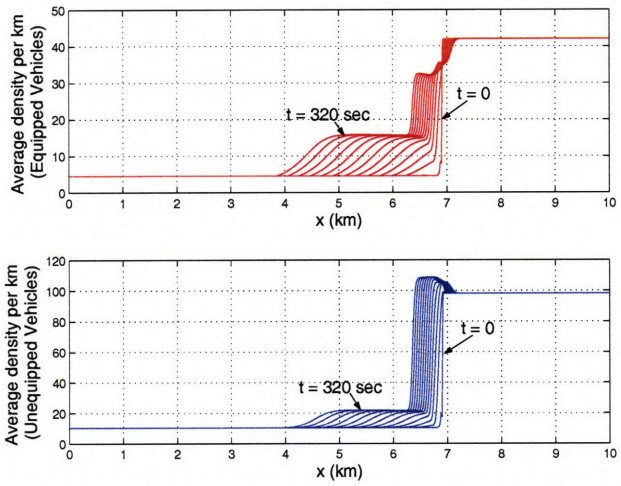

Figure 3-33: Average Density profiles of Equipped and Unequipped Vehicles (30% equipment)

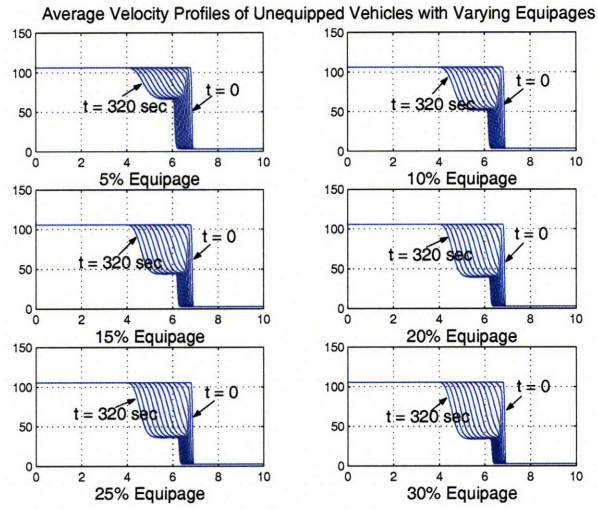

Figure 3-34: Average Velocity profiles of unequipped vehicles with varying levels of equipment

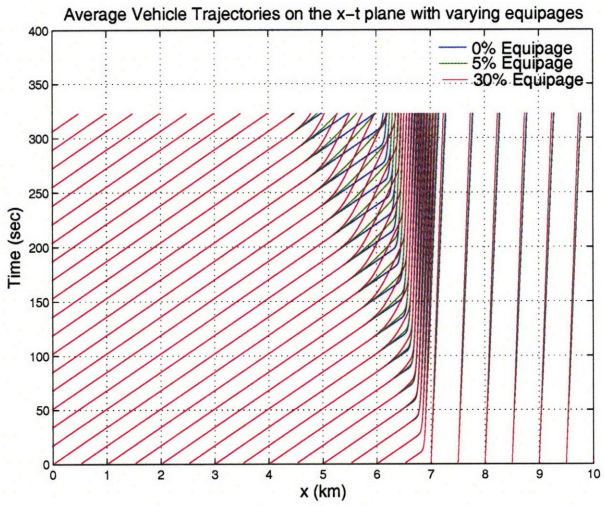

Figure 3-35: A comparison of the average driver trajectories of the unequipped vehicles on the x-t plane with varying levels of equipment

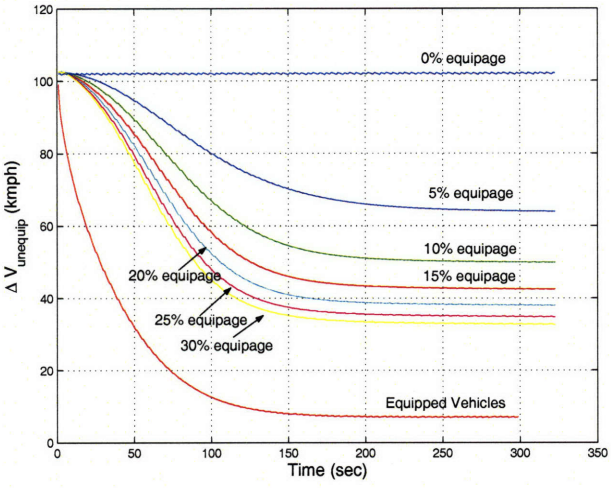

Figure 3-36: Magnitude of ΔV for different percentages of equipment

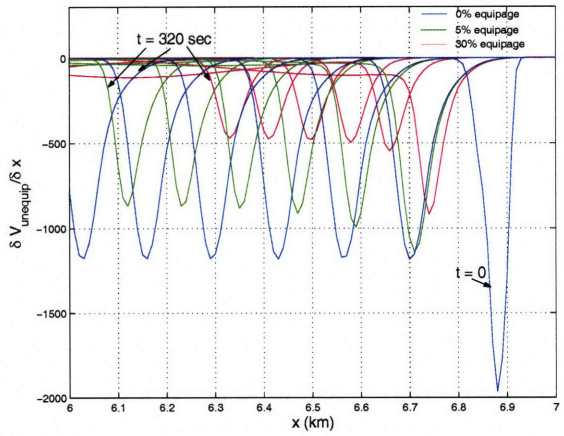

Figure 3-37: $\frac{\partial V_u}{\partial x}$ for varying levels of equipment for the Reimann Problem

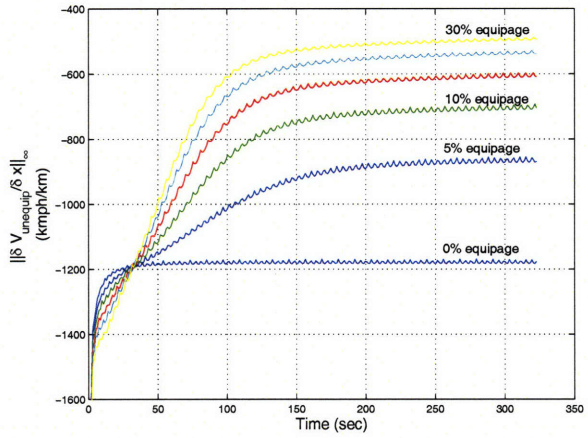

Figure 3-38: $||\frac{\partial V_u}{\partial x}||_\infty$ for varying levels of equipment for the Reimann Problem

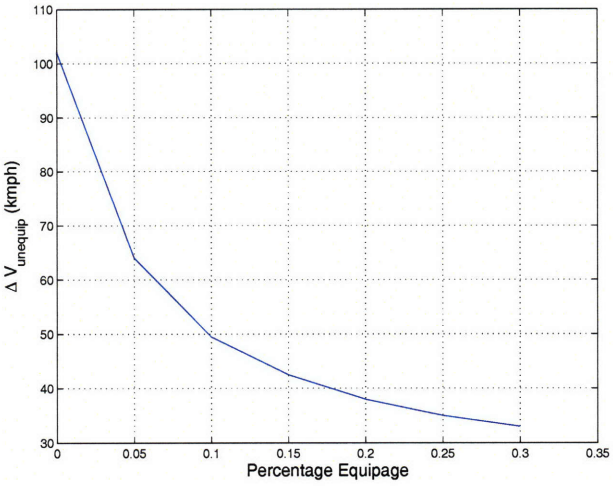

Figure 3-39: Magnitude of ΔV_u at steady state for different percentages of equipment

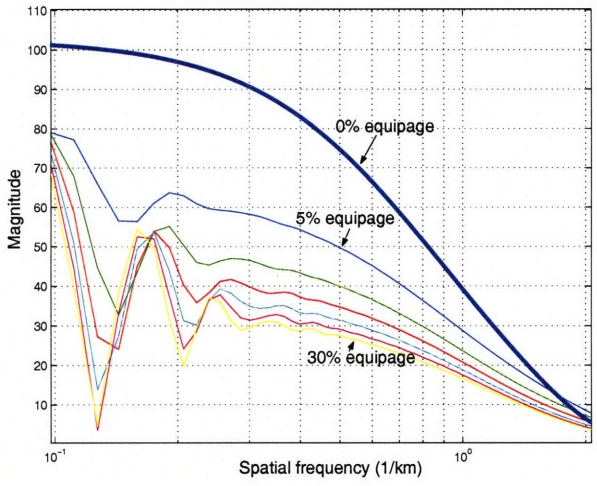

Figure 3-40: Spatial frequency content of $\frac{\partial V_u}{\partial x}$ for different percentages of equipment

we assume that information of the existence of a velocity gradient is made available to the equipped vehicles residing to the left of the point $x = 6km$, at $t = 0$; while in the second, we assume that information of low velocity conditions ahead is made available to the equipped vehicles residing to the left of the point $x = 8km$. Again, in either case, the communication wave is assumed to travel at a constant speed of 25 kmph, in the backward direction; this time originating from $x = 6km$, at $t = 0$ (in the first case) and originating from $x = 8km$, at $t = 0$ in the second. The reason that this case is interesting is because it enables us to see if and how varying levels of equipment can arrest the formation of the discontinuity, before it has developed.

Figure 3-41 shows the average velocity profiles of the equipped and unequipped vehicles for the first scenario (assuming 30% level of equipment). It is seen that the top portion of the average velocity (which had positive wave velocity when all vehicles were unequipped, i.e. it was moving forward relative to the highway), now immediately begins to move backwards as the communication wave passes through the equipped vehicles. This arrests the wave steepening effect that was present in the case of no equipment; and consequently the equipped vehicles do not experience any abrupt velocity gradient, while the unequipped vehicles experience a significantly reduced magnitude of negative velocity gradient, than they otherwise would have.

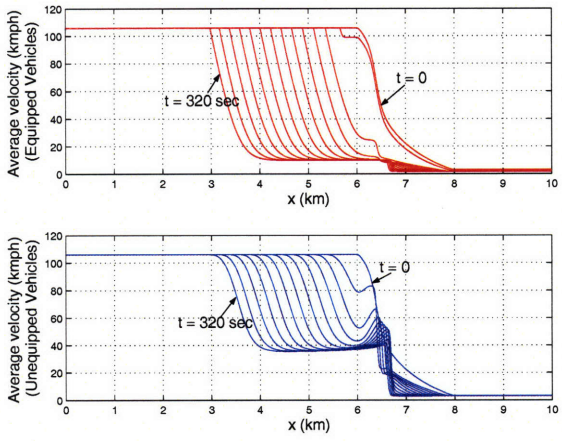

Figure 3-41: Average velocity profiles of equipped and unequipped Vehicles (30% equipment) for the continous initial condition (first information propagation scenario)

Figure 3-42 demonstrates the average velocity profile of the unequipped vehicles for

varying levels of equipment, while Figure 3-43 shows the time history of the magnitude of ΔV for the unequipped vehicles, with ΔV representing the average velocity change of the unequipped vehicles over the region where $\frac{\partial V_u}{\partial x}$ is smaller than -100 kmph/km. It is seen from Figure 3-42 that again a 5% equipment causes greatest reduction in ΔV and that above an equipment of 15%, the benefit obtained per unit increase in percentage equipment, is not significantly greater. The same effect is manifested in Figure 3-44 that shows $||\frac{\partial V_u}{\partial x}||_\infty$.

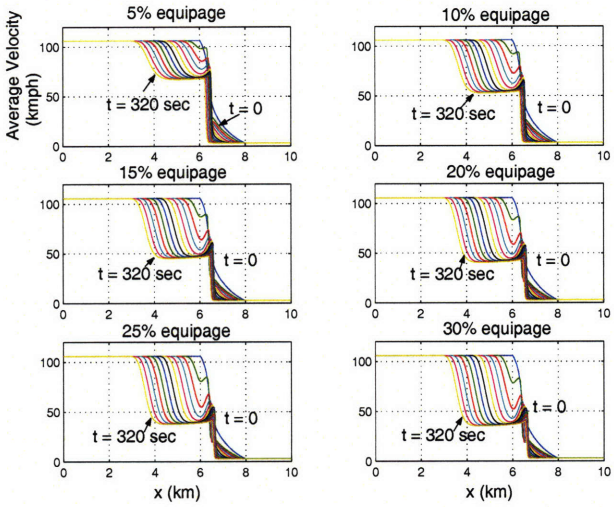

Figure 3-42: Average velocity profiles of unequipped Vehicles for varying levels of equipment for the continous initial condition(first information propagation scenario)

Figure 3-45 then shows the average velocity profile for the same initial condition, but for the second scenario, i.e. we now assume that information of the low velocity originates from $x = 8km$, and this travels backwards at the communication speed of $25kmph$. In this case, it is seen that the wave does steepen for a while - both the equipped and unequipped vehicles experience increasingly sharper negative velocity gradients for close to 3 minutes, before the smoothening effect of the slowdown warning system sets in. The reason that they experience the wave steepening for a while can be attributed to the fact that the top (high velocity) portion of the velocity wave continues to move forward for a while, before the communication wave comes upon it. This effect is also seen in Figures 3-46 and 3-47. This thus demonstrates that for

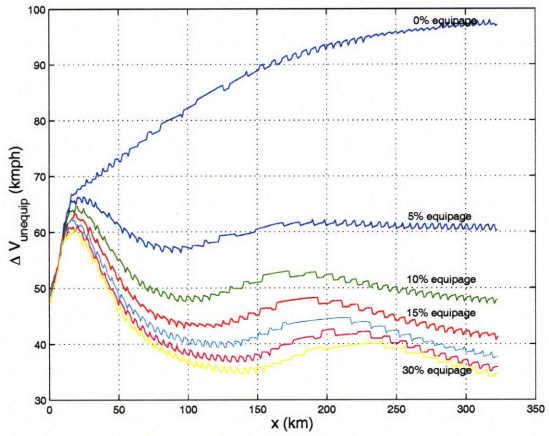

Figure 3-43: Magnitude of ΔV_u for varying levels of equipment for the continous initial condition(first information propagation scenario)

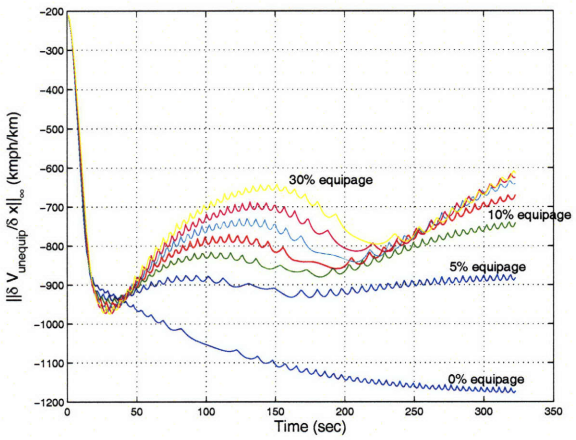

Figure 3-44: $||\frac{\partial V_u}{\partial x}||_\infty$ for varying levels of equipment for the continous initial condition(first information propagation scenario)

this initial condition, a communication speed of 25 kmph is adequate if it originates from the left end of the velocity gradient (as in the first scenario), but it is inadequate if it originates from the right end of the velocity gradient (as in the second scenario).

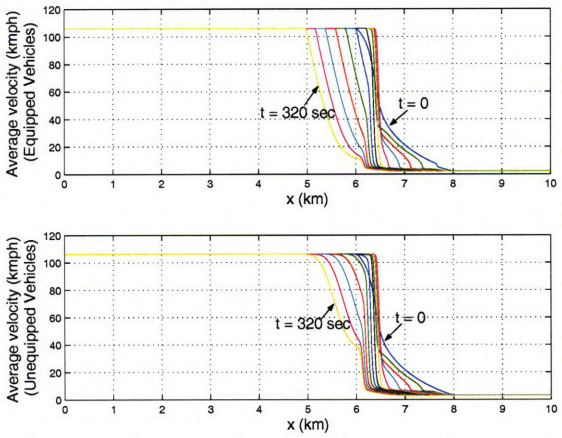

Figure 3-45: Average velocity profiles of equipped and unequipped Vehicles (30% equipment) for the continous initial condition(second information propagation scenario)

Results assuming an endogenous communication wave:

The preceding results have all been generated assuming an exogenous communication wave, i.e. the communication wave travels through the equipped vehicles at a pre-specified average rate a (which we took to be 25 kmph). In this section, we investigate the use of an endogenous communication wave in the model. We assume that whenever the average velocity of the equipped vehicles $V_e(x,t)$ at a point falls below some pre-specified threshold V_{eth}, then the warning signal is thrown backwards from that point on through a distance T_{range} (T_{range} thus specifies the transmission range of the warning signal). We investigate the use of variable values of T_{range} for a given V_{eth}, and parametrize the velocity gradients of the unequipped vehicles $\frac{\partial V_u}{\partial x}$ as a function of both the percentage of the equipped vehicles, as well as T_{range}. We do this for the Reimann Problem.

Figure 3-48 shows the average velocity profiles of the equipped and unequipped vehicles (for a 30% equipment scenario), when we assume an equipped vehicle average velocity threshold of 25 kmph accompanied with a transmission range of 400 meters.

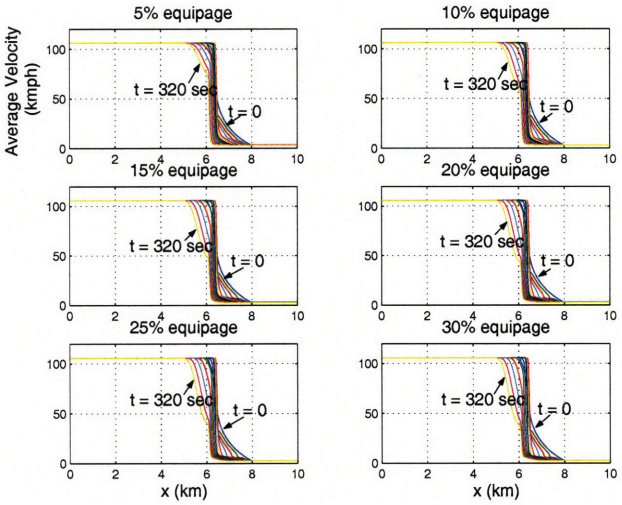

Figure 3-46: Average velocity profiles of unequipped Vehicles for varying levels of equipment for the continous initial condition(second information propagation scenario)

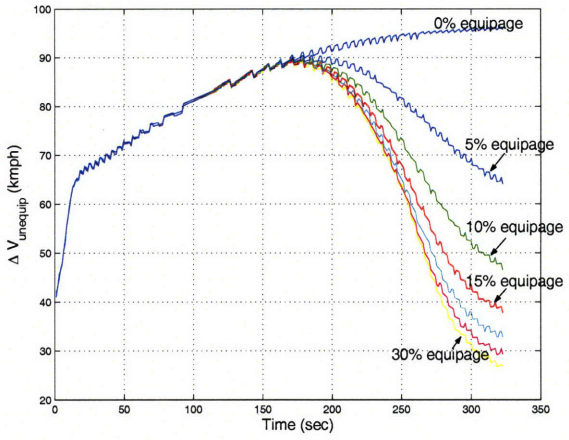

Figure 3-47: Magnitude of ΔV_u for varying levels of equipment for the continous initial condition(second information propagation scenario)

As can be seen from the figure, while the shock magnitude of the equipped vehicles is considerably weakened (as compared to the case when all vehicles were unequipped, see Figure 3-26), it is not weakened as significantly as in Figure 3-32. In the case of the unequipped vehicles, the shock magnitude is hardly reduced, if at all.

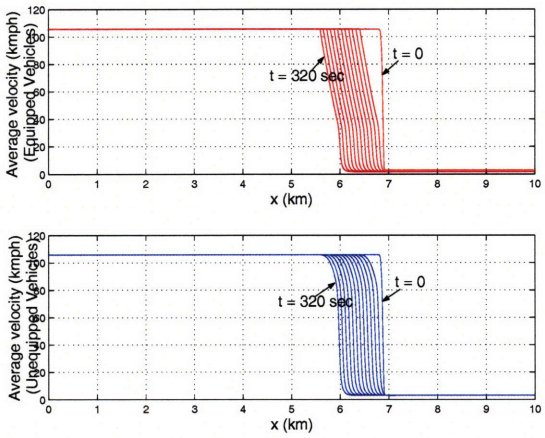

Figure 3-48: Average velocity profiles of the equipped and unequipped vehicles for the Reimann Problem for an endogenous communication wave generated using V_{eth} = 25 kmph and T_{range} = 400 meters

However, if we increase the transmission range to 500 meters, then (using the same equipped vehicle average velocity threshold as before), a considerable weakening of the shock magnitudes of both the equipped and unequipped vehicles is seen. This is brought out in Figure 3-49, which shows the average velocity profiles for this situation. Figure 3-50 shows a comparison of ΔV_u for the two different values of T_{range}, while Figure 3-51 shows a comparison of $\frac{\partial V_u}{\partial x}$. It can be clearly seen that the benefit obtained with a transmission range of 400 meters is not significant, whereas that obtained with a range of 500 meters is. The reason for this is that the larger range of 500 meters (when accompanied by a average velocity threshold of 25 kmph) enables the communication wave to travel backwards faster than the shock would have propagated when all vehicles were unequipped. If we use a higher average velocity threshold, then a smaller tranmission range would have been adequate. A higher average velocity threshold however, would increase the probability of false alarms.

Figures 3-48, 3-49, 3-50, 3-51 have all been generated for a 30% equipment sce-

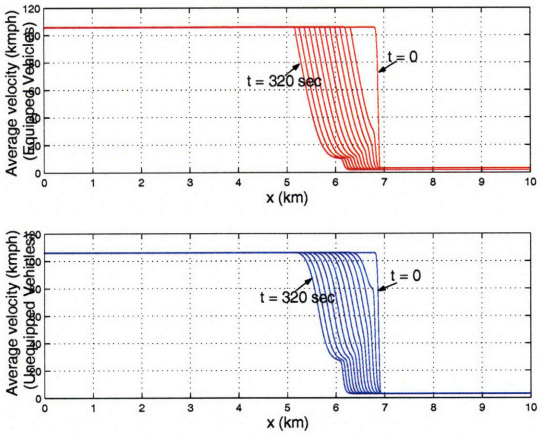

Figure 3-49: Average velocity profiles of the equipped and unequipped vehicles for the Reimann Problem for an endogenous communication wave generated using V_{eth} = 25 kmph and T_{range} = 500 meters

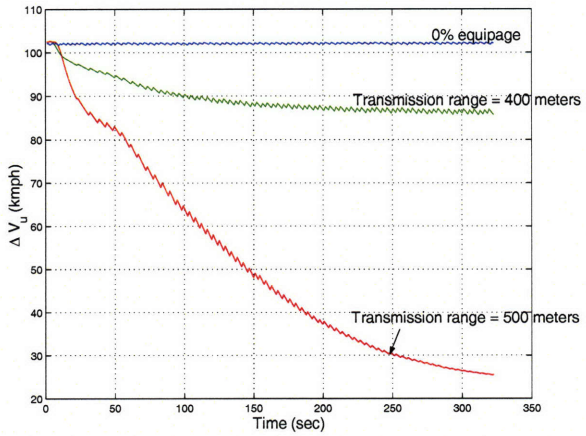

Figure 3-50: A comparison of ΔV_u for the Reimann Problem assuming 30% equipment and an endogenous communication wave generated using V_{eth} of 25 kmph

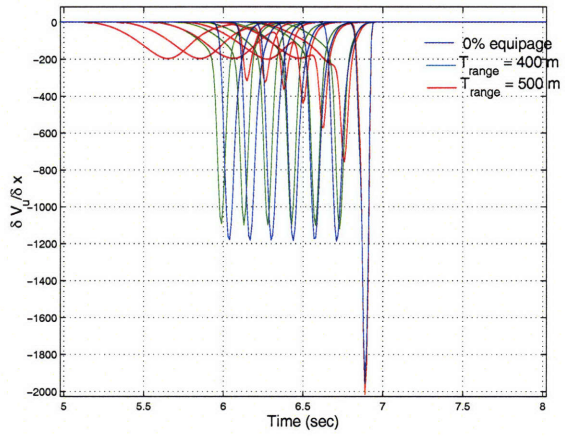

Figure 3-51: A comparison of $\frac{\partial V_u}{\partial x}$ for the Reimann Problem assuming 30% equipment and an endogenous communication wave generated using $V_{eth} = 25$ kmph

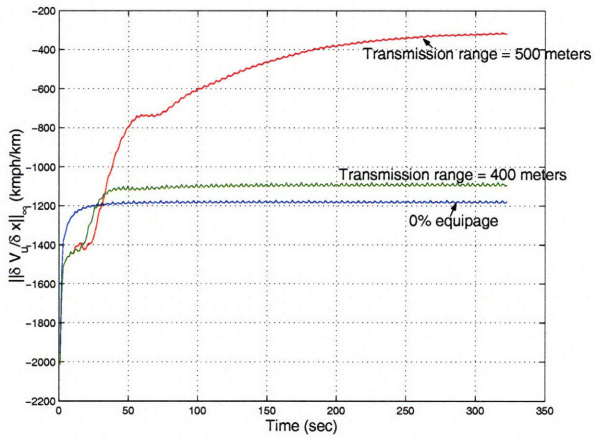

Figure 3-52: A comparison of $||\frac{\partial V_u}{\partial x}||_\infty$ for the Reimann Problem assuming 30% equipment and an endogenous communication wave generated using $V_{eth} = 25$ kmph

nario. Since they bring out the fact that the transmission range of 400 meters is inadequate for the 30% equipment scenario, it is clear that this value of T_{range} would also be inadequate for lower values of equipment. Figure 3-53 shows the behavior of the velocity gradient waves for varying percentages of equipment, while assuming $T_{range} = 500$ meters. It demonstrates that a transmission range of 500 meters, with about 15% equipment appears to be adequate for this prototype Reimann Problem.

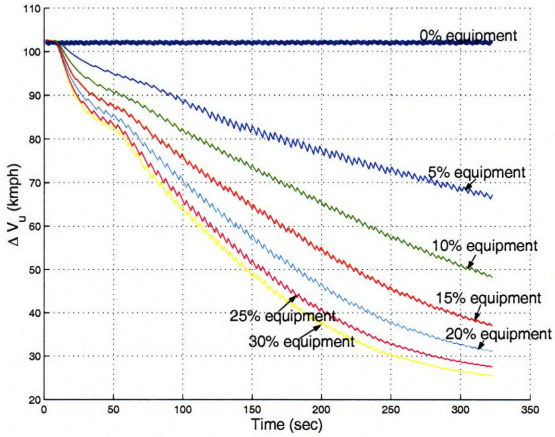

Figure 3-53: A comparison of ΔV_u for the Reimann Problem for varying equipment assuming an endogenous communication wave generated using $V_{eth} = 25$ kmph and $T_{range} = 500$ meters

3.9 A summary of what we have learnt

What constitutes an 'unsafe' driving situation, when viewed in a macroscopic (PDE-based) setting ?

Since macroscopic equations are generated by considering average behaviors of groups of vehicles, it is difficult to detect actual vehicular collisions in this setting. Large negative average velocity gradients are unsafe, because they mean that several vehicles (possibly across several lanes) have all performed a large velocity decrease over a short distance, and all at the same time. There are several ways in which these large gradients could arise:

1) An initial condition comprising discontinuities, such that these discontinuities prop-

agate (almost unchanged) along the highway - a type of Reimann Problem (Figures 3-26 and 3-37). 2) A continous initial condition with a gradual velocity gradient, that however progressively steepens with time, and eventually forms a discontinuity (Figures 3-28 and 3-44). The situation in Figure 3-28 is one wherein the high velocity portion of the wave moves forward while the low velocity portion of the wave moves backwards; till they eventually meet to form a discontinuity. However, other situations wherein all parts of the velocity wave move forward but at unequal wave velocities, such that the high velocity portion of the wave moves faster than the low velocity portion of the wave, can also lead to eventual discontinuities.

What role does partial equipment of an advance warning system play in attenuating these negative velocity gradient waves ?

We assume that along with the warning signal, the driver also receives information of the magnitude of the reduced average velocity occurring at the far-ahead location; and he subsequently attempts to reduce his desired velocity from its original value to that at the far-ahead location. As the equipped vehicles reduce their velocity, the unequipped vehicles either slow down or attempt to overtake the equipped vehicles (by passing). However, if the number of equipped vehicles/lane is large enough, then these unequipped vehicles that initially pass will still encounter other equipped vehicles; and eventually be forced to slow down. In this way, the average velocity of the unequipped vehicles gets reduced before the shock hits them.

What is the appropriate PDE model that represents a mixed communication environment, wherein far-ahead velocity information is transmitted at a finite communication speed ?

The relevant equations are Equations (53-58),(61-62). If we assume that information of the (closest) location of occurrence of the degraded velocity condition is also transmitted, then the relevant equations are Equations (53-58),(62-64).

If the advance warning propagates at a finite speed along the highway, what should be the minimum transmission range ?

The minimum transmission range would be established in conjunction with the average velocity threshold of the equipped vehicles, needed to trigger the warning

system. For a velocity threshold of 25 kmph, a transmission range of 400 meters would be inadequate, while one of 500 meters would be adequate (Figures 3-50, 3-51, 3-52). The value of the pair comprising the threshold and the transmission range, should be such that they generate a communication speed that propagates at about twice the value of the wave speed of the velocity wave.

What is the minimum level of equipment required in order to significantly weaken the velocity gradients ?

For a 50% reduction in the velocity change occurring across a discontinuity (as compared to when all vehicles were unequipped), about 15% equipment appears to be adequate (Figures 3-36, 3-38, 3-40, 3-44). Beyond this, the benefit obtained in terms of shock magnitude reduction per unit rise in density of equipped vehicles, is not significant.

Chapter 4

Experimental Results

A prototype system to test the slowdown warning concept was built. In this chapter, details of road tests that were performed to test a class of pileup crash scenarios, are discussed. The road tests were performed both before and after equipping a few cars with the system; and in each case, the driver response is evaluated. These tests demonstrate the satisfactory working of the slowdown warning concept, at least for this class of scenarios.

4.1 Prototype System

We have developed a prototype of the slow-down warning system. The system architecture is as shown in Figure 4-1, while a schematic is given in Figure 1-3. From a research standpoint, we wanted to have a low-cost test bed. We have therefore chosen a system comprising off the shelf components : a GPS receiver, a wireless transceiver, as well as a laptop computer. Using the GPS receiver, a car equipped with the warning system can determine its position and speed. (When used in a differential/WAAS enhanced mode, the errors in position and velocity are small enough for our purposes). The computer analyzes this information, and in the event of any abrupt deceleration or abnormally low speed (assumed to be 20 mph for the road tests, but is subject to refinement), it transmits a warning signal to the other cars through a wireless transceiver. Each recipient car then determines whether the sig-

nal is indeed relevant to it (i.e. whether the slowdown is occurring in the same lane as the one it is travelling in, how far ahead the slowdown is occurring, etc). If the computer determines that the warning signal it has received is indeed relevant to the car it resides in, then it issues a warning signal to the driver, alerting him/her of the impending slowdown. On the other hand, if the computer deems the warning signal to be irrelevant to the car it resides in, then no warning is issued to the driver.

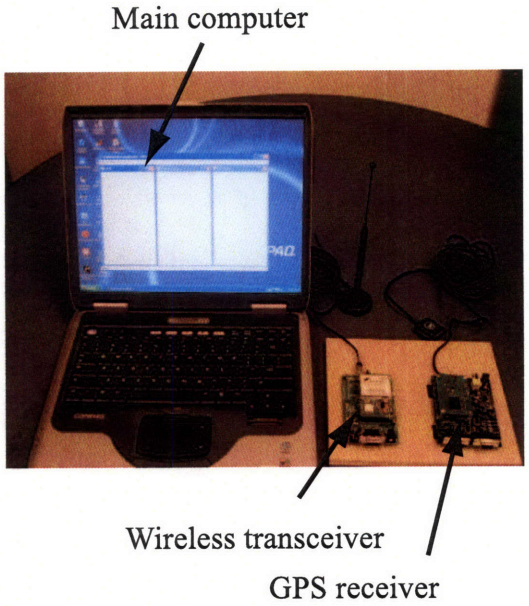

Figure 4-1: Prototype system

The above situation is illustrated through an example in Figure 4-2, which shows several cars A, B, C, D, E, F, G, H and J. Assume car A causes a hazard and therefore broadcasts a warning signal. Assuming the communication channel in the air to be homogeneous and isotropic, this signal transmitted by car A travels in an omnidirectional fashion, and thus all the cars within the communication range (viz. cars B, C, D, F, G, H and J) receive the warning signal. However, even though cars D, F, G, H and J receive the warning signal, the algorithms resident in these cars should be able to determine that the current received warning is not relevant to them, and there is therefore no need to broadcast an alert to the driver. For instance, there is no reason for the driver of car D to be alerted (even though car D has received

the warning signal) since it is too far away from car A. Similarly, the hazard caused by car A does not pose a threat to cars F, G and H, because car F is ahead of car A while car G is not in the same lane as car A. Car J is travelling in a direction opposite to that of car A, and therefore its driver also should not receive an alerting signal. If we define the warning zone as the zone in which all equipped cars (upon receipt of the warning signal), issue an alert to the driver, then this example is an illustration of the importance of a judicious design of the warning zone (as a subset of the transmission range). The warning zone should not be ahead of the car that has broadcast the signal; it should not encroach upon other lanes (if there is no reason to do so), and even in its own lane, it should be neither too large nor too small. Too large a warning zone will broadcast unnecessary false alerts to cars far behind, while too small a warning zone will not provide significantly enhanced safety.

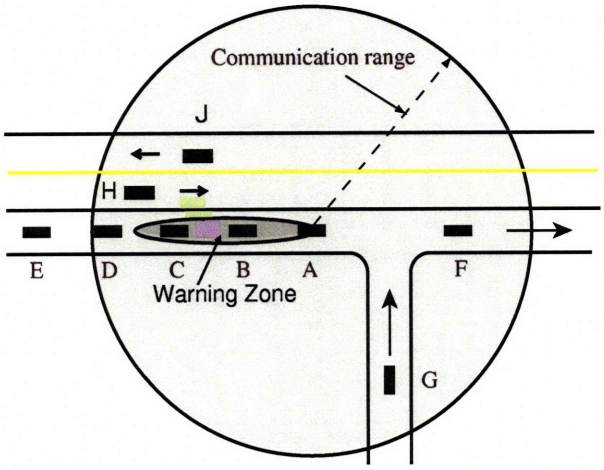

- Car A transmits a warning signal.
- Car B and C receive a warning signal, and issue a warning sign to drivers because they are in the warning zone.
- Car D, F,H,J, G receive a warning signal, but do not issue a warning sign to drivers because they are not in the warning zone.
- Car E cannot receive a warning signal because it is far way from Car A.

Figure 4-2: Illustration of the warning zone

We implemented algorithms wherein the warning signal includes information of the vehicle's past trajectory and speed. In our current prototype, a car that broadcasts a slowdown warning signal, also broadcasts information of its trajectory and velocity

for the past 450 meters of its travel. Consider the schematic scenario represented in Figure 4-2 wherein vehicle A is transmitting a warning signal, with a transmission range R. In addition to the warning signal, Vehicle A also transmits its position and velocity vector information at the GPS update rate (which can be as high as $10Hz$), for the last 450 meters of its travel. If we assume the first transmission of the warning signal by A to occur at a time $t = t_1$; then the information content transmitted by A at $t = t_1$, is as follows :

Time	East & North Posn. Co-ord.	Velocity Vector on Horizontal Plane
t_1	$E_A(t_1)$, $N_A(t_1)$	$\vec{V_A}(t_1)$
$(t_1 - \Delta t)$	$E_A(t_1 - \Delta t)$, $N_A(t_1 - \Delta t)$	$\vec{V_A}(t_1 - \Delta t)$
$(t_1 - 2\Delta t)$	$E_A(t_1 - 2\Delta t)$, $N_A(t_1 - 2\Delta t)$	$\vec{V_A}(t_1 - 2\Delta t)$
$(t_1 - 3\Delta t)$	$E_A(t_1 - 3\Delta t)$, $N_A(t_1 - 3\Delta t)$	$\vec{V_A}(t_1 - 3\Delta t)$
. . . .		
. . . .		
$(t_1 - n\Delta t)$	$E_A(t_1 - n\Delta t)$, $N_A(t_1 - n\Delta t)$	$\vec{V_A}(t_1 - n\Delta t)$

where n is such that

$\sqrt{(E_A(t_1) - E_A(t_1 - n\Delta t))^2 + (N_A(t_1) - N_A(t_1 - n\Delta t))^2)}$

$= 450$ meters. $\vec{V_A}$ represents the velocity components of A in the North and East directions.

At time t_1, (when B, H and J receive the warning signal), let their corresponding data be $E_B(t_1), N_B(t_1) \& \vec{V_B}(t_1)$; $E_H(t_1), N_H(t_1) \& \vec{V_H}(t_1)$; $E_J(t_1), N_J(t_1) \& \vec{V_J}(t_1)$ respectively.

When J receives the warning signal, it is able to determine that the warning is not relevant to it as follows : it computes the inner product of its own horizontal velocity vector $\vec{V_J}(t_1)$ with that of the transmitting vehicle $\vec{V_H}(t_1)$. When it determines that this inner product is negative, it is able to infer that the warning is not relevant to it. The one-sigma velocity error of GPS is 5 cm/sec in each axis [68], and this error is small enough for our purposes.

For vehicles B and H, the procedure to determine the relevance (or otherwise) of

the warning signal it receives from A involves the use of relative trajectories : Vehicle B computes the trajectory of A for the time interval $[t_1 - n\Delta t, t_1]$, relative to $B's$ position at t_1; and vehicle H computes the trajectory of A for the same time interval, relative to $H's$ position at t_1. A schematic of these trajectories is given in Figure 4-3.

Figure 4-3 demonstrates that since vehicle B is travelling on the same lane as vehicle A, therefore, the trajectory of A relative to B passes close to the origin; on the other hand, since vehicle H is travelling on a different lane, therefore the trajectory of A relative to H is further away from the origin. By constructing a circle around the origin (whose radius is equal to the typical width of a lane), and then determining whether the closest distance of the trajectory from the origin is less than the radius of this circle, it is possible to determine whether the recepient vehicle is travelling on the same lane as the transmitting vehicle. The typical width of a highway lane is 12 feet [65], which is 3.67 meters. The one-sigma relative position error in a differential GPS system is about 3.0 meters, of which a large contributor is multi-path reflection (1.4 meters) [66]. It is to be observed that a major contributor to multi-path reflection errors is the presence of buildings; and since there are not too many buildings found close to the highways, errors due to multi-path reflection will be much smaller, and this in turn, would lead to smaller errors in computation of the relative trajectories discussed above. [67] has reported obtaining centimeter level relative position accuracies by using a differential carrier phase GPS system on a highway. Furthermore, [69] reports the use of a Nationwide Differential Global Positioning System (NDGPS) that currently provides 1-3 m navigation accuracy, and is developing a future system called High-accuracy NDGPS which will provide 10 centimeter level accuracy or better.

In our currently developed prototype, the area of the warning zone is constant and equal to $450m$. This number was decided as follows. We assumed a nominal vehicle speed of about 65 miles per hour (which corresponds to a little under 30 meters/sec). If we conservatively assume a GPS update rate of 1 Hz (although GPS updates at rates as high as 10 Hz are currently available), then that would imply that a vehicle would have travelled about 30 meters before a fresh update on its position

and velocity would be available. We took the warning zone to be a little more than one order of magnitude higher than this number. Eventually however, the warning zone should be optimally determined in real time depending on various factors, such as traffic conditions, weather, inter-car distance, actual car velocities, etc., and we intend to extend our current technical capabilities to address this problem. Since the amount of information propagating increases with increasing numbers of equipped cars, and since the capacity of the communication system is limited, it is important to strike the right balance between transmitting too little information and too much information. The warning information transmitted by each car should comprise the minimum possible information that will just enable the recipient vehicles to determine whether the warning signal is relevant to them or not.

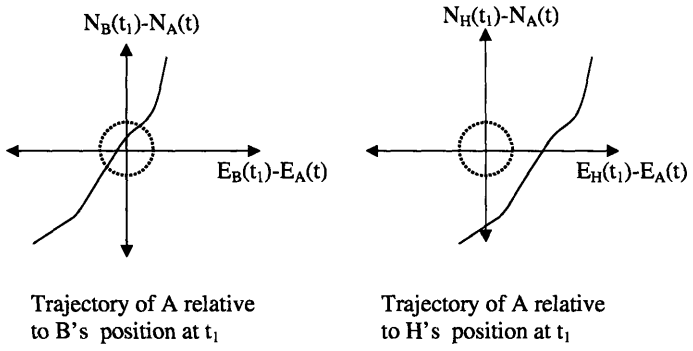

Figure 4-3: Schematic relative trajectories

4.2 Other pile-up crash scenarios

The specific scenario that we have considered in the preceeding simulation and analysis sections is as represented in Figure 4-4. The schematic shows a string of cars moving along with equal initial velocities and equal initial inter-car distances when one of the cars in the string (say car B in the figure) has to execute an abrupt deceleration (for whatever reason - say because of a deer crossing the road in front of it); and this leads to a chain reaction in all the cars driving behind car B - resulting in a pileup crash.

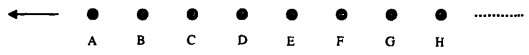

Figure 4-4: Multi-vehicle scenario I

It is easy to see that this is not necessarily the only initial condition that could lead to a pileup crash. For instance, consider the schematic represented in Figure 4-5. In this schematic, A represents a car that has already met with an accident and has come to a stop. Car B (accompanied by a string of cars behind it) is initially at a fairly large distance behind car A (say about 500 meters or more); while all the cars behind B are again driving at equal initial velocities and equal initial inter-car distances. Then, under poor visibility conditions, it is quite possible that car B may not see (or anticipate) the stopped car A, until it is too late, i.e. B is almost upon A, at which time B has to execute a sharp deceleration in order to stop before it hits A. This may then induce a chain reaction in all the cars driving behind car B; and this could result in a pileup crash too.

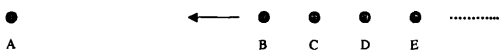

Figure 4-5: Multi-vehicle scenario II

In each of the above two scenarios, the slowdown warning system could come into play in a different way. In the first scenario, (assuming car B to be equipped), the warning system would be triggered owing to the abrupt deceleration of car B (i.e. the system would be triggered on the basis of a deceleration threshold). In the second scenario however, (assuming car A to be equipped), the warning system would be triggered owing to the zero velocity of car A (i.e. the system would be triggered on the basis of a velocity threshold); and the warning system would actually be warning the other cars behind so that they do not slam into the stopped car and create a pile-up. Of course, if car A is unequipped, then the system would again be triggered on the basis of the abrupt decleration of car B, and the warning triggering scenario would then become identical to the first one.

While it is the first scenario that has been addressed in Chapter 2 of this thesis,

it is hard to test this scenario on the road since it is dangerous for a *string* of cars to actually do very sharp decelerations on the road. In fact the only possible way to test this scenario might be on a driving simulator. In an attempt to test the *second* scenario, however, we conceived a road test experiment (discussed below). We then interspersed the road test results with simulations, to demonstrate the effects of having all unequipped/all equipped/some equipped vehicles when the second scenario above is encountered.

4.3 Discussion of the road test experiments

After developing ten prototype units of the slow-down warning system, we installed them in cars and conducted experiments on the highway to test the system. The drivers for these tests were chosen randomly (on a volunteer basis). They were given no prior instructions, other than being told to drive normally; and on receipt of the warning signal, to become more alert. We chose the Route 1 highway (North and South) since it is very well suited for these experiments. (See Figure 4-6, which shows the map of Route 1 highway. There are many spaces alongside this route that serve as good starting and ending points for the experiments).

Two-car road test experiments:

The initial experiment involved two cars, numbered 1 and 2, with car 1 being the lead car. The experiment was conducted at night to simulate the effect of low visibility. The experiment would commence with car 1 getting onto the highway, and car 2 also getting onto the highway a couple of minutes after car 1. Thus car 2 did not have car 1 in its field of vision, as car 1 had already traveled well ahead. Also, there were several other cars interspersed between cars 1 and 2. (These interspersed cars were regular cars driving on the highway and were oblivious of the conduct of this experiment). The cars were traveling at typical highway speeds.

The first car would then get off the highway at some random point, and park at some adjoining spot. As soon as it would slow down (in order to get off the highway), it would begin to emit the warning signal. If car 2 could locate car 1 and

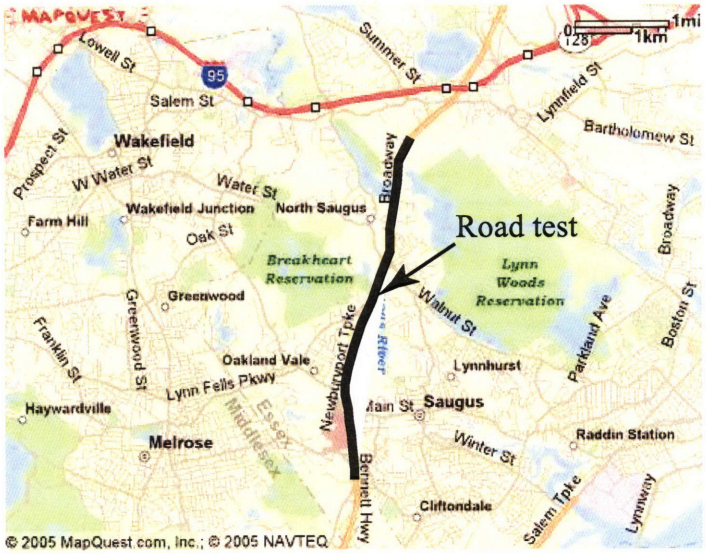

Figure 4-6: Route 1 highway in MA where the road tests were conducted

park alongside it, it was deemed to have avoided an accident, while if it overshot the location where car 1 was parked, it was deemed to have had an accident. The idea behind the experiment was that once car 1 begins to emit the warning signal, car 2 should receive the signal and get cued to slow down thus enabling it to locate car 1 and be able to park alongside it. The purpose of the experiment was two fold : The first was to see how reliably the slowdown warning equipment hardware and algorithms functioned (in warning the driver early enough), and the second was to use the driver responses (both with and without the warning system) as inputs to simulations that would test the second pile-up crash scenario discussed above.

Figure 4-7 shows the results of one such two-car road test. In this figure, the time history of the car velocities and the absolute position trajectory of the cars (as obtained from GPS) have been plotted. As can be seen from the figure, car 1 is initially traveling at about 50 mph, and then gets off the highway at about t = 100 sec, and parks at some adjoining spot. When its speed has reduced below 20 mph, it begins to emit the warning signal from t = 107 sec onwards. The (GPS obtained) location of car 1 at the instant it begins to transmit the signal, is also shown in the figure. Car 2 then begins to receive the signal when it comes to within about 350 meters of car 1 (which happens at about t = 220 sec). The instant car 2 receives

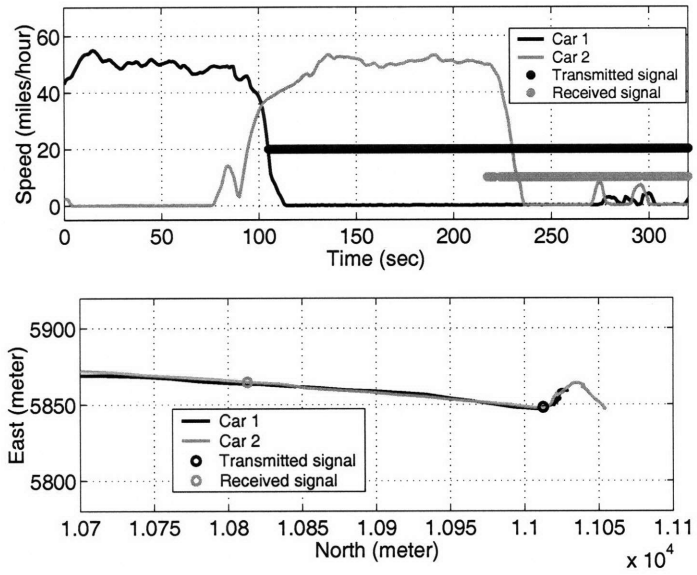

Figure 4-7: Road test with two cars

the signal, it immediately gets cued to slow down (as can be seen by the drop in its velocity), and this enables it to locate car 1.

Six-car road test experiments:

After the two-car road test, we conducted a series of six-car road tests, with varying degrees of equipment of the warning system. Figure 4-8 shows the results of a six-car road test, when all the cars were unequipped. It is seen from Fig. 4-8(b) that while car 6 could not locate car 1 at all, cars 2 and 3 actually located car 1 only after overshooting it. Thus, for the purposes of this experiment, cars 2, 3 and 6 were deemed to have collided with car 1. Cars 4 and 5, on the other hand, in spite of being able to locate car 1, had to execute very sharp decelerations the instant they actually spotted car 1.

The abrupt deceleration of car 4 in the road test is also shown on the phase plane in Figure 4-9. This plot serves as a good representation of what happens when a car driving along on the highway (with no other cars in the driver's immediate field of vision), suddenly comes upon the site of a stopped car. To demonstrate the chain reaction and the consequent pile-up crash that could be initiated on a string of cars driving behind it, we resort to simulations (since it is obviously dangerous to test

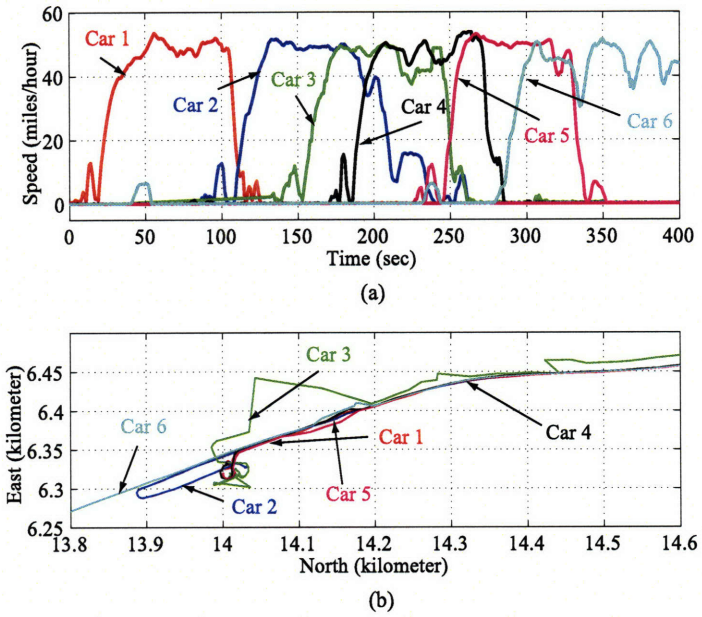

Figure 4-8: Road test with no cars equipped

such a scenario on the road). We use the approximation to the road test result of Figure 4-9 (also shown in the figure), as the velocity profile of the lead car in a 10 car simulation. The following (simulated) cars are all driving along at equal initial velocities and equal initial inter-car distances.

Figure 4-10 demonstrates what happens to the nine unequipped cars behind (that are assumed to be driving with an initial time headway of $T = 1.3sec$). The abrupt deceleration of the lead car in the simulation (which is akin to car B in Figure 4-5) initiates a chain reaction in all the following nine cars; and all of them slam into the lead car with high velocities at impact; and thus generate a pile-up crash.

Reverting this discussion back to the road tests, we then conducted a six-car road test with all cars equipped. Again, these cars were not driving as a string, i.e. each car started only a couple of minutes after the preceeding car had left, and therefore did not have the preceding experimental car in its field of vision. Again, car 1 would get off the highway at a random point; but this time it would begin to emit the warning signal (to mimick the event that car A in Figure 4-5 is now equipped). The objective of this experiment is to see if the slowdown warning equipment functions efficiently

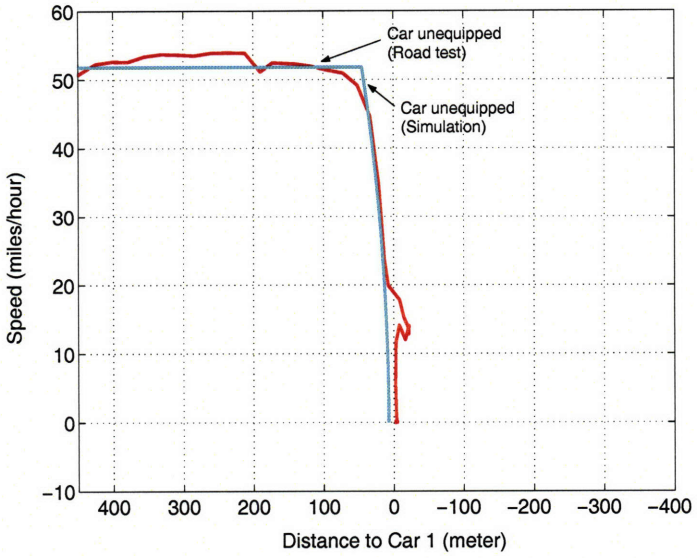

Figure 4-9: Typical phase plane plot of unequipped car

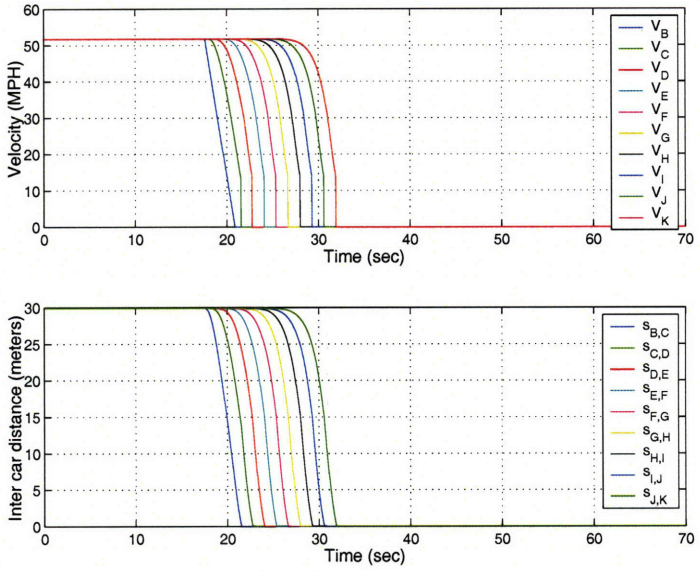

Figure 4-10: Results of a 10-car simulation (all unequipped) when the lead car suddenly comes upon the site of an accident

enough to warn the drivers of cars 2-6 (each of which independently mimicks car B in Figure 4-5), once they enter within the transmission range of car 1; and also to use the typical velocity profile of cars 2-6 to *simulate* what would happen if there were actually a string of cars (of varying degrees of equipment) driving behind the mimicked car B.

Figure 4-11 then shows the results of a road-test experiment with all six cars equipped. Figure 4-11(a) also shows the time instants when each car began to receive the warning signal, while Figure 4-11(b) also shows the location of each car at that time. It can be seen that all the cars began to receive the warning signal sufficiently early, and that enabled them to slow down well in advance, and locate car 1 successfully. Thus in this experiment, all the cars were deemed to have avoided colliding with car 1.

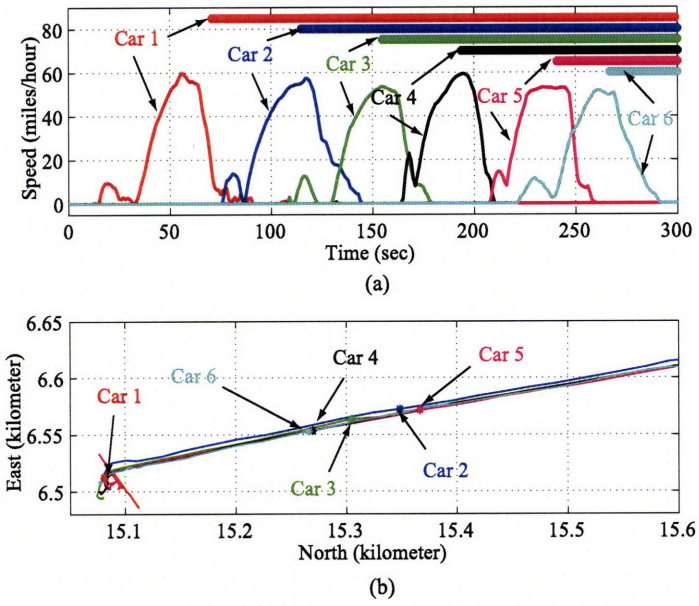

Figure 4-11: Road test with all cars equipped

The gradual deceleration of car 4 in the road test (when equipped) is shown on a phase plane in Figure 4-12. It can be seen that due to the early warning it receives, it begins to slow down earlier (than it otherwise would have, if it were unequipped); and the consequence is that it executes a far smoother deceleration profile (than when it was unequipped). From the road test experiments, it was observed that there could

be either of two typical phase plane plots of an equipped vehicle - one denoted as Profile A and the other denoted as Profile B. Qualitatively, Profile B constitutes a continous decrease in velocity by the equipped car till it reaches close to the location of the accident. Profile A constitutes first a velocity decrease till the car reaches an intermediate velocity; the car then travels at this velocity for a short distance before it performs a second velocity reduction that brings it to rest just before the accident location.

We again use an approximation to the velocity response of this car and use this approximation as the velocity of the lead car in a 10-car simulation, with all the following cars equipped. The results of this simulation using Profile A are shown in Figure 4-13, while that using Profile B are shown in Figure 4-14. All the equipped cars are able to take anticipative action (by increasing their time headways), and thereby avoid collisions, as indicated by the fact that their velocities drop smoothly to zero simultaneously with their inter-car distances dropping to zero.

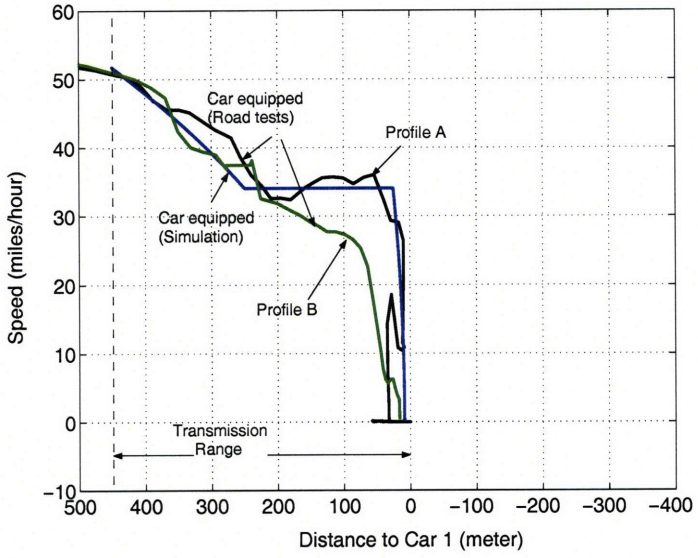

Figure 4-12: Typical phase plane plot of equipped car

Figure 4-15 then shows the result of having only the first five cars of the string equipped and the last five cars of the string unequipped, and with the lead car having executed a velocity reduction of the form of Profile B, on receipt of the warning

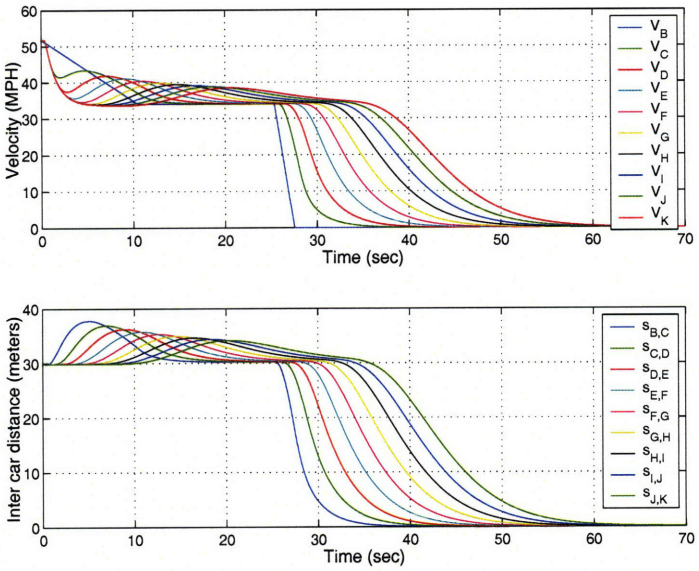

Figure 4-13: Results of a 10-car simulation (all equipped) with velocity profile of the lead car being as in Profile A from the road test

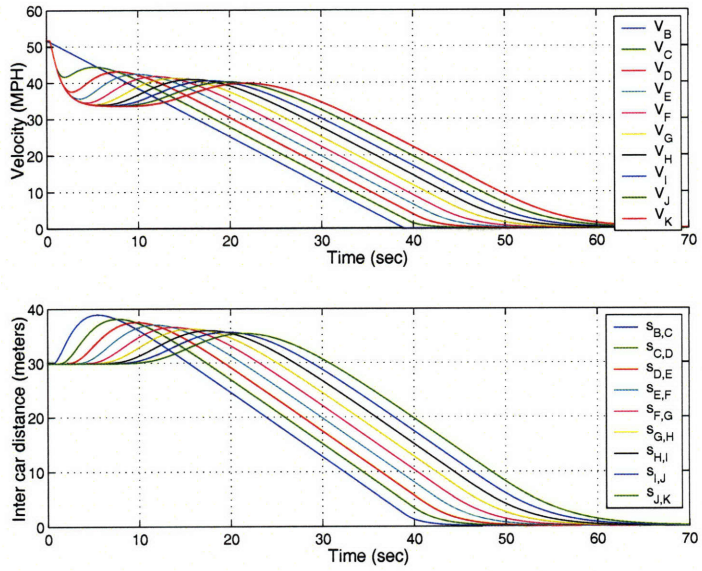

Figure 4-14: Results of a 10-car simulation (all equipped) with velocity profile of the lead car being as in Profile B from the road test

signal. It can be seen that the presence of the first five equipped cars enables even the unequipped cars behind to slow down early enough to avoid an accident. Figure 4-16 again shows the responses corresponding to a different equipment scenario. Figure 4-17 shows the responses when the lead car performs a velocity reduction of the form of Profile A.

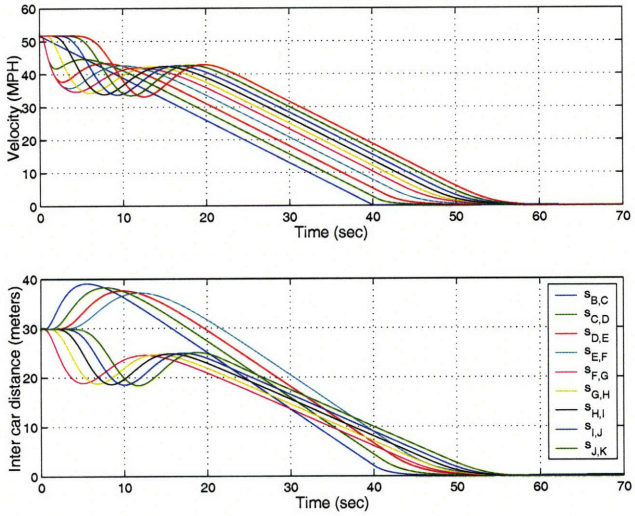

Figure 4-15: Results of a 10-car simulation (some equipped) with velocity profile of the lead car being as in Profile B

Figures 4-18 and 4-19 then consider the scenario when the car in the pre-existing accident is unequipped, and therefore does not broadcast a warning signal. The equipped cars behind the lead car then get warned only on the basis of the sudden deceleration of the lead car (i.e. on the basis of a deceleration threshold). Figure 4-18 shows the situation when all the cars (with the exception of the car in the pre-exisiting accident) are equipped, and Figure 4-19 shows the corresponding situation when only some cars (again, barring the car in the pre-existing accident) are equipped.

The next experiment was conducted to test the effect of partial equipment. Only cars 1, 2, 4 and 6 were equipped. In this experiment, after car 1 left, car 2 started after about 50 seconds, and all of cars 3-6 followed behind car 2 almost immediately. Also, for this experiment, no other highway cars were allowed to come in between cars 2 to 6. The idea behind this was to test if the unequipped cars (viz. cars 3 and 5)

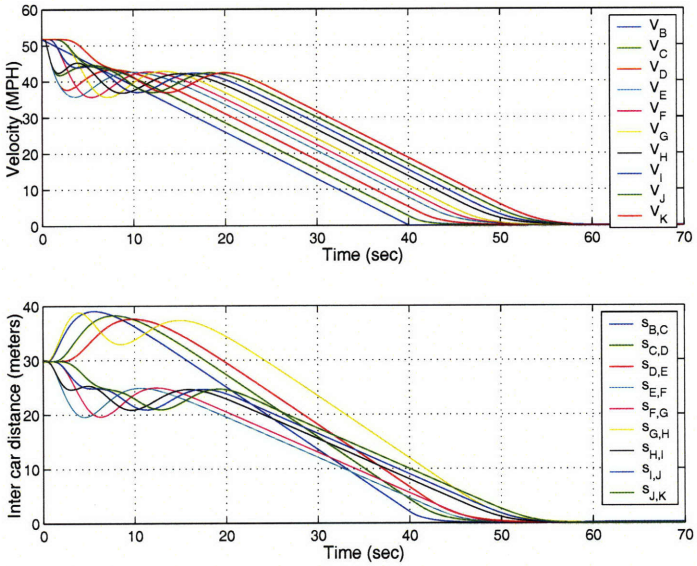

Figure 4-16: Results of a 10-car simulation (some equipped) with velocity profile of the lead car being taken from the road test : Only cars A, B, C, D, E, H are equipped

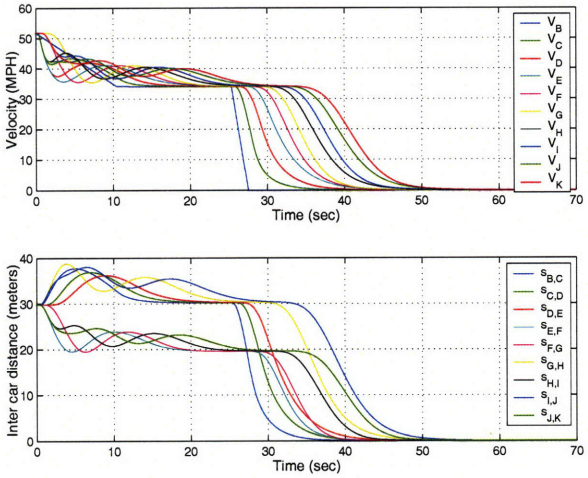

Figure 4-17: Results of a 10-car simulation (some equipped) with velocity profile of the lead car being as in Profile A

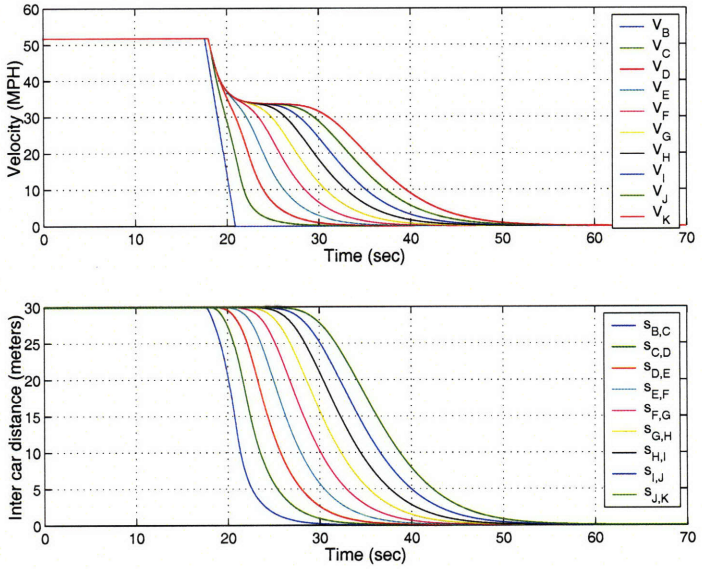

Figure 4-18: Results of a 10-car simulation (all equipped - except for the car in the pre-existing accident)

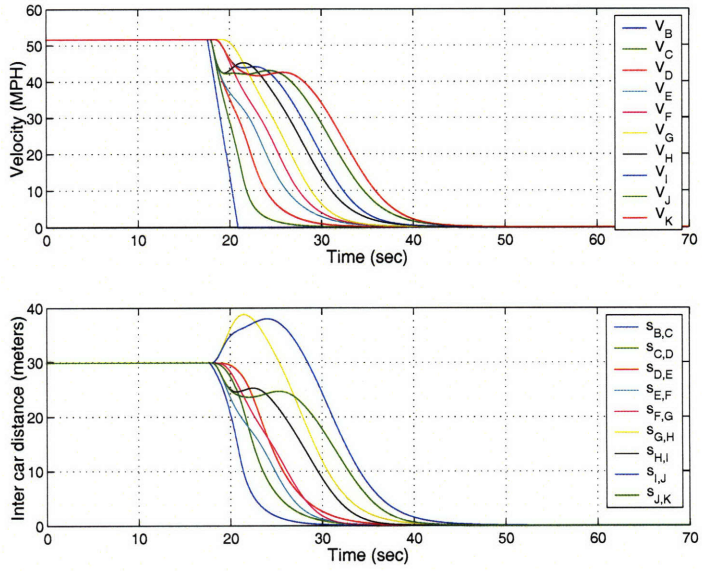

Figure 4-19: Results of a 10-car simulation (some equipped - The car in the pre-existing accident is unequipped)

could get cued into slowing down by the brake-lights of the equipped car immediately ahead of them (viz. cars 2 and 4, respectively) sufficiently early, to enable them to locate car 1 successfully.

The results are shown in Figure 4-20, from which it can be seen that this was indeed the case. Even the unequipped cars could locate car 1 successfully, along with the equipped cars. Thus, in this experiment too, all cars were deemed to have avoided colliding with car 1.

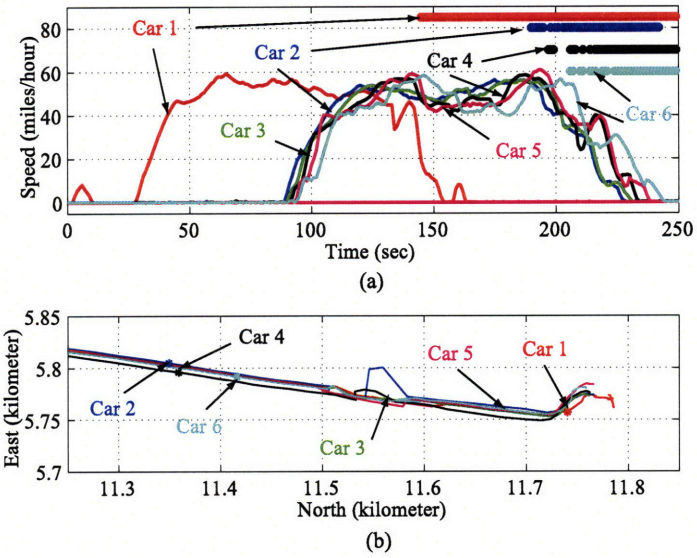

Figure 4-20: Road test with some cars equipped

Figure 4-21 then shows a comparative study of the deceleration behavior of car 4 in two different experiments, one in which the car was unequipped and one in which the car was equipped. These are plotted on a phase portrait showing the velocity of car 4 versus the distance to car 1. It is seen that in the case when car 4 was unequipped, even though it was actually able to locate car 1, it had to decelerate very sharply at the last possible moment. The same car, when it was equipped however, was able to execute a more gradual deceleration when it began to receive the warning signal.

Figure 4-22 shows a similar comparative study of car 5 in three different experiments: (a) Car 5 was unequipped and there was no equipped car ahead of it. (b) Car 5 was equipped. (c) Car 5 was unequipped but car 4 (immediately ahead of it) was

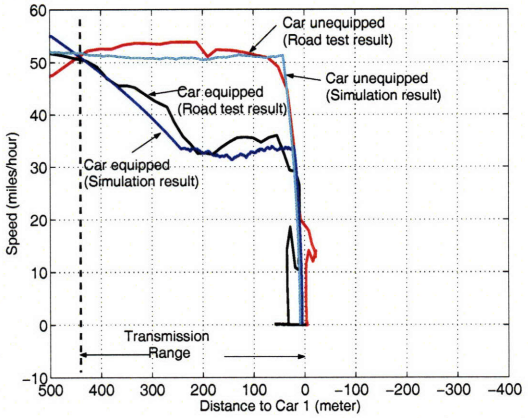

Figure 4-21: Phase Portrait of car 4 for different experiments

equipped. It is seen that in case (a), car 5 overshot the location of car 1 (and was therefore deemed to have collided with car 1). In case (b), it received the warning signal early enough to enable it to decelerate gradually and locate car 1. In case (c), car 5 got cued into slowing down by the brake-lights of car 4 (which itself was equipped) about 450 meters from car 1, and this enabled it to begin to decelerate early enough, and again locate car 1.

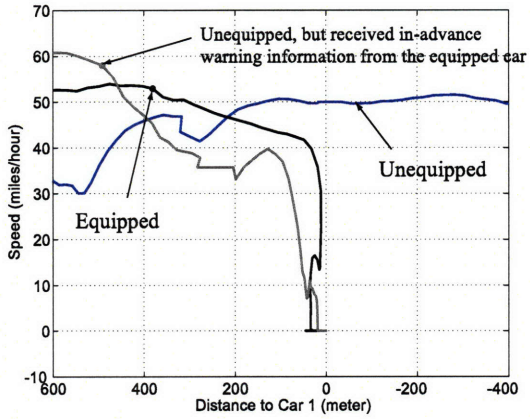

Figure 4-22: Phase Portrait of car 5 for different experiments

Chapter 5

Summary and Future Work

5.1 Summary and Conclusions

In this thesis, we deal with the problem of safety of an automotive multi-vehicle system in a mixed communication environment. This mixed environment comprises of some vehicles specially equipped to receive advance information of a hazardous situation occurring far ahead on the highway (and beyond the driver's visual range), randomly mixed amongst other unequipped vehicles that are capable of receiving only local, near-neighbor information. The specific safety problem that we deal with concerns the alleviation of pile-up crashes on the highway - with the equipped vehicles being alerted to the possibility of the occurrence of a pile-up crash, by means of a slowdown warning system, that informs them of the presence of a hazard ahead. We use both microscopic and macroscopic models, in which we study the effects of varying information content communicated to the driver of an equipped vehicle.

In the microscopic modeling approach, the problem is formulated as a single lane problem, and the notion of safety is defined as one of collision avoidance. It has been discussed in the literature, that there exist some initial conditions under which string instability can occur, and the occurrence of string instability is a factor that can lead to pile-up crashes. It is assumed that besides transmitting the warning of an impending slowdown ahead, no further information is made available to the driver of an equipped vehicle. Furthermore, the alerting information is transmitted at a near

infinite speed. We make the reasonable assumption that in such situations, the driver of an equipped vehicle, on receipt of a warning, increases his time headway to the vehicle ahead. If all the vehicles are equipped, then the trend of string instability can be totally eliminated; whereas if some vehicles are equipped, then there is the prevalence of mixed string stability - in which scenario, some parts of the vehicular string are stable, while others are not. It is demonstrated how the presence of a few equipped vehicles can serve to keep the level of string instability below the threshold that would lead to pile-up crashes. Furthermore, certain sufficient conditions are determined, under which it can be guaranteed that pile-up crashes would not occur. These sufficient conditions govern both - the minimum number of equipped cars required to be present in the string; as well as the set of precise distributions of equipped cars required to be present in the string.

In the macroscopic modeling approach, the problem is formulated as a multi-lane problem, and the notion of safety is defined as one of attenuating large negative velocity gradients/shocks on the highway, that otherwise pass through unattenuated/amplified (when all vehicles are unequipped). In this approach, we assume that in addition to the alerting signal, the driver of an equipped vehicle also receives information of the velocity conditions occurring far ahead. However, the alerting signal is assumed to be propagate through the equipped cars, at a finite propagation speed. Different initial conditions, such as a Reimann Problem which comprises of an initially discontinous condition; and an initially continous condition that propagates with time to evolve into a discontinuity (when all vehicles are unequipped) are studied. The evolution of the shock/velocity gradients, for different levels of equipment are parametrized.

A prototype of a slowdown warning system was built. Road tests to verify the performance of the slowdown warning concept, as well as evaluate the driver response to an accident scenario, both with and without the system, were conducted. The results of these road tests, demonstrating satisfactory performance of the slowdown warning equipment hardware (subject to good communication links) are also presented in this thesis.

5.2 Future Work

The results obtained using microscopic models in Chapter II, assume simplified driver-vehicle models that possess identical dynamics. Future work could include using more sophisticated models wherein the vehicles in a string do not all have the same dynamics. Furthermore, while the current model assumes that, on receipt of a slowdown warning signal, only the time delay and time headway of a driver switches to a new set of values; subsequent work could involve switching the driver gains as well (since this too could be considered a reasonable modeling assumption). The current model also assumes deterministic values of the model parameters; establishing theorems that govern the required number and distribution of equipped vehicles in a string, so as to result in zero collisions with stochastic model parameters could be explored. An extension of the microscopic model to a multi-lane scenario can also be explored.

The results obtained using macroscopic models in Chapter III use a separate continuity and momentum conservation-like equation for each of the equipped and unequipped vehicles, with a closing expression for the velocity variance. Future work could include using a dynamic equation for the velocity variance for the equipped and unequipped vehicles respectively. It could also include removing the assumption that along with the warning signal, the value of the degraded average velocity at the far-ahead point is transmitted; this assumption could be replaced by one wherein the equipped vehicles increase their time headways in response to a warning signal (as has been done in the microscopic analysis).

The experimental results in Chapter IV test the slowdown warning concept only for a particular class of pileup crash scenarios. Methods would have to be devised that enable testing of the warning concept for a larger class of pileup crash scenarios.

On a broader scale, this thesis explores situations wherein some agents that have access to non-local information are mixed with other agents that have access to only local information. In this thesis, the motion dynamics of the agents evolve along one spatial dimension. Attempts could be made to generalize this work to situations where the agent dynamics evolve in two or even three dimensions.

Bibliography

[1] CNN News, "Five seriously hurt in 194-vehicle California pileup," Nov. 3, 2002.

[2] CNN News, "Massive pile-up near Ga.-Tenn. line kills 4," March 14, 2002.

[3] Boston Globe News, "Sixty six vehicle California Pileup," April 2, 2004.

[4] Boston Globe News, "Rains trigger 30 car pileup on I-93," August 4, 2003.

[5] P. I. Richards, "Shock Waves on the Highway," *Operations Research, Vol. 4, No. 42, 1956, pp. 209-229.*

[6] J. K. Hedrick, R. Sengupta, Q. Xu, Y. Kang, C. Lee, "Enhanced AHS Safety Through the Integration of Vehicle Control and Communication," *California PATH Research Report UCB-ITS-PRR-2003-27, September 2003.*

[7] X. Y. Lu, J. K. Hedrick, M. Drew, "ACC/CACC - Control Design, Stability and Robust Performance," *Proc. Of the American Control Conference, May 8-10, 2002.*

[8] P. Seiler, A. Pant, K. Hedrick, "Disturbance Propagation in Vehicle Strings," *IEEE Transactions on Automatic Control, Vol. 49, No. 10, October 2004.*

[9] A. R. Girard, J. B. de Sousa, J. K. Hedrick, "An Overview of Emerging Results in Networked Multi-Vehicle Systems," *Proc. of the 40th IEEE Conference on Decision and Control, December 2001.*

[10] Q. Xu, K. Hedrick, R. Sengupta, J. VanderWerf, "Effects of Vehicle-vehicle/roadside-vehicle Communication on Adaptive Cruise Controlled High-

way Systems," *Proc. of the 56th IEEE Vehicular Technology Conference, Vol. 2, September 2002.*

[11] S. Kato, S. Tsugawa, K. Tokuda, T. Matsui, H. Fujii, "Vehicle control algorithms for cooperative driving with automated vehicles and intervehicle communications," *IEEE Transactions on Intelligent Transportation Systems, Vol. 3, No. 3, September 2002, pp. 155-161.*

[12] J. Carbaugh, D. Godbole, R. Sengupta, "Tools for safety-Throughput analysis of vehicle automation systems," *Proc. Of the American Control Conference, Vol. 3, 1997.*

[13] J. Carbaugh, D. Godbole, R. Sengupta, "Safety and capacity analysis of automated and manual highway systems," *Transportation Research C (6), 1998.*

[14] A. Bose, P. A. Ioannou, "Analysis of Traffic Flow with Mixed Manual and Semi-automated Vehicles," *IEEE Transactions on Intelligent Transportation Systems, Vol. 4, No. 4, December 2003, pp. 173-188.*

[15] A. Bose, P. A Ioannou, "Mixed manual/semi-automated traffic: a macroscopic analysis," *Transportation Research Part C 11 (2003), pp. 439-462.*

[16] R. E. Chandler, R. Herman, and E. W. Montroll, "Traffic dynamics: Studies in car following," *Operations Research, Vol. 6, pp. 165-184, 1958.*

[17] J. S. Tyler, "The Characteristics of Model Following Systems as Synthesized by Optimal Control," *IEEE Transactions on Automatic Control, Vol. AC-9, pp. 485-498, 1964.*

[18] G. O. Burnham, J. Seo and G. A. Bekey, "Identification of Human Driver Models in Car Following," *IEEE Transactions on Automatic Control, Vol. 19, pp. 911-915, 1974.*

[19] D. C. Gazis, R. Herman, and R. Rothery, "Nonlinear follow-the-leader models of traffic flow," *Operations Research, Vol. 9, 1961.*

[20] D. Swaroop and J. K. Hedrick, "String Stability of Interconnected Systems," *IEEE Transactions on Automatic Control, pp. 349-357, Vol. 41, No. 3, March 1996.*

[21] D.T Mcruer and E.S Krendel, "Mathematical Models of Human Behavior," *AGARD, AGARD-AG-188, 1974.*

[22] Claire Tomlin, George J.Pappas and Shankar Sastry, "Conflict Resolution for Air Traffic Management : a Study in Multi-Agent Hybrid Systems," *IEEE Transactions on Automatic Control*, Vol. 43, No. 4, April 1998.

[23] Claire Tomlin, Ian Mitchell and Ronojoy Ghosh, "Safety Verification of Conflict Resolution Maneuvers," *IEEE Transactions on Intelligent Transportation Systems*, Vol. 2, No. 2, June 2001.

[24] Ching-Yao Chan and Han-Shue Tan, "Feasibility Analysis of Steering Control as a Driver-Assistance Function in Collision Situations," *IEEE Transactions on Intelligent Transportation Systems*, Vol. 2, No. 1, March 2001.

[25] Takeshi Sakaguchi, Atsuya Uno, Shin Kato and Sadayuki Tsugawa, "Cooperative Driving of Automated Vehicles with Inter-Vehicle Communications," *Proc. of the IEEE Intelligent Vehicles Symposium 2000*, pp. 516-521, 2000.

[26] Bishop, "A survey of Intelligent Vehicle Applications World-Wide," *Proc. of the IEEE Intelligent Vehicles Symposium 2000*, pp. 25-30, 2000.

[27] Christoph Mertz, Sue McNeil and Charles Thorpe, "Side Collision Warning Systems for Transit Buses," *Proc. of the IEEE Intelligent Vehicles Symposium 2000*, pp. 344-349, 2000.

[28] I.D Couzin, J. Krause, N.R Franks and S.A Levin, "Effective leadership and decision-making in animal groups on the move," *Nature, Vol. 433, February 2005.*

[29] M. H. Lighthill, G. B. Whitham, "On kinematic waves II : A theory of traffic flow on long, crowded roads," *Proc. Of the Royal Society of London Ser. A 229, pp. 317-345, 1945.*

[30] H. J. Payne, "Models of Freeway Traffic and Control, " *Simulation Council, 1971.*

[31] G. B. Whitham, "Linear and Nonlinear Waves, " *Wiley, 1974.*

[32] C. Daganzo, "Requiem for second-order fluid approximation to traffic flow, " *Transportation Research Part B 29 (4), 1995, pp. 277-286.*

[33] H. M. Zhang, "A Theory of Nonequilibrium Traffic Flow, " *Transportation Research B, Vol. 32, No. 7, 1998, pp. 485-498.*

[34] A. Aw and M. Rascle, "Resurrection of second order models of traffic flow ? " *SIAM Journal of Applied Math., 60(3), 2000, pp. 916-938.*

[35] , M. Rascle, "An Improved Macroscopic Model of Traffic Flow: Derivation and Links with the Lighthill-Whitham Model, " *Mathematical and Computer Modelling 35 (2002), pp. 581-590.*

[36] J. M. Greenberg, "Extensions and Amplifications of a Traffic Model of Aw and Rascle, " *SIAM Journal of Applied Math, Vol. 62, No. 3, pp. 729-745.*

[37] R. M. Colombo, "A 2 x 2 Hyperbolic Traffic Flow Model, " *Mathematical and Computer Modelling, 35, 2002, pp. 683-688.*

[38] D. Helbing, "Improved fluid dynamic model for vehicular traffic, " *Physics Review E 51, pp. 3164-3169, 1995.*

[39] D. Helbing, A. Hennecke, V. Shvetsov and M. Treiber, "Micro- and Macro-Simulation of Freeway Traffic, " *Mathematical and Computer Modelling 35, 2002, pp. 517-547.*

[40] D. Helbing, "Gas-kinetic derivation of Navier-Stokes-like traffic equations, " *Physical Review E 53, March 1996, pp. 2366-2381.*

[41] M. Treiber, A. Hennecke and D. Helbing, "Derivation, properties and simulation of a gas-kinetic-based, nonlocal traffic model, " *Physical Review E 59, January 1999, pp. 239-253.*

[42] P. Nelson, "Traveling wave solutions of the diffusively corrected kinematic wave model, " *Math. Comp. Modeling, Special Issue on Traffic Flow Modeling, vol. 35, pp. 561-580, 2002.*

[43] S. P. Hoogendoorn and P. H. L. Bovy, "Continuum modeling of multiclass traffic flow, " *Transportation Research, Part B 34, 2000, pp. 123-146.*

[44] N. Bellomo and M. Delitala, "On the Mathematical Theory of Vehicular Traffic Flow I. Fluid Dynamic and Kinetic Modelling, " *Mathematical Models and Methods in Applied Sciences, Vol. 12, No. 12, 2002, pp. 1801-1843.*

[45] E. Angelis, "Nonlinear hydrodynamic models of traffic flow modeling and mathematical problems, " *Math. Comp. Modeling, vol. 29, pp. 83-95, 1999.*

[46] Bonzani, "Hydrodynamic models of traffic flow: Driver's behavior and nonlinear diffusion, " *Math. Comp. Modeling, vol. 31, pp. 1-8, 2000.*

[47] E. N. Holland and A. W. Woods, "A continuum model for the dispersion of traffic on two-lane roads, " *Transportation Research Part B, Vol. 31, No. 6, 1997, pp. 473-485.*

[48] C. F. Daganzo, "A continuum theory of traffic dynamics for freeways with special lanes, " *Transportation Research Part B, Vol. 31, No. 2, 1997, pp. 83-102.*

[49] A. Klar and R. Wegener, "A hierarchy of models for multilane vehicular traffic I: Modeling, " *SIAM Journal of Applied Mathematics, Vol. 59, No. 3, 1999, pp. 983-1001.*

[50] I. Prigogine and R. Herman, "Kinetic theory of vehicular traffic, " *Elsevier, 1971.*

[51] S. L. Paveri-Fontana, "On Boltzmann like treatments for traffic flow, " *Transportation Research Part B, Vol. 9, pp. 225-235, 1975.*

[52] A. Klar, and R. Wegener, "Enskog-like kinetic models for vehicular traffic, " *Journal of StaSurveys on Mathematics for Industry, vol. 6, pp. 215-239, 1996.*

[53] A. Klar, and R. Wegener, "Kinetic derivation of macroscopic anticipation models for vehicular traffic, " *SIAM Journal of Applied Mathematics, vol. 60, pp. 1749-1766, 2000.*

[54] A. Klar, R. D. Kune and R. Wegener, "Mathematical models for vehicular traffic, " *Surveys on Mathematics for Industry, vol. 6, pp. 215-239, 1996.*

[55] P. Nelson, "A kinetic model of vehicular traffic and its associated bimodal equilibrium solution, " *Transp. Theory Stat. Phys. , vol. 24, pp. 383-409, 1995.*

[56] R. Wegener and A. Klar, "A kinetic model for vehicular traffic derived from a stochastic microscopic model, " *Transp. Theory Stat. Phys., vol. 25, pp 785-798, 1996.*

[57] A. Schadschneider, "Statistical physics of traffic flow, " *Physica A285, 101, 2000.*

[58] L. Arlotti, N. Bellomo, and E. De Angelis, "Generalized kinetic models: Mathematical structures and applications, " *Math. Models Methods Appl. Sci., vol. 12, pp. 567-592, 2002.*

[59] Y. Sone, "Kinetic theory and fluid dynamics, " *Birkhauser Boston, 2002.*

[60] P. P. J. M. Schram, "Kinetic theory of gases and plasmas, " *Kluwer academic publishers, 1991.*

[61] Kai-Chung Chu, "Optimal Decentralized Regulation of a String of Coupled Vehicles, " *IEEE Transactions on Automatic Control, June 1974.*

[62] X. Liu, A. Goldsmith, S. Sonia Mahal and J. K. Hedrick, "Effects of Communication Delay on String Stability in Vehicle Platoons, " *IEEE Intelligent Transportation Systems Conference Proceedings, August 2001.*

[63] Swaroop D. and K. R. Rajagopal, "Intelligent Cruise Control Systems and Traffic Flow Stability, " *Transportation Research Part C, 1999.*

[64] J. Yi, H. Lin, L. Alvarez and R. Horowitz, "Stability of Macroscopic Traffic Flow Modeling through Wavefront Expansion, " *Transportation Research Part B, 2003.*

[65] R. Shah, C. Nowakowski and P. Green, "U.S Highway Attributes Relevant to Lane Tracking," *University of Michigan, UMTRI Technical Report 98-34, 1998.*

[66] "GPS Errors and Estimating Your Receiver's Accuracy," *http://www.edu-observatory.org/gps/gps_accuracy.html*

[67] T.M Nguyen, J.W Sinko and R.C Galijan, "Using Differential Carrier Phase GPS to Control Automated Vehicles," *Proceedings of the 40th Midwest Symposium on Circuits and Systems, Sacramento, CA, August 1997, pp. 493-496*

[68] D.M Bevly, J.C Gerdes, C. Wislon and G. Zhang, "The Use of GPS Based Velocity Measurements for Improved Vehicle State Estimation," *Proceedings of the American Control Conference, Chicago, Illinois, June 2000, pp. 2538-2542.*

[69] "Nationwide Differential Global Positioning System Program Fact Sheet, " *http://www.tfhrc.gov/its/ndgps/02072.htm*

[70] D. Swaroop, "String Stability of Interconnected Systems - An application to Automated Highway Systems, " *Ph.D Dissertation, University of California at Berkeley, December 1994.*

[71] M.T Moreno, D. Jiang and H. Hartenstein, "Broadcast Reception Rates and Effects of Priority Access in 802.11-Based Vehicular Ad-Hoc Networks, " *Proceedings of VANET 04, October 2004, pp. 10-18.*

[72] W.F Phillips, "A kinetic model for traffic flow with continuum implications, " *Transportation Planning and Technology, 1979, Vol. 5, pp. 131-138.*

[73] F.J Alexander and A.L Garcia, "The Direct Simulation Monte Carlo Method, " *Computers in Physics, Vol. 11, No. 6, Nov/Dec. 1997, pp. 588-593.*

[74] D. Helbing, "Theoretical foundation of macroscopic traffic models, " *Physica A, Vol. 219, 1995, pp. 375-390.*

[75] D. Helbing, "Derivation, properties, and simulation of a gas-kinetic-based, nonlocal traffic model, " *Physical Review E, Vol. 59, No. 1, January 1999, pp. 239-253.*

[76] Z. Tan and P.L Varghese, "The $\Delta - \epsilon$ method for the Boltzmann Equation, " *Journal of Computational Physics, Vol. 110, 1994, pp. 327-340.*

[77] H.M Zhang, "Structural properties of solutions arising from a nonequilibrium traffic flow theory, " *Transportation Research B, Vol. 34, 2000, pp. 583-603.*

[78] D. Helbing, "Macroscopic dynamics of multilane traffic, " *Physical Review E, Vol. 59, June 1999, pp. 6328-6339.*

[79] H.M Zhang, "Analyses of the stability and wave properties of a new continuum traffic theory, " *Transportation Research B, Vol. 33, 1999, pp. 399-415.*

[80] J. Lygeros and N. Lynch, "Conditions for safe deceleration of strings of vehicles, " *California PATH Research Report UCB-ITS-PRR-2000-2, January 2000.*

[81] *http://www.ntsb.gov*